

UTILIZATION OF BIOCHAR FROM WASTEWATER SLUDGE FOR WASTEWATER EFFLUENT AND REUSE

Eustina Musvoto, Farai Mhlanga, Vimbai Kasonde, Linamandla Ponco, Leslie Petrik and David Ikumi



**WATER
RESEARCH
COMMISSION**

TT 940/24



Utilization of Biochar from Wastewater Sludge for Wastewater Effluent and Reuse

Report to the
Water Research Commission

by

***Eustina Musvoto, Farai Mhlanga, Vimbai Kasonde, Linamandla Ponco,
Leslie Petrik and David Ikumi***

TruSense Consulting Services (Pty) Ltd.

**WRC Report No. TT 940/24
ISBN 978-0-6392-0647-9**

September 2024

Obtainable from

Water Research Commission
Bloukrans Building, Lynnwood Bridge Office Park
4 Daventry Street
Lynnwood Manor
PRETORIA

orders@wrc.org.za or download from www.wrc.org.za

This is the final report of WRC project no. C2021/2023-00432.

DISCLAIMER

This report has been reviewed by the Water Research Commission (WRC) and approved for publication. Approval does not signify that the contents necessarily reflect the views and policies of the WRC, nor does mention of trade names or commercial products constitute endorsement or recommendation for use.

EXECUTIVE SUMMARY

Wastewater contains a wide range of both inorganic and organic micro-pollutants like heavy metals and endocrine disrupting compounds (EDCs) that are known to be detrimental to human and environmental health. Most municipal wastewater treatment plants (WWTPs) apply biological wastewater treatment processes (e.g. activated sludge, biofilters and ponds) that are not capable of removing most of these micro-pollutants. Tertiary treatment (e.g. biosorption, adsorption, oxidation and advanced oxidation, ion exchange, membrane filtration and extraction) is therefore required to remove micro-pollutants from final effluent to meet regulatory compliance. Activated carbon (AC) adsorption is the most applied technique due to its simplicity, effectiveness and adaptability to various wastewater types and reuse applications. However, commercially available activated carbons produced from coal are costly and environmentally unsustainable. To reduce costs and ensure long-term sustainability, a diverse range of materials (e.g. sawdust, wood chips, crop waste, waste tyres, etc.) have been explored. In recent years research has shown that using sludge from WWTPs as an adsorbent is also a promising option.

This project investigated the feasibility of using activated carbon produced from pyrolysis of wastewater sludge hydrochar for micropollutant removal from wastewater. The hydrochar was derived from processing combined primary and waste activated sludge using the emerging enhanced hydrothermal polymerization (EHTP) technology (a catalysed hydrothermal carbonisation process). The performance of the sludge hydrochar-derived activated carbon (HC-AC) was compared with commercial coal-based granular activated carbon (C-GAC) through laboratory-scale and small-scale column adsorption tests. The objective of the study was to assess the performance and viability of HC-AC as a low-cost alternative adsorbent, promoting the valorization of sludge within a circular economy framework. Other ACs were also evaluated during the project.

Laboratory scale experiments were carried out in two phases. In the first phase standard laboratory scale jar adsorption tests were conducted to determine the adsorption kinetics and isotherms for both C-GAC and HC-AC using a solution containing lead (II) ions. Pb (II) was selected as an indicator metal because it is one of the most toxic heavy metals that is most likely to be present in significant quantities in wastewater receiving industrial effluent. The results showed that the performance of HC-AC was similar to C-GAC with both having an adsorption capacity of 1.5 mg/g and 99% removal of Pb (II) at equilibrium. The second phase conducted similar jar adsorption tests to investigate the performance of both C-GAC and HC-AC in removing selected heavy metals from secondary clarifier effluent collected from a full-scale biological nutrient removal (BNR) activated sludge plant. The heavy metals were selected from the South African National Standard (SANS) 241 for potable water.

Table 1 summarises the performance of both C-GAC and HC-AC in removing the selected heavy metals.

The performance of HC-AC and C-GAC was closely similar for all elements except for Fe where C-GAC exhibited a significantly higher adsorption capacity. The order of adsorption was Fe > Ni > Mn > Zn for C-GAC and Fe > Ni > Zn > Mn for HC-AC.

Table 1: Adsorption Capacities and % Removals-Laboratory Scale Studies Phase II

Heavy Metal	Adsorption Capacity (mg/g)		Removal (%)	
	HC-AC	C-GAC	HC-AC	C-GAC
Iron	47.2	63.1	78	78
Manganese	25.7	26.6	57	67
Nickel	16.8	15.8	73	69
Zinc	6.6	8.2	67	64

Pilot small-scale column tests were conducted at a full-scale BNR activated sludge plant using secondary clarifier effluent. The maximum adsorption capacity and percentage removals before breakthrough was observed for both HC-AC and C-GAC are given in Table 2.

Table 2: Summary of Adsorption Capacities and % Removals-Pilot Scale Studies

Heavy metal	Adsorption Capacity (mg/g)		Removal (%)	
	HC-AC	C-GAC	HC-AC	C-GAC
Iron	35.4	30.7	94	93
Manganese	9.9	11.3	86	86
Nickel	13.6	10.3	90	89
Zinc	1.7	2.8	82	85

The performance of the two adsorbents using the small pilot-scale adsorption columns was closely similar. The order of adsorption was Fe > Ni > Mn > Zn for both C-GAC and HC-AC.

The study demonstrated that hydrochar produced from processing sludge in a novel thermochemical conversion process can be successfully converted to activated carbon through pyrolysis under a nitrogen atmosphere. The HC-AC performed as efficiently as commercial C-GAC in the removal of Pb (II) ions in a single-metal solution at laboratory scale. HC-AC performance was also demonstrated to be closely similar to that of C-GAC in removing heavy metals from a multi-metal solution through laboratory and pilot column tests using final effluent from a BNR activated sludge plant as the adsorbate. Based on the study results, it appears to be feasible to process sludge in a catalysed hydrothermal carbonisation type technology such as EHTP and convert the produced hydrochar to activated carbon that can be used for tertiary treatment of final effluent from WWTPs. However, further studies are required to investigate viability of using sludge derived HC-AC in full-scale tertiary treatment adsorption plants. Such studies could include investigations into other activation methods (physical, chemical), removal of ash and heavy metals and regeneration and reuse of the HC-AC. Feasible configurations for tertiary treatment processes that incorporate adsorption using sludge hydrochar derived activated carbon with other tertiary treatment technologies, leading to

innovative low-cost treatment processes for water recycling and reclamation schemes within a circular economy also need to be further investigated.

ACKNOWLEDGEMENTS

The authors wish to acknowledge the contributions of the following Reference Group members:

Dr JN Zvimba	Water Research Commission (Research Manager)
Dr SW Sötemann	City of Cape Town
Mr R Moodliar	eThekwini Municipality
Ms N Khosa	Ekurhuleni Water Care Company
Prof LF Petrik	University of the Western Cape
Dr V Masindi	Magalies Water
Mr CM Esterhuysen	City of Tshwane

The project was only possible with the co-operation of a number of individuals and institutions. The authors therefore wish to record their sincere thanks to the following institutions as well as the following members of their staff:

eThekwini Municipality

Mr A Somiah
Mr D Govender
Ms N Dlamini
Mr X Nocanda

University of Cape Town

Mr J Matesun

TruSense Consulting Services (Pty) Ltd

Ms N Ngwenya
Ms T Basi
Mr C Sikhosana
Mr N Hlophe

University of KwaZulu-Natal

Dr S Septien
Mr T Zikhalala

TABLE OF CONTENTS

EXECUTIVE SUMMARY	III
ACKNOWLEDGEMENTS	VI
CHAPTER 1 BACKGROUND	1
1.1 INTRODUCTION	1
1.2 PROCESSES FOR REMOVAL OF MICROPOLLUTANTS FROM WASTEWATER	2
1.3 PROJECT OBJECTIVES	3
1.4 PROJECT TASKS	4
1.4.1 <i>Task 1: Literature Review</i>	4
1.4.2 <i>Task 2: Production of Hydrochar Activated Carbon</i>	4
1.4.3 <i>Task 3: Phase1 Laboratory Studies</i>	4
1.4.4 <i>Task 4: Phase 2 Laboratory Studies</i>	4
1.4.5 <i>Task 5: Pilot Scale Studies</i>	4
1.4.6 <i>Task 6: Project Report</i>	5
CHAPTER 2 LITERATURE REVIEW	6
2.1 INTRODUCTION	6
2.2 TERTIARY TREATMENT TECHNOLOGIES FOR HEAVY METAL REMOVAL FROM WASTEWATER EFFLUENT	8
2.3 HEAVY METAL REMOVAL FROM WASTEWATER EFFLUENT THROUGH ADSORPTION	9
2.3.1 <i>Adsorption Fundamentals</i>	9
2.3.2 <i>Activated Carbon</i>	10
2.3.3 <i>Processing, Activation and Characterisation of Adsorbents</i>	15
2.3.4 <i>Adsorption Kinetics</i>	17
2.3.5 <i>Adsorption Isotherms</i>	18
2.3.6 <i>Adsorption in Packed Bed Columns</i>	20
2.3.7 <i>Parameters Affecting the Fixed-bed Column Process</i>	23
2.3.8 <i>Breakthrough Analysis in Adsorption Tests</i>	23
CHAPTER 3 LABORATORY SCALE STUDIES	25
3.1 INTRODUCTION	25
3.2 PRODUCTION OF HYDROCHAR	25
3.3 PYROLYSIS OF HYDROCHAR TO PRODUCE ACTIVATED CARBON	26
3.4 CHARACTERIZATION OF ACTIVATED CARBONS	28
3.5 ADSORPTION EXPERIMENTS	29
3.5.1 <i>Methylene Blue Adsorption</i>	31
3.5.2 <i>Lead (II) Adsorption</i>	35
3.5.3 <i>Multi-Metal Adsorption Studies using Wastewater from BNR Plant</i>	40
3.6 SUMMARY AND DISCUSSION	40
CHAPTER 4 PILOT SCALE ADSORPTION STUDIES	43
4.1 INTRODUCTION	43

4.2	DESIGN OF PILOT-SCALE ADSORPTION COLUMNS	43
4.3	SMALL-SCALE PILOT COLUMN ADSORPTION TESTS	45
4.3.1	<i>Phase 1 Adsorption Column Tests Results</i>	46
4.3.2	<i>Phase 2 Adsorption Column Test</i>	54
CHAPTER 5	CONCLUSIONS AND RECOMMENDATIONS	61
REFERENCES	64
APPENDICES	70
APPENDIX A	LABORATORY SCALE STUDIES	70
APPENDIX B	ADSORPTION COLUMN TESTS RESULTS -HEAVY METALS	93
APPENDIX C	TESTS ON WOOD DERIVED ADSORBENTS	98

LIST OF TABLES

Table 2-1: Advantages and Limitations of Generally Applied Techniques for Heavy Metal Removal from Wastewater Effluent (Adapted from various Sources)	8
Table 2-2: Performance of Worldwide Selected Waste-derived Activated Carbon for Organic and Inorganic Pollutants from Aqueous Solutions (Adapted from Ngeno et al.,2022).	12
Table 2-3: Adsorption Kinetics Models (<i>Tejada-Tovar et al., 2022</i>)	18
Table 2-4: Adsorption Isotherm Models	19
Table 3-1: Percentage weight loss and yield	28
Table 3-2: Properties of adsorbents	29
Table 3-3: Adsorption Capacities and Kinetic parameters for MB Adsorption onto GAC and HC-AC	34
Table 3-4: Isotherm Parameters for MB Adsorption onto GAC and HC-AC	35
Table 3-5: Kinetic Parameters for Pb(II) ions onto C-GAC and HC-AC	39
Table 3-6: Isotherm Parameters for the Adsorption of Pb (II) Ions onto GAC and HC-AC	39
Table 3-7: Summary of Adsorption Capacities and % Removals-Laboratory Scale Studies	40
Table 4-1: Typical Values for Design and Operation in GAC filters (Cecen, 2012)	44
Table 4-2: Design and operating parameters of adsorption columns	44
Table 4-3: Comparison between SST Effluent Average Concentrations and SANS 241-2015 Standard Limits	46
Table 4-4: Summary of Adsorption Capacities and Percentage Removals for Selected Heavy Metals in SST Effluent	48
Table 4-5: Adsorption Capacity Break through Points for C-GAC and MN-GAC	52
Table 4-6: Summary of adsorption capacities and % removals for selected EDC compounds in SST effluent	52
Table 4-7: Summary of Adsorption Capacities and % Removals-Pilot Scale Studies	55
Table 5-1: Properties of adsorbents	73
Table 5-2: Parameters for the methylene blue initial concentration test	79
Table 5-3: Parameters for the methylene blue contact time test	79
Table 5-4: parameters for the methylene blue pH test	81
Table 5-5: parameters for the methylene blue dosage test	83
Table 5-6: Parameters for the Lead pH test	85
Table 5-7: Parameters for the Lead adsorbent dosage test	86
Table 5-8: Parameters for the Lead initial concentration test	87
Table 5-9: Parameters for the Lead contact time test	89
Table 5-10: Parameters for adsorbent dosage test using wastewater.	90
Table 5-11: Parameters for contact time test using wastewater.	90
Table 5-12: Summary of Adsorption Capacities and % Removals-Laboratory Scale Studies	91
Table 5-13: Summary of the presence and absence of functional groups on GAC and HC-AC.	92
Table 5-14: Photos of Some of the Locally Sourced Activated Carbons used in the Laboratory and Pilot Scale Adsorption Tests	99
Table 5-15: Physical Characteristics of Waste Wood Derived Green ACs from Khula Village	100
Table 5-16: Characteristics of the Activated Carbons Analysed to Date	101

LIST OF FIGURES

Figure 2-1: Breakthrough Characteristics in a Fixed-bed GAC Adsorber (Cecen, 2012)	24
Figure 3.1: Schematic of horizontal tube furnace used for pyrolysis	27
Figure 3.2: Thermogram of HC-PS-WAS	27
Figure 3.3: Images of hydrochar before annealing and after annealing at different temperatures	28
Figure 3.4: Effect of pH on Adsorption of MB (initial concentration: 7.5 mg/L; solution volume: 100 mL, contact time: 130 min for C-GAC, and 280 min for HC-AC; adsorbent dose: 0.2 g/100 mL); pH: 2-11)	31
Figure 3.5: Effect of Contact Time on Adsorption of MB (initial MB concentration: 7.5 mg/L; solution volume: 100 mL, contact time: 370 min; adsorbent dose: 0.2 g/100 mL; pH 6.5)	32
Figure 3.6: Effect of Adsorbent Dosage on Adsorption of MB (initial MB concentration: 7.5 mg/L; solution volume: 100 mL, contact time: 130 min for C-GAC, and 280 min for HC-AC; adsorbent dose: 0.1-1(g/100 ml); pH 8 for C-GAC and pH 11 for HC-AC)	33
Figure 3.7: Effect of pH on the adsorption of Pb (II) ions (initial Pb (II) concentration: 5.3 mg/L; solution volume: 100 mL, contact time: 120 min; adsorbent dose: 0.2 g/100 mL); solution pH: 2-8)	36
Figure 3.8: Effect of Adsorbent Dosage on the Adsorption of Pb (II) ions (initial concentration: 5.3 mg/l; solution volume: 100 ml, contact time: 120 min; adsorbent dose: 0.1-1 g/100 ml; solution pH: 7)	37
Figure 3.9: Effect of contact time on the adsorption of Pb (II) ions (initial Pb(II) concentration: 9.1 mg/L; solution volume: 100 mL, contact time: 150 min; adsorbent dose: 0.6 g for C-GAC and HC-AC, 0.8 g for AW-AC; solution pH: 7).	38
Figure 4-1: Pilot Scale Adsorption Column Rig before Installation at BNR Activated Sludge Case Study Plant	43
Figure 4-2: Removal of Iron from SST effluent by various adsorbents	47
Figure 4-3: Percentage removal of Iron from SST effluent by various adsorbents	47
Figure 4-4: Removal of Nickel from SST effluent by various adsorbents	47
Figure 4-5: Percentage removal of Nickel from SST effluent by various adsorbents	47
Figure 4-6: Breakthrough curve for Fe adsorption on C-GAC	50
Figure 4-7: Breakthrough curve Mn adsorption on C-GAC	50
Figure 4-8: Breakthrough curve Ni adsorption on C-GAC	50
Figure 4-9: Breakthrough curve Zn adsorption on C-GAC	50
Figure 4-10: Breakthrough curve for Fe adsorption on MN-GAC	51
Figure 4-11: Breakthrough curve for Mn adsorption on MN-GAC	51
Figure 4-12: Breakthrough curve for Ni adsorption on MN-GAC	51
Figure 4-13: Breakthrough curve for Zn adsorption on MN-GAC	51
Figure 4-14: Removal of selected EDCs from SST effluent by various adsorbents	53
Figure 4-15: Removal of selected EDCs from SST effluent by various adsorbents	53
Figure 4-16: Removal of Iron from SST effluent by C-PAC	56
Figure 4-17: % Removal of Iron from SST effluent by C-PAC	56
Figure 4-18: Removal of Manganese from SST effluent by C-PAC	56

Figure 4-19: % Removal of Manganese from SST effluent by C-PAC	56
Figure 4-20: Removal of Iron from SST effluent by HC-AC	57
Figure 4-21: % Removal of Iron from SST effluent by HC-AC	57
Figure 4-22: Removal of Manganese from SST effluent by HC-AC	57
Figure 4-23: % Removal of Manganese from SST effluent by HC-AC	57
Figure 4-24: Breakthrough curve for Fe adsorption on C-PAC	59
Figure 4-25: Breakthrough curve for Mn adsorption on C-PAC	59
Figure 4-26: Breakthrough curve for Zn adsorption on C-PAC	59
Figure 4-27: Breakthrough curve for Fe adsorption on HC-AC	60
Figure 4-28: Breakthrough curve for Mn adsorption on HC-AC	60
Figure 4-29: Breakthrough curve for Zn adsorption on HC-AC	60
Figure 5.1: Scanning electron micrographs of C-GAC and HAC	76
Figure 5.2: Raman spectra of GAC and HC-AC	77
Figure 5.3: EDS spectrum of GAC, and HC-AC	78
Figure 5.4: Effect of contact time on adsorption of MB (initial concentration: 7.5 mg/L; solution volume: 100 mL, contact time: 370 min; adsorbent dose: 0.2 g/100 mL; pH 6.5)	80
Figure 5.5: Effect of pH on adsorption of MB (initial concentration: 7.5 mg/L; solution volume: 100 mL, contact time: 130 min for GAC, 160 min AW-AC and 280 min for HC-AC; adsorbent dose: 0.2 g/100 mL); pH: 2-11)	81
Figure 5.6: Effect of adsorbent dosage on adsorption of MB (initial concentration: 7.5 mg/L; solution volume: 100 mL, contact time: 130 min for GAC, 160 min for AW-AC and 280 min for HC-AC; adsorbent dose: 0.1-1(g/100 ml); pH 8 for GAC and AW-AC, pH 11 for HC-AC)	83
Figure 5.7: Effect of pH on the adsorption of Pb (II) ions (initial concentration: 5.3 mg/L; solution volume: 100 mL, contact time: 120 min; adsorbent dose: 0.2 g/100 mL); solution pH: 2-8)	85
Figure 5.8: Effect of adsorbent dosage on the adsorption of Pb (II) ions (initial concentration: 5.3 mg/L; solution volume: 100 mL, contact time: 120 min; adsorbent dose: 0.1-1 g/100 mL; solution pH: 7)	87
Figure 5.9: Effect of initial concentration on the adsorption of Pb (II) ions (initial concentration: 1.9-14.3 mg/L; solution volume: 100 mL, contact time: 120 min; adsorbent dose: 0.6 g for GAC and HC-AC, 0.8 g for AW-AC; solution pH: 7)	88
Figure 5.10: Effect of contact time on the adsorption of Pb (II) ions (initial concentration: 9.1 mg/L; solution volume: 100 mL, contact time: 150 min; adsorbent dose: 0.6 g for GAC and HC-AC, 0.8 g for AW-AC; solution pH: 7)	89
Figure 5.11: FT-IR spectra of GAC and HAC	91
Figure 5-12: Removal of Manganese from SST effluent by various adsorbents	94
Figure 5-13: Percentage removal of Manganese from SST effluent by various adsorbents	94
Figure 1-1: Removal of Zinc from SST effluent by various adsorbents.....	96
Figure 1-2: Percentage removal of Zinc from SST effluent by various adsorbents.....	96
Figure 5-16: Removal of Zinc from SST effluent by various adsorbents	94
Figure 5-17: Percentage removal of Zinc from SST effluent by various adsorbents	94
Figure 5-18: Removal of selected EDCs from SST effluent by various adsorbents	95
Figure 5-19: Removal of selected EDCs from SST effluent by various adsorbents	96
Figure 5-20: Removal of selected EDCs from SST effluent by various adsorbents	97

Figure 5-21: Pilot Scale Column Test Calibration for the Various ACs. AW-AC and PC-AC had broken beds with some particles floating to the surface while wastewater could not flow through SD-AC causing pooling in the column. C-GAC had a normal bed 103

Figure 5-22: Pilot Scale Column Test Calibration for the Various ACs. After washing off fines, soaking and removing floating particles, the AW-AC and PC-AC column beds remained intact similar to GAC 105

LIST OF ABBREVIATIONS

AC	Activated Carbon
ASTM	American Society for Testing and Materials
AW-AC	Alien Wood-Activated Carbon
AWWA	American Water Works Association
BET	Brunauer-Emmet-Teller
COD	Chemical Oxygen Demand
DAF	Dissolved Air Flotation
EDS	Energy Dispersive X-Ray Spectroscopy
EHTP	Enhanced Hydrothermal Polymerization
EPA	Environment Protection Agency (USA)
FT-IR	Fourier Transform Infrared
ICP-OES	Inductively Coupled Plasma-Optical Emission Spectroscopy
GAC	Granular Activated Carbon
HC-AC	Hydrochar Derived Activated Carbon
HCL	Hydrochloric Acid
HNO ₃	Nitric Acid
MB	Methylene Blue
MBN	Methylene Blue Number
NaOH	Sodium Hydroxide
PAC	Powdered Activated Carbon
Pb	Lead
SEM	Scanning Electron Microscopy
SST	Secondary Settling Tank
TGA	Thermogravimetric Analysis
TSS	Total Suspended Solids
UV-VIS	Ultraviolet-Visible Spectroscopy
WHO	World Health Organization
WWTP	Wastewater Treatment plant

This page was intentionally left blank

CHAPTER 1 BACKGROUND

1.1 Introduction

South Africa is inherently water scarce and the impacts of climate change have exacerbated pressure on the country's meagre water resources. Municipalities are therefore turning to wastewater reuse. National policy and position papers such as the National Water Resource Strategy, Water Reconciliation Studies, National Development Plan and the Water and Sanitation Master Plan acknowledge the need for wastewater reuse (Graham, 2019). A study by Kalebaila et al. (2020) estimated the quantity of wastewater generated from South African municipal wastewater treatment facilities and the portion that can potentially be reused. Nationally, about 824 municipal wastewater collector and treatment plants provide an estimated collective hydraulic capacity of 6,509 MI/day. Sixty five percent of the hydraulic capacity (~4,000 MI/d) is provided by 59 wastewater treatment plants (WWTPs) classified as macro (i.e. have a capacity >25 MI/day). The estimated potential water reuse capacity for the macro wastewater treatment facilities is ~2,500 MI/d. Therefore, the study by Kalebaila et al. (2020) estimates that 62.5% of the wastewater inflow at large WWTPs can potentially be reused.

Several initiatives to implement water recycling and reclamation schemes (WR&R) have been undertaken by municipalities. One of the oldest WR&R schemes is eThekweni Municipality's Durban Water Recycling (DWR) plant that treats about 47.5 MI/d of effluent from the Southern WWTP to near potable standards for sale to industrial customers. Other notable schemes include:

- Beaufort West 2.3 MI/d direct potable reuse of wastewater effluent scheme that produces SANS Class 1 standard drinking water.
- Olifants River catchment scheme that reuses approximately 38 MI/d and 205 MI/d from domestic and industrial WWTPs for various purposes including industrial process water, irrigation and in mining.

Other municipalities are also planning to implement WR&R schemes to mitigate the impacts of severe drought that are experienced throughout the country. After suffering a severe water crisis in 2018, the City of Cape Town's water strategy now includes both wastewater reuse and desalination to increase resilience and reduce the risk of severe water shortages in future. eThekweni Municipality is also planning to upgrade the DWR plant to produce 10-20 MI/d of potable water as well as implement WR&R schemes at Northern and KwaMashu WWTPs.

Successful implementation of WR&R schemes is built on 3 key principles (i) providing reliable treatment of wastewater to meet strict water quality requirements for the intended reuse application, (ii) protecting public health and (iii) gaining public acceptance (Asano and Bahri, 2011). All three principles require effective and affordable treatment technologies.

1.2 Processes for Removal of Micropollutants from Wastewater

Wastewater contains a wide range of both inorganic and organic micro-pollutants that are discharged into sewers by households and industries as well as through stormwater runoff. These include heavy metals and organic compounds such as endocrine disrupting compounds (EDCs) that are known to be detrimental to human and environmental health (WHO, 2013; Marques-Pinto et al., 2013). South Africa has regulations that stipulate limits for heavy metals in treated wastewater effluent that is discharged into the environment or reused for various purposes. Although the detrimental impact of EDCs is acknowledged, there are not yet regulations limiting EDCs in wastewater effluent.

Most municipal WWTPs apply biological wastewater treatment processes such as activated sludge, biofilters and ponds that are not capable of removing most of the micro-pollutants. A variety of tertiary treatment processes (e.g. biosorption, adsorption, oxidation and advanced oxidation, ion exchange, membrane filtration and extraction) have proved to be effective for the removal of these micropollutants.

Adsorption is reported as the most widely applied tertiary treatment process for the removal of pollutants from wastewater treatment effluent (Chung et al., 2015; Aljamali et al., 2021; Chowdhury et al., 2022). Because of its relatively straightforward design, ease of operation, affordability, energy efficiency and insensitivity to toxic pollutants, adsorption is preferred to alternative methods of treatment (Yagub et al., 2014; Tan and Hameed, 2017).

Activated carbon is the preferred adsorbent in adsorption processes because of its high adsorption capacity for various types of contaminants (particularly heavy metals), high surface area and pore volume, ease of usage and maintenance. Powdered activated carbon (PAC) and granular activated carbon (GAC) have both been proven to be effective adsorbents in removing not only heavy metals but certain EDCs and dissolved organic carbon.

Commercially used ACs are produced mostly from coal, which is not only expensive, but also environmentally unsustainable. It is reported that about 1.7 million tons of coal based activated carbon is produced per year (Nowicki et al., 2015). Continued coal production at these high rates and the associated environmental impacts is not sustainable. Therefore, to reduce costs for conventional type ACs, a diverse range of materials have been explored as alternative sources (e.g. sawdust, waste tyres, prawn shell, mango seed kernel, wood chips, wheat straws, lemon peel, etc.), paving a pathway for practical application of green adsorbents.

Sludge from WWTPs is one such alternative which has been investigated and found desirable due to its high organic content. It is an unavoidable by-product of wastewater treatment that, in recent years, has been accepted by the wastewater sector as a resource from which valuable materials can be extracted.

The possible use of sludge as a precursor for AC production and subsequent application for tertiary treatment of effluent provides an alternative relatively low-cost adsorbent and promotes valorisation of sludge within a circular economy. Promotion of circular economy within the wastewater sector and converting WWTPs into resource recovery facilities is viewed as one of the key strategies to achieving long term sustainability in the South African wastewater sector. Furthermore, the transition to green adsorbents offers several advantages including low cost, improved efficiency, adsorbent regeneration and reduction of waste disposal challenges as waste is converted to commercially valuable activated carbon (Namasivavam and Kavitha, 2002, El-Wakil et al., 2015;).

1.3 Project Objectives

To provide the South African water sector with options for activated carbons for use in full scale WR&R schemes this project aimed to investigate the viability of using activated carbon produced from sludge hydrochar to remove micropollutants from wastewater. The specific objectives of the project were as follows:

- Investigate the application of activated carbon, produced from hydrochar (HC-AC) generated from processing wastewater sludge in the EHTP technology, to remove selected micropollutants from final effluent discharged from a biological nutrient removal (BNR) activated sludge plant (ASP)
- Compare the performance of the HC-AC with coal based granular activated carbon (C-GAC)
- Conduct laboratory studies to determine the adsorption kinetic models for HC-AC and C-GAC
- Conduct pilot scale column tests to assess the feasibility of using the HC-AC in full-scale plants.

The project was conducted in collaboration with Municipality A that is investigating using low-cost adsorbents in their WR&R schemes. The experimental work focused on the production of HC-AC, characterization of the adsorbents and assessing their performance. Experiments were conducted in three stages as follows:

- Comprehensive characterization of activated carbons (adsorbents) using standard procedures
- Laboratory scale batch jar tests to determine optimal adsorption parameters, adsorption kinetics and isotherms, adsorption capacities and removal efficiencies of the adsorbents
- Batch tests conducted using mono-element solutions containing Pb(II) ions, methylene blue solutions and clarifier effluent from a full scale BNR activated sludge plant
- Pilot scale adsorption column tests

The adsorption column rig was installed at a selected BNR activated sludge plant. Four identically sized adsorption columns running in parallel and operating in continuous mode were setup. Performance of the adsorbents in removing selected heavy metals listed in the South African drinking water standard (SANS 241), from secondary clarifier effluent was assessed and compared.

As part of this project, to assist Municipality A, preliminary high-level evaluation to determine feasibility of using waste wood derived activated carbons as adsorbents for tertiary treatment of wastewater effluent was also conducted.

1.4 Project Tasks

The project was undertaken in 6 major tasks as follows:

1.4.1 Task 1: Literature Review

Relevant literature, covering adsorption, adsorption kinetics and isotherms, types of adsorbents, sludge derived activated carbon and analytical tests for activated carbon characterisation were reviewed. Available literature on adsorption is extensive hence only the most relevant work is presented in this report. The findings from literature were used to develop the procedures adopted in the laboratory and pilot scale adsorption studies and to interpret the results from the studies.

1.4.2 Task 2: Production of Hydrochar Activated Carbon

A combination of primary sludge (PS) and waste activated sludge (WAS) was collected from a full-scale BNR activated sludge plant and used to generate hydrochar using the enhanced hydrothermal polymerization (EHTP) process. Pyrolysis was used to convert hydrochar to activated carbon.

1.4.3 Task 3: Phase1 Laboratory Studies

In the first phase of laboratory studies, standard laboratory scale jar adsorption tests were conducted to determine the adsorption kinetics and isotherms for both C-GAC and HC-AC using a solution containing Pb (II) ions. Similar adsorption studies were conducted to determine the adsorption kinetics and isotherms for both C-GAC and HC-AC using methylene blue solution. The adsorption capacities and removal efficiencies for the two adsorbents were also determined.

1.4.4 Task 4: Phase 2 Laboratory Studies

Standard laboratory scale jar adsorption tests were conducted to investigate the performance of both C-GAC and HC-AC in removing selected heavy metals from secondary clarifier effluent collected from the same full-scale BNR activated sludge plant where the pilot scale column tests were conducted. The heavy metals were selected from the South African National Standard (SANS) 241 for potable water.

1.4.5 Task 5: Pilot Scale Studies

A small pilot scale column rig was setup at a full-scale BNR activated sludge plant to assess the performance of the activated carbons in removing heavy metals regulated in SANS 241 and selected

endocrine disrupting compounds (carbamazepine, Bisphenol A and Triclosan) from secondary clarifier effluent.

1.4.6 Task 6: Project Report

A project report incorporating the outputs from the above tasks was prepared. The report is structured as follows:

Chapter 1: Background

Chapter 2: Literature Review

Chapter 3: Laboratory Scale Studies

Chapter 4: Pilot Scale Studies

Chapter 5: Conclusions and Recommendations

Appendices

CHAPTER 2 LITERATURE REVIEW

2.1 Introduction

Water scarcity is a reality for many countries around the world including South Africa. The National Water and Sanitation Master Plan states that South Africa will require 17% more water in 2030 than is currently available (Department of Water and Sanitation, 2018). Assessment of the water demand, supply and vulnerability to water scarcity in the major municipalities in South Africa by Walters and Steyn, (2022) indicated that at least two metropolitan municipalities (eThekweni and Nelson Mandela Bay), need an increase in water reuse activities. Furthermore, it is projected that the impacts of climate change will increase in South Africa which could worsen the national water deficit (IPCC, 2022). The anticipated 2050 climate and population growth projections for the major municipalities indicate that five of the eight metros would see a reduction in the mean annual precipitation, while all (except one) would see a drastic increase in population growth (CSIR, 2019). An increase in population coupled with increased drought conditions in future will result in an increase in potable, industrial and irrigation water demand in South Africa. It is therefore critical that water reuse forms part of the water and wastewater management strategy of the country. Reuse of treated wastewater to augment water supplies reduces vulnerability to droughts, population growth and water-supply constraints. It can therefore play a key role in improving water security in water-scarce countries such as South Africa (Toze, 2006; Tortajada, 2021).

The potential water reuse capacity is an important factor in the implementation of water reuse strategies. Although it is not possible to ascertain an exact figure for reuse potential, estimates have been provided from various studies. A study by Kalebaila et al. (2020) determined that South Africa has approximately 824 wastewater collector and treatment facilities, that provide an estimated collective hydraulic capacity of 6,509 MI/day. Sixty five percent of the hydraulic capacity (4,000 MI/d) is provided by 59 wastewater treatment facilities classified as macro wastewater treatment works (i.e. have a capacity of >25 MI/day). The reported estimate of potential water reuse capacity for the macro wastewater treatment works is 2,500 MI/d. Although some water reuse schemes have been implemented in the country, there is still a need for additional formal water reuse projects/schemes to expand current reuse volumes (CSIR, 2019). Existing water reuse schemes include:

- the advanced purification demonstration plant at Zandvliet WWTP commissioned in 2019, in the City of Cape Town
- Beaufort West 2.3 MI/d direct potable reuse of wastewater effluent scheme commissioned in 2010 that produces SANS Class 1 standard drinking water
- Oliphants River catchment scheme that reuses approximately 38 MI/d and 205 MI/d from domestic and industrial WWTPs for various purposes including industrial process water, irrigation and in mining.

- Durban Water Recycling plant commissioned in May 2001 and treats about 47.5 Ml/d of effluent from the Southern WWTP to near potable standards. The reclaimed water is sold to industrial customers. According to a study in 2018, the reclaimed water was cheaper at R2.80/m³ than potable water at R5.40/m³ (World Bank, 2018).
- Optimum Water Reclamation Plant located near Hendrina in Mpumalanga

Successful implementation of WR&R schemes is generally dependent on 3 key principles (i) providing reliable treatment of wastewater to meet strict water quality requirements for the intended reuse application, (ii) protecting public health and (iii) gaining public acceptance (Asano and Bahri, 2011). All three principles require effective and affordable treatment technologies.

Wastewater contains a wide range of both inorganic and organic micro-pollutants that are discharged into sewers by households, industries as well as through stormwater runoff. Industries such as mining operations, pulp and paper mills, metal plating factories, fertilizer production, battery manufacturing and many others, produce wastewater contaminated with heavy metals (Fu and Wang 2011). Heavy metals are elements having atomic weights between 63.5 and 200.6 and a specific gravity greater than 5.0 (Srivastava and Majumder, 2008). A significant number of the metals are potentially harmful to human health, aquatic life and the environment (da Silva Oliveira et al., 2007; Lakherwal, 2014; Agoro et al., 2020). Some heavy metals easily dissolve in water and tend to bioaccumulate in living organisms making them highly hazardous (Agoro et al. 2020). Metals such as Iron (Fe), Arsenic (As), Cadmium (Cd), Chromium (Cr), Copper (Cu), Manganese (Mn), Mercury (Hg), Nickel (Ni), Lead (Pb) and Zinc (Zn) which are normally present in wastewater in trace amounts are highly toxic even in minor quantities.

In recent years, new pollutants, usually referred to as “contaminants of emerging concern (CECs)” have also raised concern in the water sector. Emerging contaminants are synthetic or naturally occurring chemicals or any microorganisms that are not commonly monitored in the environment but have the potential to enter the environment and cause known or suspected adverse ecological and/or human health effects (Rosefeld and Feng, 2011). These include pharmaceuticals, pesticides, industrial chemicals, surfactants, personal care products and natural and artificial hormones. Some of these compounds are classified as endocrine-disrupting compounds (EDCs). Emerging contaminants are consistently being found in wastewater, drinking water, surface and ground water sources and have been linked to potentially negative impacts in human health such as neurological disorders, immune dysfunction, harm to the reproductive system and congenital anomalies (Grova et al., 2019; Matta et al., 2020). CECs are persistent, non-biodegradable, and bio-accumulative (Kanamarlapudi et al., 2018; Omo-Okoro et al., 2018). As a result, there is a significant shift towards regulation of CECs from WWTPs in most countries.

Many municipal WWTPs apply conventional biological treatment processes (e.g. activated sludge, biofilters, ponds) that were not designed to remove micropollutants during secondary treatment. Even where

chemical treatment is applied (e.g. in chemically enhanced primary sedimentation or biological excess phosphorus removal).

Regulations for WR&R stipulate much lower limits for heavy metals than for effluent from secondary treatment. Therefore, tertiary treatment of effluent from secondary treatment processes is required to meet the higher standards for WR&R schemes. Usually, various treatment technologies are coupled together in order to achieve the required standard for the reuse purpose.

2.2 Tertiary Treatment Technologies for Heavy Metal Removal from Wastewater Effluent

Feasible treatment technologies for the removal of heavy metals from wastewater effluent include chemical precipitation, ion exchange, chemical oxidation, evaporation, reverse osmosis, ultrafiltration, membrane filtration, electrodialysis and adsorption. A summary of the advantages and limitations of these technologies is given in Table 2-1.

Table 2-1: Advantages and Limitations of Generally Applied Techniques for Heavy Metal Removal from Wastewater Effluent (Adapted from various Sources)

Removal Techniques	Advantages	Limitations
Adsorption	<ul style="list-style-type: none"> • Simple design and operation • High efficiency (up to 99%) • Cost-effective – Low capital and operating cost • pH range is wide (2-12) • High metal-binding capabilities, so most of the metals can be removed • Regenerative and non-toxic 	<ul style="list-style-type: none"> • Performance depends on adsorbent • Produces waste (spent adsorbent/disposal problems) • Regeneration of used adsorbents is necessary in some cases
Evaporation	<ul style="list-style-type: none"> • Pure effluent 	<ul style="list-style-type: none"> • High operational cost • Generate sludges/ disposal problems • High energy consumption (25-50 kW per ton of evaporated water)
Ion exchange	<ul style="list-style-type: none"> • Possible to regenerate resin • High quality effluent • Rapid separation • Small footprint 	<ul style="list-style-type: none"> • Effluent pre-treatment mostly required • Ionic competition and matrix fouling • High total cost due to frequent resin cleaning and sludge disposal • High pH sensitivity
Electrodialysis	<ul style="list-style-type: none"> • High selectivity for separation 	<ul style="list-style-type: none"> • Operating costs are high due to high energy consumption and membrane fouling • Bulky sludge production
Membrane filtration	<ul style="list-style-type: none"> • Small footprint • High separation selectivity 	<ul style="list-style-type: none"> • High capital cost • High operational and maintenance costs for membrane fouling, 3.5 times higher than that of the electrodialysis
Chemical precipitation	<ul style="list-style-type: none"> • Low cost 	<ul style="list-style-type: none"> • Generates large amounts of sludge. • Sludge difficult to dispose/Additional disposal cost

Each removal method has its own set of pros and cons. However, adsorption is the most popular and commonly applied as a separation, purification, and detoxification process at full-scale in wastewater treatment. The benefits of adsorption of heavy metals over other conventional methods include design simplicity, economical, metal selective, regenerative, absence of toxic sludge generation and high efficiency (Tripathi & Ranjan, 2015).

2.3 Heavy Metal Removal from Wastewater Effluent through Adsorption

2.3.1 Adsorption Fundamentals

Adsorption describes the mechanism by which a material called the adsorbate (in a gaseous or liquid bulk) binds on the surface of a solid material known as an adsorbent (El-Dairi *et al.*, 2014). It has been found to effectively remove both organic and inorganic pollutants especially emerging contaminants that are stubborn to remove by conventional biological wastewater treatment technologies. The mechanism of adsorption has been reported as comprising of three stages:

1. Diffusion of molecules from the bulk phase towards the interface space (external diffusion)
2. Diffusion of molecules inside the pores (internal diffusion); diffusion of molecules in the surface phase (surface diffusion)
3. Adsorption of the adsorbate in the active sites of the adsorbent. (Tan and Hameed, 2017; Wang and Guo, 2020; Musah *et al.*, 2022).

The process is generally classified into two types, namely physisorption (physical adsorption) and chemisorption (chemical adsorption). In physisorption, the adsorbate molecules adhere to the adsorbent's surface with a weak interaction force, usually electrostatic Van der Waals' forces. Due to the weak nature of this pairing, physisorption is usually reversible, allowing for desorption and reuse of the adsorbent. Conversely, chemisorption is a result of the formation of strong chemical bonds between the adsorbate and adsorbent involving mechanisms such as ion exchange, complexation, electrostatic attraction and surface precipitation (Harun and Sazali, 2020; Musah *et al.*, 2022; Raji *et al.*, 2023). The removal efficiency of pollutants through adsorption is dependent on factors such as the adsorbent surface area, the presence of surface functional groups on the surface of the adsorbent and the dosage of the adsorbent in the contaminated solution (Li *et al.*, 2002). It is also influenced by parameters such as pH, initial solute concentration, temperature and contact time (Yagub *et al.*, 2014; Raji *et al.*, 2023).

An adsorbent is a solid substance (in rare cases a liquid) used to remove molecules or ions from liquid or gas bulks as they stick to its surface. As adsorption is a surface process, a good adsorbent is generally characterized by possessing a porous structure which is an indicator of high surface area (Gupta *et al.*, 2009; El-Dairi *et al.*, 2014; Crini *et al.*, 2019). Other properties of importance when considering the suitability of an adsorbent include low cost, high adsorption capacity, appropriate pore distribution and diameter, as well as the presence of suitable surface functional groups (Mariana *et al.*, 2021).

Various solid adsorbents in their original or modified forms have been applied to remove trace elements such as heavy metals from wastewater. Activated carbons, zeolites, clay, mesoporous silica, polymeric resins, (Tan and Hameed, 2017; Raji et al., 2023). Nanosized metal oxides, various wastes and advanced adsorbents have been tested at experimental scale and applied at full scale as well, for multi-metal removal from wastewaters and aqueous solutions.

2.3.2 Activated Carbon

The term “activated carbon (AC)” is broad and encompasses carbonized materials exhibiting a large surface area, porosity as well as high reactivity (Cuhadaroglu and Uygun, 2008; Bhatnagar et al., 2013; Heidarinejad et al., 2020). AC is the most widely used adsorbent for tertiary treatment of wastewater effluent to remove heavy metals and other micropollutants. Compared to other adsorbents, AC is an adsorbent with the highest capacity, produces high quality effluent and is made from carbonaceous material which is readily available.

Elemental carbon is the main constituent of activated carbon (85-95%). Heteroatoms like oxygen, nitrogen as well as sulphur are also present depending on the type of raw material, preparation and activation process. AC is commonly produced from coal, which is non-renewable and has negative environmental impacts compelling the need to explore alternative environmentally friendly, cost-effective sources of adsorbents. (Danish and Ahmad, 2018).

Raw Materials for Activated Carbon

Traditional Commercial Raw Materials

The market for AC is huge and was valued at US\$4-5 billion in 2023 with a projected compound annual growth rate of 5.6% until 2032. The main driver for the market growth is the increased use in water and wastewater treatment which had the highest revenue share at 42% in 2023. Coal, coconut shell and wood-based ACs collectively dominate the market, with coal-based AC the most dominant constituting around 50-60% of the total market.¹ Historically, coal-based AC has been favoured because it is an extremely effective adsorbent due to its large surface area, pore structure and high degree of surface reactivity. However, coal is a non-renewable resource and the production of coal-based AC has negative environmental impacts. Studies have shown that coal-based AC has a much higher negative environmental impact in terms of global warming, acidification and eutrophication potential compared to biomass-based activated carbon which is from renewable raw materials (Yong et al., 2022).

Apart from the negative environmental impacts of coal-based ACs, activated carbons produced using raw materials with dominant market share like coal, coconut shell and wood are expensive to purchase and regenerate. The increased demand of AC and fluctuation in raw material availability further increases prices. Therefore, to reduce costs for conventional type activated carbons, a diverse range of materials have been

¹ “Estimates from various market research reports, e.g. Fortune Business Insights (2023); The Brainy Insight (2023); Kingpin Market Research (2023)”

explored as alternative sources (e.g. sawdust, waste tyres, prawn shell, mango seed kernel, wood chips, wheat straws, lemon peel, orange peel, tree barks, rice husks, maize cobs, hazelnut husks, etc.) paving a pathway for practical application of green adsorbents. Transition to these sources of materials offers several advantages including low cost, improved efficiency, adsorbent regeneration and reduction of waste disposal issues as waste is converted to commercially valuable activated carbon.

Waste-Derived Raw Materials

Various waste materials have been investigated as raw materials to produce adsorbents for the removal of various pollutants from domestic, municipal and industrial wastewaters over the years. A study by Ngeno et al. (2022) used literature data to compile and critique recent research on water purification studies in Africa using waste-based adsorbents including ACs. The study concluded that waste materials that are readily available from agriculture and industry are suitable raw materials for producing effective adsorbents that can be applied in water treatment in Africa. Since most African Countries have financial constraints and cannot afford more expensive technologies, use of waste materials is a cost-effective alternative. More research is however required to further understand the technical, financial and environmental impacts to ensure optimal and sustainable full-scale implementation.

The same study also reviewed literature data from various countries on the performance of waste derived adsorbents in removing different organic and inorganic pollutants from aqueous solutions including wastewater. A summary of the performance of waste derived ACs from the study by Ngeno et al. (2022) is given in Table 2-2. There are very data from Africa indicating that more studies are required on waste derived ACs in Africa.

A review of some commonly used waste-based AC precursors is given below.

Pinewood

Pinewood is readily available and its various tree parts can extract heavy metals from wastewater. In studies by Thakur et al. (2021), the bark showed a high affinity for Pb, Cu, Cd, Ni and Zn in that order, with the selectivity for Cu, Cd and Ni almost at par. The temperature at which pinewood is pyrolysed influences the adsorptive capacity of the biochar product. For pyrolysis performed at 300 and 400/450°C, Pb removal efficiencies are 4.3 mg/g and 4.1 mg/g respectively (Kyzas & Kostoglou, 2014). Adding 0.11-3.6 N sulphuric acid modifies pine sawdust to reach an 86% Cr removal efficiency at pH 2. High removal efficiencies were observed for cobalt, nickel and Zn at pH 7 (Argun et al., 2005). The implication is that specific heavy metals can only be effectively removed from wastewater with sawdust at a particular pH.

Table 2-2: Performance of Worldwide Selected Waste-derived Activated Carbon for Organic and Inorganic Pollutants from Aqueous Solutions (Adapted from Ngeno et al., 2022).

Location	Pollutants	Adsorbents	Adsorbates	Max adsorption capacity/	Time (h)	PH	T (°C)	References
Worldwide								
USA	Dyes	Activated carbon (AC) from Cashew nut shells.	Methylene Blue (MB)	476 mg/g	24	7	25	Spagnoli et al. (2017)
Pakistan		AC from used tea leaves.	MB dye	321 mg/g	12	7	30	Mohmood et al. (2017)
Turkey		AC from active sludge	Crystal violet	62.1 mg/g	2.5	6	25	Shabza et al. (2019)
Brazil		AC from palm fibres	MB dye	110.8-162.5 mg/g	1	6	30	Maia et al. (2021)
USA/South Korea	Heavy metals	Biochar from loblolly pine	Cd ²⁺	167 mg/g	24	7.5	25	Park et al. (2017)
Viet Nam		AC from banana peel	Cu ²⁺ Ni ²⁺ Pb ²⁺	14.3 mg/g 27.4 mg/g 34.5 mg/g	24	6.1-6.5	25	To et al. (2017)
Brunei		AC from sugarcane bagasse	Cx ⁶⁺	9.7 mg/g	2	6.5	26	Kerri et al. (2020)
Hungary China		Pomegranate peel powder AC from tangerine seed	Ammonium Metolcarb Pirimicarb Methiocarb	9.11 mg/g 39.37 mg/g 93.4 mg/g	2 0.25	6 7	25 30	Hodur et al. (2023) Wang et al. (2020)
Spain		AC from sludge	Acetamidiprid Thiamethoxam Imidacloprid	129 mg/g 127 mg/g 166 mg/g	24-144	7	25	Sanz-santos et al. (2021)
China Hong Kong	Emerging pollutants	Waste tea-based AC. AC from palm kernel shell	Oxytetracycline Atenolol Acebutolol carbamazepine	0.69 mmol/g 0.67 mmol/g 0.72 mmol/g	30 24	- 7	30 25	Kan et al. (2017) To et al. (2017)
Brazil		AC from macauba palm	Bisphenol A Ethinylestradiol Amoxicillin	0.15 mmol/g 0.10 mmol/g 0.07 mmol/g	24	5.5	25	Moura et al. (2018)
Africa								
Botswana	Nickel (ii) and Cobalt (ii) ions	Vinegar-Treated eggshell Waste Biomass		78.70% and 76.53% respectively				Stevens and Batlokwa (2017)
Zimbabwe	Methylene blue	Biochar and Fe ₂ O ₃ -biochar nanocomposite derived from pulp and paper sludge		50 mg/g and 33 mg/g respectively				Chaukura et al. (2017)
Nigeria	dye	Activated carbon from sawdust		98.5%				Eletta et al. (2018)
Kenya	Caffeine and ciprofloxacin pharmaceuticals	Water hyacinth biochar		>60%				Ngeno et al. (2016)
Nigeria	Crude oil	Chemically and Thermally Modified Coconut (Cocos nucifera) Husks		Between 12.11 g/g and 16.84 g/g				Agarry et al. (2020)

Sawdust

Sawdust is favoured as an adsorbent because it is easily sourced from sawmills at low prices. Its biodegradability makes disposal safe and convenient. The wood particles contain hemicellulose, lignin and cellulose which have adsorptive properties (Lakherwal, 2014; Meez et al., 2021). Kyzas & Kostoglou (2014) pegged the adsorption efficiency for Cr(VI) at 20.7 mg/g from liquid solutions. The ability of sawdust to adsorb heavy metals can be enhanced by adding acid and the type of acid depends on the source tree of the sawdust. One example is modifying oak sawdust with hydrochloric acid for heavy metal adsorption. The maximum removal efficiency was 84% for Cr at pH 3, 82% for Ni at pH 8 and 93% for Cu at pH 4 (Argun et al., 2007).

Agricultural by-products

Most low- and middle-income countries (LMICs) in Africa and Latin America have utilised agricultural by-products as biosorbents for removal and recovery of metal ions. Agricultural by-products are considered more affordable and abundant for use. Most of these agricultural by-products are generated from waste of staple foods native in the countries. Agricultural wastes include yam peels, fluted pumpkin, cassava peels, orange, banana peels, sweet potato peels, plantain peels, rice-husks, sawdust, coconut fibres, vegetables, etc. (Okoro & Okoro, 2011; Kyzas & Kostoglou, 2014; Ayob et al., 2021). The adsorbents have been found to remove >90% of heavy metals like Pb, Zn and Cd.

Wastewater Sludge

Sludge is an unavoidable by-product of WWTPs. Sludge management is a huge challenge to wastewater utilities because of the large quantities produced, strict disposal regulations and the associated high handling and treatment costs. To mitigate these challenges, sludge management strategies have shifted towards valorisation of sludge through energy generation, beneficial use and resource recovery. The conversion of sludge to AC is one such use which has been explored in recent years.

Sludge is favoured as an activated carbon precursor due to its high organic content and its carbonaceous nature. The preparation of sludge derived AC is reported to be via mostly carbonization and then further activation by physical means using carbon dioxide, steam or air. An alternative is chemical activation before carbonization using chemical agents such as H_2SO_4 , $ZnCl_2$, KOH , H_3PO_4 as this significantly enhances the surface area and as a result the adsorption capacity (Hadi et al., 2015; Puccini et al., 2017). The produced AC has been reported as having surface areas ranging between 100-600 mg_2/g . Sewage derived ACs have also been found to be as efficient as conventional ACs in the removal of common heavy metals (e.g. Pb, Cu, Zn, Cd, Hg) from aqueous solutions and wastewater (Li et al., 2016); Salini et al., 2018; Al-Mahbashi et al., 2023).

Types of Activated Carbon

Activated carbons can be generically classified based on their processing techniques, size, and industrial applications. The main classifications are granular activated carbon (GAC), powdered activated carbon

(PAC), extruded activated carbon (EAC), bead activated carbon (BAC), polymer-coated carbon, impregnated AC and woven carbon (Ganjoo et al., 2023). Each type of activated carbon has its advantages and is selected based on factors such as the specific contaminants present in the water, the desired treatment efficiency and the operating conditions of the treatment system. Based on market research reports, PAC (~ 50%) and GAC (~40%) dominated the market in 2023.

Granular Activated Carbon (GAC)

Granular activated carbon (GAC) adsorption has been used successfully for the advanced (tertiary) treatment of municipal and industrial wastewater. Typically, GAC adsorption is utilized in wastewater treatment as a tertiary process following conventional secondary treatment or as one of several unit processes consisting of physical-chemical treatment. In WWTPs utilizing biological secondary treatment, GAC adsorption is generally located after filtration and prior to disinfection (EPA, 2000).

GAC has the capacity to adsorb the relatively small quantities of soluble organics and inorganic compounds such as nitrogen, sulfides, and heavy metals remaining in the wastewater following biological or physical-chemical treatment. In practice, a GAC system consists of carbon contactors, virgin and spent carbon storage, carbon transport systems and carbon regeneration systems. The carbon contactors are fabricated as steel columns or steel or concrete rectangular tanks in which the carbon is placed to form a “filter” bed (EPA, 2000). Inside the columns, the AC is held in place by an underdrain system at the bottom of the contactor. To achieve treatment, wastewater is applied at the top of the column, flows downward through the carbon bed and is withdrawn at the bottom of the column. Provisions for backwash and surface wash of the carbon bed are required to prevent buildup of excessive head loss due to accumulation of solids and to prevent the bed surface from clogging. The regeneration of the AC is accomplished by thermal processing in a special kiln or multiple hearth furnaces. Approximately 5 to 10 percent of the carbon is destroyed in the regeneration process or lost during transportation and must be replaced with virgin carbon. Repeated regeneration degrades the carbon particles until an equilibrium is eventually reached providing predictable long term system performance (EPA, 2000).

Prior to the design and implementation of GAC systems, a pilot plant study should be conducted to determine if the technology will meet discharge permit requirements and to quantify key parameters such as optimum flow rate, bed depth and operating capacity on a particular wastewater. This information is required to determine the dimensions and number of carbon contactors required for continuous treatment. The sizing of carbon contactors is based on contact time, hydraulic loading rate, carbon bed depth and number of contactors (EPA, 2000).

Powdered Activated Carbon

Powdered activated carbon (PAC) is used as an adsorbent in wastewater treatment mainly for the removal of non-biodegradable pollutants after biological treatment. PAC has a higher fraction of mesopores than GAC and thus allows for more rapid intraparticle diffusion (Real et al., 2017; Suzuki, 1991).

The application of PAC involves contacting of the adsorbent with the solution to be treated for a prescribed time followed by separation to obtain a treated effluent. The application of PAC in this manner proves to be mostly impractical compared to GAC adsorbers. In wastewater treatment, PAC can be added at different points in the wastewater treatment process to remove micropollutants. The application of PAC into biological treatment in which PAC is held in suspension is generally favoured compared to applications in which PAC is used in stationary form (Cecen and Akatas 2012). In most wastewater treatment applications PAC is added as dry powder or as an aqueous solution before or simultaneously to the flocculation step. In some cases, the separation is done after the addition of the flocculants in a sedimentation tank. Sand filtration usually follows to further remove solid particles present in the effluent. The advantages of PAC lie in the flexibility of dosing based on the level of water pollution and reduced investment costs since existing aeration and secondary settling tanks are used.

2.3.3 Processing, Activation and Characterisation of Adsorbents

As alternatives to industrial adsorbents generally derived from finite resources (such as coal, lignite and peat), the precursors to sorbents should be easily accessible, cheap and non-toxic. The carbon or oxygen content should also be high to increase bonding possibilities between the sorbent and the sorbate. Other attributes include thermal resistance, resistance to wear, recyclability and narrow pore diameters (Ali et al., 2012). This leads to increased exposed surface area and, hence, an elevated surface capacity and fast kinetics for adsorption. Further, the sorbents should also be easily desorbed thereafter thus enabling regeneration without releasing undesirable substances into the aqueous media (Kumar et al., 2019; Omo-Okoro et al., 2018). Most waste biomaterials have been found to fulfil most, if not all, of those desired properties for the preparation of carbonaceous adsorbents. Additionally, they are a renewable resource. Usually, these waste materials, often bio-based ones, are used without thermal or chemical pretreatment or are pyrolyzed to obtain low-cost biochars that are alternatives to activated carbon. These carbonaceous chars can further be activated to improve their porosity and surface chemistry (Ali et al., 2012).

Activation of Adsorbents

In general, adsorbents are processed and/or activated using both physical and chemical methods. Some bio-based sorbents (biosorbents) are used directly as dried powdered biomass. The majority, however, are transformed into carbonaceous materials through pyrolysis, a process of decomposing organic material through heating at elevated temperatures with neither oxygen nor halogen. This converts the material to carbon. Heating rate and duration of carbonization and activation are the most significant variables during pyrolysis since they influence the ultimate pore structure, surface area and chemical properties of the

resultant carbon. The resultant material constitutes an inflexible carbonaceous char containing pores packed with tarry pyrolysis deposits and necessitates activation to expand the internal surface area of the char thus increasing porosity (Ali et al., 2012; Omo-Okoro et al., 2018; Adeniyi and Ighalo, 2019).

Activation may be achieved chemically or physically consequently obtaining activated carbons with diverse forms and dimensions given the varying pathways of activation. In chemical activation, chemical modifiers are infused into the biomass. Commonly used chemical activators include zinc chloride ($ZnCl_2$), phosphoric acid (H_3PO_4), sulphuric acid (H_2SO_4), potassium hydroxide (KOH), sodium hydroxide (NaOH), potassium sulphide (K_2S) and potassium thiocyanate (KCNS). These chemically modifying groups most of which contain oxygen, sulphur and nitrogen are known to improve the adsorption and cation-exchange capacities. Once the biomass is saturated with the activators, it is then dehydrated to minimize tar formation and volatilization during pyrolysis (Ali et al., 2012; Omo-Okoro et al., 2018.; Adeniyi and Ighalo, 2019; Agarry et al., 2020).

The advantages of chemical activation technique has some strengths include low activation temperatures of activation, shorter reaction time, reduced energy costs and increased material yield. The used material may however be environmentally hazardous. The cost of adsorbent development depends on the method of chemical activation, duration of pyrolysis and temperatures used (Omo-Okoro et al., 2018).

Physical activation is the direct reaction between the carbonized char and an activator, which are mostly oxidizing agents like steam, carbon dioxide (CO_2) and air. Physical activators are clean, easy to handle and environmentally friendly but have a lower yield. Just like chemical activation, the main objective is to rid the structure of tarry amorphous carbon in the interstitial layers thus increasing the porosity and making the internal surface area accessible (Ali et al., 2012). Nanotechnology has also been employed in producing nanocomposites from waste materials. Nanoscale structures atomic and molecular sizes are within 1-100 nm. Nanocomposites are materials synthesized from varied materials put together and structured into nanoscale size to increase their functionality and reactivity (Omo-Okoro et al., 2018). Most nanocomposites have been manufactured from metals and agricultural waste materials and have been found to work exceptionally well in water treatment (Okello et al., 2017).

Characterisation of Adsorbents

Adsorbents are characterized to determine their textural and surface characteristics before and after adsorption. This includes surface area, porosity, crystallite size, particle size, thermal stability, surface morphology, and functional groups responsible for adsorption (Oyewo et al., 2016). High porosity (and consequently an extensive surface area with more specific adsorption sites and faster kinetics) is the fundamental characteristic of a good adsorbent. Several characterization methods can be conducted on adsorbents including X-ray diffraction, which has been employed for mineralogical phase identification and quantification and measurement of crystallite size. The scanning electron microscope (SEM) and

transmission electron microscopy (TEM) are used for inspecting surface morphology. Fourier Transform infrared FTIR spectrometry has also been used to determine surface functional groups of adsorbents pre- and post- adsorption (Choina et al., 2015; Onwuka et al., 2016; Oyewo et al., 2016; Souza et al., 2017).

2.3.4 Adsorption Kinetics

The main purpose of studying adsorption kinetics is to describe the rate of solute uptake and the retention of the solute from the aqueous phase to the solid phase interface (adsorbent) under a set of given parameters (Batool *et al.*, 2018; Tejada-Tovar *et al.*, 2022). The kinetics can also be used to evaluate the performance of the adsorbent (Wang and Guo, 2020). The design of adsorption systems largely relies on the rates calculated from the kinetic studies of adsorption (Yagub *et al.*, 2014). Of the mathematical models developed to describe the kinetics of adsorption of dyes, metal ions and other compounds in aqueous solution over the years, the pseudo first order and pseudo second order kinetic models have been the most widely applied and compared (Qiu *et al.*, 2009; Simonin, 2016; Tan and Hameed, 2017).

Pseudo first order kinetic and pseudo second order kinetic models

The Pseudo-first order (PFO) kinetics first proposed by Lagergren in 1988 and the pseudo-second order (PSO) kinetics have been extensively compared in literature (Ho and McKay, 1999a & 1999b). Most studies report the superiority of the PSO equation to that of the PFO when it comes to fitting data from adsorption experiments (Yagub et al., 2014; Tan and Hameed, 2017). This effect is possibly as a result of treating the experimental data with the linearized equations of the PFO and PSO, which give the plots $\log(q_e - q_t)$ versus time (t) and t/q_t versus time (t) respectively where:

- q_e is the removal capacity at equilibrium
- q_t is the removal capacity at time t and
- t is the time.

The correlation coefficient of the PSO is likely to be higher and closer to one as both the x and y axis of the PSO plot contain the variable t. The PFO describes the adsorption rate of the solute onto the adsorbent based on the adsorption capacity. The model assumes that the rate of adsorption is proportional to the difference between the maximum capacity at equilibrium and the capacity at any time, i.e. $(q_e - q_t)$. Its linearized integral form and the plot used to derive its constants (k_1 and q_e) are given in Table 2-3 below. The PSO is used to calculate the initial rate of sorption and is especially applicable on small amounts of initial concentration whereas the PFO is favoured at high initial concentration (Mokhena et al., 2016, (Batool et al., 2018). It assumes that the rate of uptake is second order with respect to the surface sites that are available on the adsorbent and that the rate limiting step may be chemical adsorption

(Tan and Hameed, 2017; Hubbe, Azizian and Douven, 2019). The linearized integral form of the model and the plot used to derive its constants k_2 and q_e are depicted in Table 2-3.

Table 2-3: Adsorption Kinetics Models (Tejada-Tovar et al., 2022)

Model	Integrated Equation	Plot	Parameters
Pseudo-first order	$\begin{aligned} & \text{Log}(q_e - q_t) \\ & = \text{Log}q_e - \frac{k_1}{2.303}t \end{aligned}$	$\text{Log}(q_e - q_t) \text{ vs } t$	q_t = adsorption capacity at any time t mg/g
			q_e = adsorption capacity at equilibrium mg/g
			k_1 =Lagergren's constant (min^{-1})
			t = time (min)
Pseudo-second order	$\frac{t}{q_t} = \frac{1}{k_2 q_e^2} + \frac{1}{q_e} t$	$\frac{t}{q_t} \text{ vs } t$	k_2 =pseudo-second order constant (min^{-1})

It has been observed that the q_e value obtained from the PFO equations is usually farther away from the value obtained experimentally when compared to that obtained by the PSO equations which is often less but closer. Thus the wide applicability of PSO over PFO stems more from a mathematical basis than it does from a physical one. The added advantage of using PSO is that the q_e value is not required for fitting the experimental data (Musah et al., 2022).

2.3.5 Adsorption Isotherms

Adsorption isotherms are mathematical models that are crucial to comprehending the mechanism of adsorption by illustrating the interaction between the adsorbate and the surface of the adsorbent and providing information regarding the adsorption capacity at given operating conditions (Yagub et al., 2014; Musah et al., 2022; Tejada-Tovar et al., 2022). A number of isotherms including Elovich, Freundlich, Langmuir, Redlich-Peterson, and Temkin have been published in literature (Batoool et al., 2018). The Langmuir (1918) and Freundlich (1906) are the two most widely employed isotherms. The Langmuir and Freundlich isotherm equations are given in Table 2-4

Langmuir Isotherm

The Langmuir isotherm is based on the basic assumption that the adsorption process occurs at specific homogeneous sites on the adsorbent surface (Chung et al., 2015; Tejada-Tovar et al., 2022). The isotherm also assumes:

- That each adsorbent has fixed adsorption sites on its surface and that at specific parameters, a portion of these sites may be occupied by adsorbate.
- Only one entry can be accommodated on each site of adsorption on the adsorbent surface.
- There is no interaction between adsorbate occupying different adsorption sites.

- Each adsorption site has the same heat of adsorption and is unaffected by the percentage of sites occupied by the adsorbate.

Based on these assumptions, the Langmuir adsorption isotherm is valid only for monolayer adsorption (Musah et al., 2022). Four linear forms of the Langmuir are usually presented in literature. The linear equations have been used to express the Langmuir isotherm and the plots also displayed alongside these equations have been used to deduce the Langmuir constants K_L and q_{max} . From these same plots, the separation factor, R_L which indicates the nature of the isotherm can also be determined using the following equation:

$$R_L = \frac{1}{(1 + K_L \cdot C_i)}$$

where K_L is the Langmuir constant and C_i is the initial concentration of the adsorbate. If the R_L value falls between 0 and 1, i.e. $0 < R_L < 1$, then the isotherm is deemed favourable (Chung et al., 2015; Musah et al., 2022; Tejada-Tovar et al., 2022).

Table 2-4: Adsorption Isotherm Models

Model	equation	Plot	Parameters
Langmuir 1	$\frac{1}{q_e} = \left(\frac{1}{K_L \cdot q_{max}} \right) \cdot \frac{1}{C_e} + \frac{1}{q_{max}}$	$\frac{1}{q_e} \text{ vs } \frac{1}{C_e}$	q_e = the solute mass adsorbed per unit adsorbent mass at equilibrium (mg/g) q_{max} = maximum adsorption capacity (mg/g) C_e = adsorbate concentration at equilibrium (mg/l) K_L = Langmuir constant related to the affinity of the adsorbent for the adsorbate Ref 3 (Osmari <i>et al.</i> , 2013)
Langmuir 2	$q_e = q_m - \frac{1}{K_L} \frac{q_e}{C_e}$	$q_e \text{ vs } \frac{q_e}{C_e}$	
Langmuir 3	$\frac{q_e}{C_e} = q_m K_L - K_L q_e$	$\frac{q_e}{C_e} \text{ vs } q_e$	
Langmuir 4	$\frac{C_e}{q_e} = \frac{1}{q_m K_L} + C_i$	$\frac{C_e}{q_e} \text{ vs } C_e$	
Freundlich	$\text{Log } q_e = \frac{1}{n} \text{Log } C_e + \text{Log } K_F$	$\text{Log } q_e \text{ vs } \text{Log } C_e$	K_F = Freundlich constant, related to the adsorption capacity of the adsorbent (mg/g) n = adsorption intensity of the adsorbent according to its heterogeneity Ref 3 (Tejada-Tovar <i>et al.</i> , 2022)

Freundlich isotherm

The Freundlich isotherm is an empirical model occasionally employed as a tool for data description due to the mathematical simplicity of its equation and its aptitude for characterizing non-linear adsorption processes across a range of adsorbate concentrations (Chung et al., 2015; Musah et al., 2022). Unlike the

Langmuir model that assumes that the adsorption process occurs at specific homogeneous sites with the same heat of adsorption, the Freundlich isotherm assumes a heterogeneous adsorption surface with unequal available sites with different adsorption energies (Yagub, Sen and Ang, 2012). It is typically used to quantify the relationship between the amount of adsorbate removed per unit weight of adsorbent and the adsorbate concentration still present in solution at equilibrium (Musah et al., 2022). The isotherm is formulated as per the equation in Table 2-4 then its constants K_F and n can be formulated from the plot of $\text{Log } q_e$ vs $\text{Log } C_e$ (Yagub, Sen and Ang, 2012; Batool et al., 2018; Musah et al., 2022). If the K_F value falls within the range of 1-20, and the n value is above 1, then adsorption is considered promising and the data fits the model well (Batool et al., 2018). The value of the linear regression coefficient R^2 is used to determine which model best fits the adsorption data (Yagub et al., 2014).

2.3.6 Adsorption in Packed Bed Columns

For the adsorption technique to be available for industrial application, packed bed columns in continuous systems must be evaluated in support of scaling up to industrial scale. Currently there is a gap in the application of fixed bed columns for adsorption in continuous systems, despite several researchers having investigated the application of biosorption at higher scale in continuous systems (Ramrakhiani et al. 2016; Martín-Lara et al. 2017). Therefore, pilot scale studies are required to demonstrate high removal efficiencies before plant scale up can be carried out. Rapid small scale column tests (RSSCTs) and pilot scale adsorption columns are generally used to evaluate and predict adsorption media performance before scaling up.

Rapid Small-Scale Column Studies

RSSCTs are scaled-down columns packed with smaller-diameter adsorption media that receive higher loading rates to reduce the duration of experiments significantly. This method uses scaling relationships that allow correlation of lab-scale column results operated at accelerated flow rates to full scale column performance.

The RSSCT method as developed by Frick (1982) to predict the behaviour of full-scale columns based on the performance of small-scale columns has been extensively applied by various researchers over time, with the most prominent being by Crittenden and his research group (Crittenden et al., 1986a; 1987; 1989; 1991). The RSSCT uses fixed-bed mass transfer models to scale down the full-scale design to a much smaller column. Significantly smaller GAC granules than those used in full-scale adsorbers are used, in order to take advantage of the fact that the rate of adsorption is proportional to the inverse of the particle diameter squared and thus the breakthrough in the small columns occur in a matter of days. The appropriate scale-up equations are used to (i) design the small-scale columns based on the characteristics of the full-scale column and (ii) transform the small-scale column data into a prediction of the full-scale column behaviour.

The method does not require extensive isotherm or kinetic studies to obtain the full-scale performance prediction and the amount of water required is reasonable for the small-scale column tests to be conducted in a laboratory, thereby avoiding the laborious on-site test work that also require a continuous supply of raw water.

The three parameters critical for proper design of the RSSCT include empty bed contact time (EBCT), the hydraulic loading and the AC bed length inside the small-scale column. The proper EBCT scaling between the small-scale column (SC) and the full-scale or “large” column (LC) can be determined using the equations described by Crittenden et al. (1991). The RSSCT has been successfully used to predict the full or pilot-scale performance. Surveys of past comparisons of the RSSCT to full-scale data for many waters and for several different adsorbates has also been conducted. Unfortunately, the scaling relationships are usually not known beforehand, requiring researchers to either test both scaling equations in order to choose the more appropriate relationship for the field situation, or conduct batch kinetic tests using different sizes of carbon particles to establish a relationship between the particle size and the surface diffusivity.

Although the RSSCT method provides great cost and time savings over pilot-plant studies, careful consideration must be taken when applying the findings as the approach has its limitations as follows:

- a) the RSSCT tests are conducted with a single sample, which may not be representative of the seasonal water quality variations at the full-scale facility
- b) the short duration of the RSSCT tests precludes the development of sufficient biomass and related contaminant biodegradation that is observed in full-scale adsorbers, which may cause differences in the breakthroughs
- c) RSSCT scaling method for predicting the performance of adsorption systems experiencing significant preloading was found inadequate because of the inability to accurately scale the preloading effect (Summers et al., 1989; Speth and Miltner, 1989; Speth, 1991; Crittenden et al., 1991; Knappe et al., 1997). Summers et al. (1989) proposed preloading of the small GAC particles and then performing a small-scale column test in order to increase the precision in predicting the large-scale columns. One drawback of initial preloading of the GAC particles for column tests is determining the appropriate preloading time.

Therefore, implementing such an experiment requires multiple elements to ensure that similarity between the small-scale column and full-scale adsorber is maintained.

These elements include:

- data from a full-scale or larger scale adsorber must be readily available to adequately compare the results from the RSSCTs.
- Information regarding the large-scale column carbon regarding its type, capacities, bulk densities, and void fraction is necessary to ensure adequate similarity.

- Proper scaling of the small-scale column and amount of carbon used as well as the type of pump and piping to build the system and limit dead zones are needed.

Additional precautions are required to prevent change in the characteristics of the water. Furthermore, proper analysis is fundamental in the success of such test work. With the proper set-up and if the RSSCT is capable of predicting the performance of the large-scale adsorber, then different tests can be undertaken to help determine how adsorption columns should be used in the future.

Fixed Bed Continuous Adsorption Column Studies

A fixed-bed GAC column is used mostly for contacting wastewater with GAC. Fixed-bed carbon adsorbers may be operated under pressure or gravity flow. Wastewater is applied at the top of the carbon column, flows downward through the carbon bed and is withdrawn at the bottom of the column. As the wastewater flows through the column, the contaminants are adsorbed. The carbon is held in place with a drain system at the bottom of the contactor. Provisions for backwash and surface wash of the carbon bed are required to prevent build-up of excessive head loss due to accumulation of solids and to prevent the bed surface from clogging.

The main reactor configurations for GAC adsorption systems are the fixed (packed), expanded and fluidized beds. A downflow adsorber with low fluid velocities essentially functions as a fixed-bed reactor. Fixed-bed operation provides filtration as well as adsorption. The fixed-bed configuration is suitable in the case of low strength wastewaters containing little or no suspended solids.

This system generally works with unsteady rate-controlled processes. The adsorption phenomenon takes place in a particular fixed region of the bed with the effluent in the moving phase. Once the adsorption in the fixed-bed zones becomes saturated (also known as mass transfer zone MTZ), the effluent passes through the bed towards the output. The downstream and upstream movement of the effluent in the column bed is ensured by a pump at definite flow rate.

Adsorption column studies are easier in operation and design, obtain a high yield and treat large quantities of wastewater. The most applicable technique in column studies is the fixed-bed column due to cyclic sorption and desorption (Kumar et al., 2011). The breakthrough curve is a significant component of the column adsorption studies as it explains the effluent concentration-over-time profile. The S-shape of the breakthrough curve depends on the nature of the wastewater treated (Vinodhini, 2010). In this study, the breakthrough curve for the adsorption of the selected pollutants will be plotted and interpreted in the context of application of the adsorption column technique in EDCs and heavy metal removal, by adsorbents.

Batch mode adsorption studies provide essential operating parameters and provide practical operational information about specific adsorbents. The advantages of fixed-bed columns over batch studies are that they can be operated in single, series, and in parallel. Column mode studies are based on the parameters

such as fixed-bed height, breakthrough curve, and flow rate. These techniques are efficient, reliable and the most common ones for the removal of pollutants from water and wastewater (Gupta et al., 2016).

2.3.7 Parameters Affecting the Fixed-bed Column Process

Bed Height and Diameter

Heavy metal ion removal is mainly dependent on the quantity of adsorbents inside the fixed-bed column. The higher surface area has more binding sites and functional groups for metal biosorption in aqueous solution. The breakthrough curve generally increases by increases in bed height and diameter (Rangabhahiyam et al., 2016). Other researchers have looked at the effect of bed height and diameter on removal efficiencies of individual pollutants and made recommendations on the most optimal parameters for adsorption. This study will use real effluent from a typical WWTP and monitor the removal of selected pollutants at a particular bed height and column diameter.

Flowrate

As the flow rate increases, the rate of pollutant removal decreases. The breakthrough curve becomes steeper and reaches the optimum state. The equilibrium state is reached quickly due to the high residence time between adsorption and pollutant concentration. Studies show that breakthrough time decreases with increasing flow rate. Similarly, saturation time decreases (Lakshmi pathy et al., 2015).

Pollutant Concentration

The initial pollutant concentration with a linear flow rate effluent determines the rate of breakthrough time. The sorption of the pollutant changes with increasing concentration as well as bed height. The diffusion process depends on the inlet metal concentration. In this study the initial concentration of the selected pollutants present in the untreated effluent will be monitored at the start of each adsorption column run.

2.3.8 Breakthrough Analysis in Adsorption Tests

The adsorption of contaminants takes place in zone A, called the mass transfer zone (Figure 2-1). While in operation, the transfer zone moves in the direction of flow. As this zone moves downwards, the saturation zone (Zone-Sat) is generated, which is saturated with pollutants and is in equilibrium with the influent concentration. The plot of effluent concentration divided by influent concentration (S/S_0) as a function of elapsed time, processed volume, or bed volume generates the “breakthrough curve”. The point at which a predetermined concentration (S_B) appears is defined as the “Breakthrough point”. This point is rather arbitrary and is selected according to purity requirements.

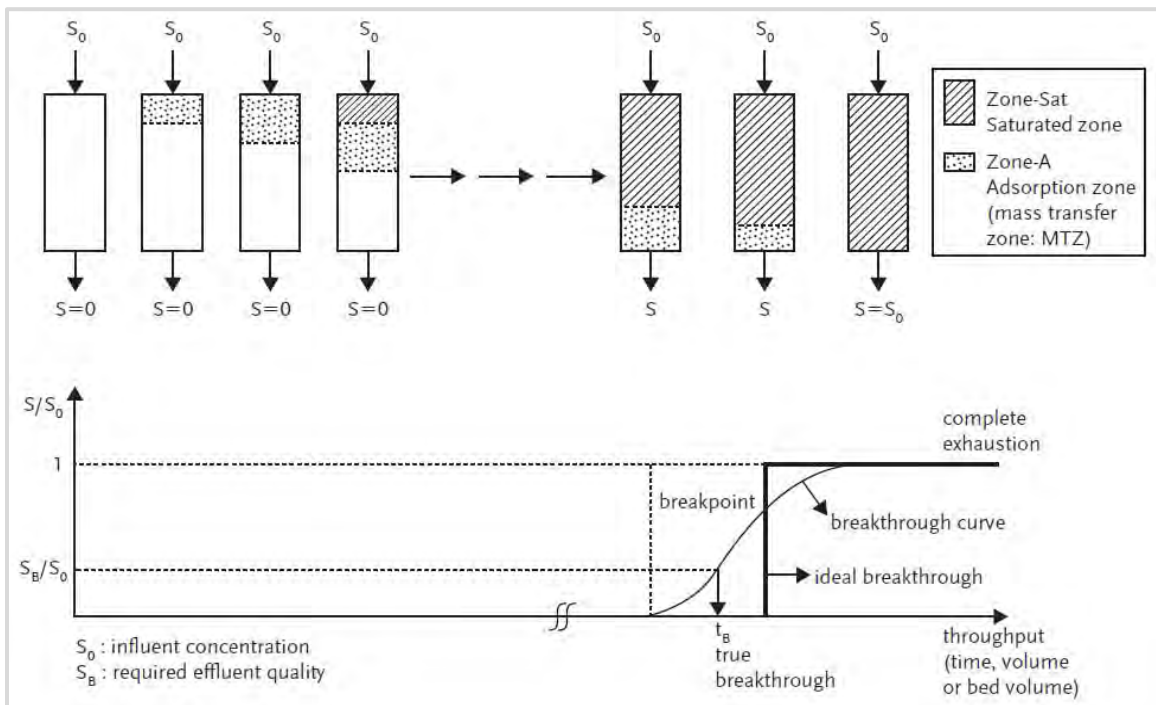


Figure 2-1: Breakthrough Characteristics in a Fixed-bed GAC Adsorber (Cecen, 2012).

CHAPTER 3 LABORATORY SCALE STUDIES

3.1 Introduction

The main objective of this study was to investigate the feasibility of using activated carbon produced from sludge hydrochar via pyrolysis for micropollutant removal from wastewater. The experimental work focused on the production of hydrochar activated carbon (HC-AC), characterization of the HC-AC and commercial coal based granular activated carbon (C-GAC) and assessing the performance and viability of HC-AC against commercial GAC. The relationship between different adsorption parameters and micropollutant removal rates was investigated. The adsorption capacity and removal efficiencies of the HC-AC and GAC were determined for a solution containing Pb (II) ions, a solution containing methylene blue and for wastewater (secondary clarifier effluent) collected from a full-scale biological nutrient removal (BNR) activated sludge plant in South Africa. The removal of selected micropollutants by each adsorbent was evaluated and a comparison of the two adsorbents was carried out.

To assist Municipality A in selecting low-cost adsorbents for planned WR&R schemes, a preliminary evaluation of commercial macadamia nut derived activated carbon (MN-AC) and selected waste wood derived activated carbons was also conducted at pilot scale. Furthermore since HC-AC is in powdered form, commercial coal-based PAC was also evaluated during the pilot scale studies.

This section of the report contains a summary of the procedure adopted for the preparation of the sludge based hydrochar activated carbon and the experimental work procedures followed in the adsorption studies. The experimental procedures were grouped into three main categories:

- Comprehensive characterization of activated carbons (adsorbents)
- Laboratory scale batch tests
- Pilot scale adsorption column tests

Pilot scale adsorption column studies are discussed in detail in Chapter 4.

3.2 Production of Hydrochar

Hydrochar was produced by processing combined primary sludge (PS) and waste activated sludge (WAS) in the enhanced hydrothermal polymerization (EHTP) process, an emerging catalysed hydrothermal carbonization type process (Musvoto et al., 2018). The sludge was obtained from a full-scale biological nutrient removal (BNR) activated sludge plant in South Africa. PS and WAS were collected from primary settling tanks and the dissolved air flotation (DAF) thickening units respectively. A catalyst solution was mixed with a portion of the composite sludge and fed into the EHTP reactor. The contents of the reactor were then heated to a temperature of $210 \pm 5^\circ\text{C}$ at a residence time of 60 minutes. After the set time had elapsed, the reactor was cooled to room temperature and the contents of the reactor (hydrochar and

supernatant) were poured into a container and then separated. The solid portion (hydrochar) was dried and stored.

3.3 Pyrolysis of Hydrochar to Produce Activated Carbon

Prior to pyrolysis, thermogravimetric analysis was carried out on the hydrochar to ascertain its chemical stability and identify the best temperature for pyrolysis. The pyrolysis method in this study was adapted from a procedure published by Saha et al. (2019).

Hydrochar from the EHTP process was pyrolyzed in a Labofurn tubular furnace under inert conditions. Nitrogen gas (N₂) was pumped into the furnace to create these conditions. The hydrochar was pyrolyzed at three different temperatures; 175, 425 and 600°C. A mass of 5 to 6 g of the hydrochar was placed into two ceramic boats which were placed at the centre of a quartz tube that was inserted into the tubular furnace. The tube had an airtight inlet cap and outlet nozzle connected to pipes to allow for the flow of nitrogen gas throughout the pyrolysis process at a volumetric flow rate of 0.1 l/min, to prevent any unwanted combustion or gasification. Nitrogen gas was passed through the quartz tube for a minute before the furnace was turned on to ensure that the atmosphere was inert. The pyrolysis procedure was performed in two steps. In the first step, the furnace was heated from ambient temperature to 100°C at a rate of 10°C/min. The temperature was then maintained at 100°C for 1 min to stabilize the temperature and to ensure the removal of moisture from the hydrochar. In the second step, the furnace was heated from 100°C to the set pyrolysis temperature at a rate of 20°C/min, which was followed by a dwelling time of 60 minutes at the same temperature. Thereafter, the furnace was allowed to cool to room temperature by natural cooling.

Once at room temperature, the nitrogen flow was cut off and the pyrolyzed hydrochar was weighed to ascertain loss of mass due to the pyrolysis process. It was then transferred to a Fisherbrand centrifuge tube and stored in a desiccator until further analyses.

A schematic of a horizontal tube furnace used for pyrolysis is give in Figure 3.1.

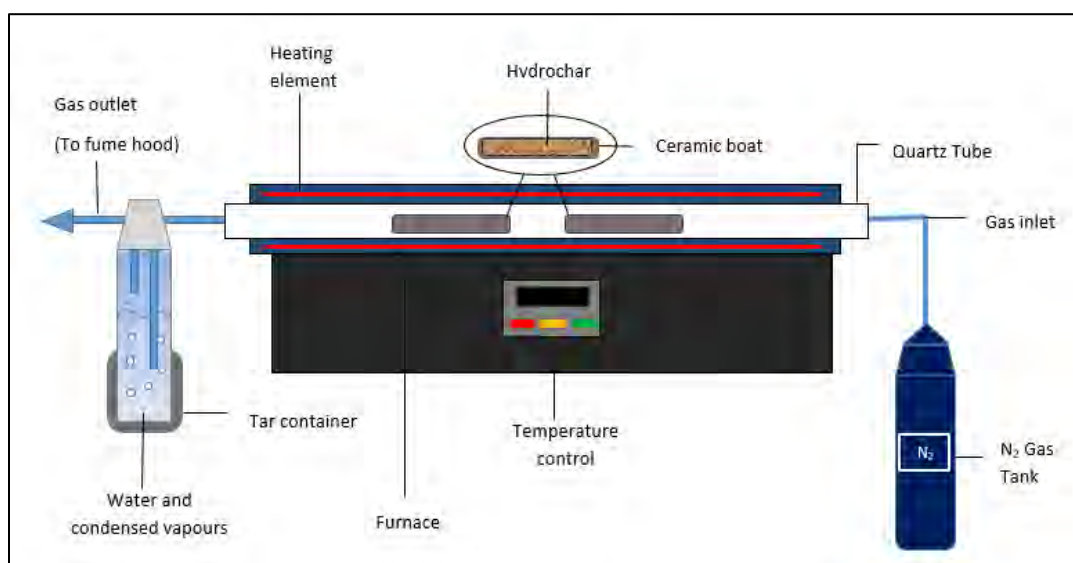


Figure 3.1: Schematic of horizontal tube furnace used for pyrolysis.

Figure 3.2 depicts the thermogram of hydrochar, (HC-PS-WAS).

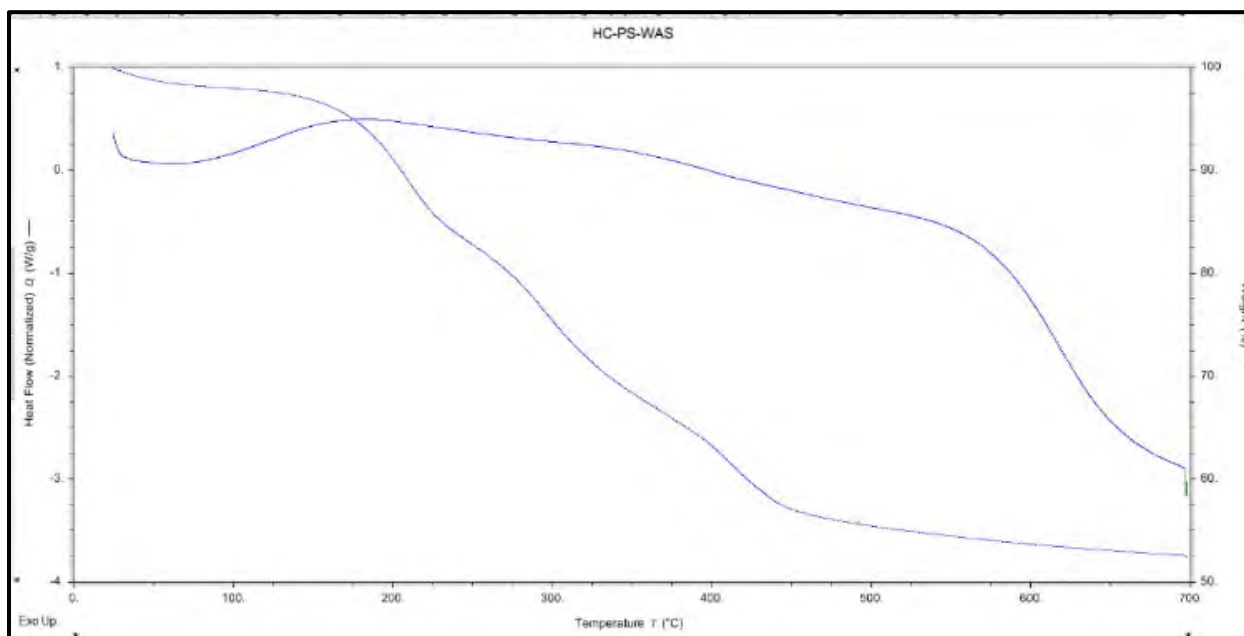


Figure 3.2: Thermogram of HC-PS-WAS

Three distinct steps can be observed from the temporal derivative mass curve in Figure 3.2. The first step from 25-175°C, a steep drop from 200-450°C, followed by a moderate decline from 450°C with the plot becoming constant towards 700°C. The initial step between 25°C and 175°C shows a weight loss of about 6.5% and can be ascribed to the release of moisture and volatile matter and the sharp decline and drastic weight loss of about 41% between 200°C and 450°C is attributed to the decomposition of proteins and low molecular weight polymers. The third and last step showed weight loss of about 2.5% that continued

to 700°C resulting from further decomposition of the hydrochar and formation of ash (De Filippis *et al.*, 2013). Based on the decomposition profile depicted in the TGA (Figure 3.2), three temperatures were chosen and further investigated to produce activated carbon. The percentage weight loss and yield results obtained are displayed in Table 3-1.

Table 3-1: Percentage weight loss and yield

Pyrolysis temperature(°C)	175	425	600
Weight loss (%)	7	43	51
Yield (%)	91	57	49

Figure 3.3 shows (a) hydrochar before pyrolysis, (b) pyrolysed product at 175°C, (c) pyrolysed product at 425°C, and (d) pyrolysed product at 600°C.

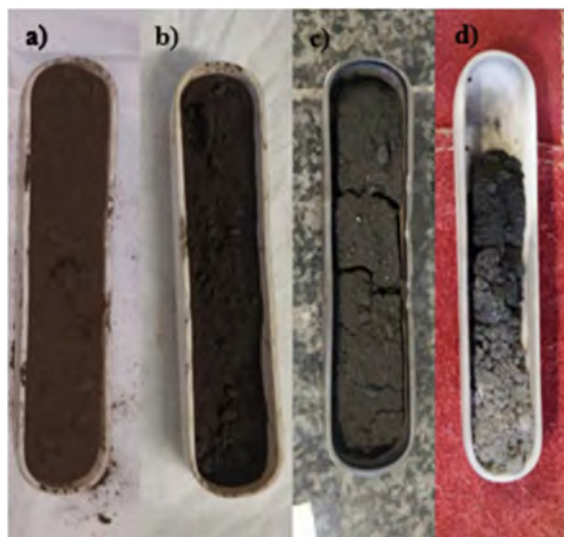


Figure 3.3: Images of hydrochar before annealing and after annealing at different temperatures.

Of the three temperatures, the pyrolyzed product at 600°C had the lowest carbon yield (49.2%) and it showed signs of ashing. As a result, it was excluded from any further investigation. Though the pyrolyzed product at 175°C had a high carbon yield (91%) when compared to that at 425°C (57%), the product resulting from pyrolysis at 425°C was chosen as the best one to be used for the adsorption tests as it had a higher BET surface area and iodine number (97 mg²/g and 111 mg/g respectively) when compared to that at 175°C (88 mg²/g and 74 mg/g respectively). The pyrolyzed product at 425°C referred to as HC-AC was used for further adsorption test work.

3.4 Characterization of Activated Carbons

Characterization tests were conducted on both C-GAC and HC-AC. The activated carbons were tested for moisture content, ash content, iodine number, particle size, attrition, bulk density, pH and surface area.

The moisture content and ash content were determined using the procedure adopted from the European Chemical Industry Council (CEFIC, 1986). The iodine test was conducted as outlined in the American Society for Testing and Materials (ASTM D4607-94, 2006). The particle size distribution was determined as outlined in the American Water Works Association (AWWA B604-74; Comm Rep, 1974). The attrition test was determined as reported by Toles et al. (2000). The bulk density was determined as outlined in ASTM D2854-96 (2000). The pH was determined as outlined in Singh et al. (2017b). Analytical techniques such as scanning electron microscopy (SEM), Fourier-transform infrared spectroscopy (FTIR), energy dispersive X-ray spectroscopy (EDS), Raman spectroscopy, thermogravimetric analysis (TGA), and Brunauer-Emmett-Teller (BET) were used to determine the surface properties and thermal stability of the activated carbons. Results obtained from these tests are summarise in Table 3-2.

Table 3-2: Properties of adsorbents

Parameter	Units	C-GAC	HC-AC
Moisture content	(%)	3.78	3.36
iodine number	(mg/g)	1,198	111
Surface area (BET N ₂)	(m ² /g)	1,050 ^a	97
Particle size	(µm)	850-1,180	75-150
Attrition	(%)	32	-
Bulk density	(g/cm ³)	0.48	0.31
Ash content	(%)	2.4	62.8
pH		5.1	2.6

^a value from supplier

A detailed discussion of the characteristics of C-GAC and HC-AC is presented in Appendix A. While the physical and chemical characteristics of activated carbon can give some insight into the potential adsorption behaviour of the activated carbons, actual adsorption tests with the specific activated carbon and the adsorbates of interest yield the most useful information.

3.5 Adsorption Experiments

Batch adsorption experiments were conducted by mixing a known amount of the adsorbent (C-GAC or HC-AC) with a known volume of an aqueous solution containing adsorbate (methylene blue, Pb (II) ions or WWTP secondary clarifier effluent) of known concentration in a series of 250 ml conical flasks. The mixture was shaken at a constant temperature using an orbital shaker set at 150 rpm for a set period. At pre-selected time intervals, 2 ml of solution were withdrawn from the mixture using a syringe with a needle to minimize the removal of the adsorbent from the flask. The retrieved samples were filtered using a 0.45 µm syringe filter and analysed to determine the residual concentration of the adsorbate in the reaction mixture. The residual concentrations were determined as follows:

a) Methylene blue

The absorbance before and after adsorption was measured using an Ultraviolet visible spectrophotometer (GBC UV-VIS 920) at a wavelength of 663 nm. A narrow width quartz cuvette with dark walls was used for analysis of the samples. The resultant concentration was calculated using the equation obtained from the calibration curve.

b) Lead (II)

The concentration was measured using inductively coupled plasma atomic emission spectroscopy (Varian 710 ICP-OES), which employs the use of a torch and has a nebulizer to generate an argon plasma. The instrument was calibrated with a blank and 1, 5, 10, and 100 ppm LGC 1586 spectra scan multi element standard. The samples were analysed three times and the average reading was taken using a 10% deviation.

Adsorption experiments were conducted by varying initial solution pH, contact time, adsorbent dose and initial adsorbate concentration. Details of the fixed and varied parameters for the experiments used in the adsorption studies are summarised in Appendix A.

The concentration of the adsorbate adsorbed was determined as the difference between the initial and final concentration in the sample solutions. At least two replicates were run in parallel for each experiment and the average values were used for further calculations. The removal efficiency was determined using Equation 3.1

$$\% \text{ Removal} = \frac{C_0 - C_t}{C_0} \times 100 \quad (3.1)$$

Where

- C_0 is the initial adsorbate concentration, (mg/l),
- C_t =the adsorbate concentration at time t, (mg/l).

The term q is defined as the amount of adsorbate adsorbed on a certain amount of adsorbent (mg/g). Adsorption capacity at time t, q_t (mg/g) is expressed as Equation 3.2. The amount of adsorption at equilibrium, q_e (mg/g), is obtained from Equation 3.3.

$$q_t = \frac{(C_0 - C_t)V}{W} \quad (3.2)$$

Where

- C_0 and C_t (mg/L) are the concentrations of the liquid phase of the dissolved substance at the initial time and desired time t, V is the volume of the solution and m is the mass of the adsorbent (g).

$$q_e = \frac{(C_0 - C_e)V}{W} \quad (3.3)$$

Where

- C_e (mg/l) is the adsorbate concentration at the time of equilibrium.

3.5.1 Methylene Blue Adsorption

Methylene blue (MB) is a synthetic cationic dye which is an odourless, dark green powder at room temperature and dissolves in aqueous solutions to form a deep blue colour. Its molecular formula is $C_{16}H_{18}ClN_3S \cdot xH_2O$, and it has a molecular weight of 319.85 g/mol and a peak absorption (λ_{max}) of 663 nm (Khan *et al.*, 2022). Studies of MB adsorption are performed widely to evaluate the mesoporosity of adsorbents and as a model of visual pollution (Bestani *et al.*, 2008). MB is one of the most common pollutants used to evaluate the removal capacity of porous carbon material and other carbons. The adsorption capacity of MB could be an indication of the mesoporous nature because its molecule size is higher than 2 nm (El-Berry *et al.*, 2022).

Effect of pH

The optimum pH for the adsorption process was investigated by varying the pH of the solutions between 2 and 11 using 0.1 M HCL and NaOH solutions. The percentage removal of MB by GAC increased from 97.7% at pH 2 to attain maximum removal of 99.1% at pH 8. This slight increment over the pH range indicates that the adsorbent performed effectively across the pH range studied. However, the sludge derived HC-AC, attained its maximum removal of 99.0% at pH of 11 which was similar to the optimum pH for MB removal reported by Fan *et al.*, (2017). A graphical representation of the results is shown in Figure 3.4

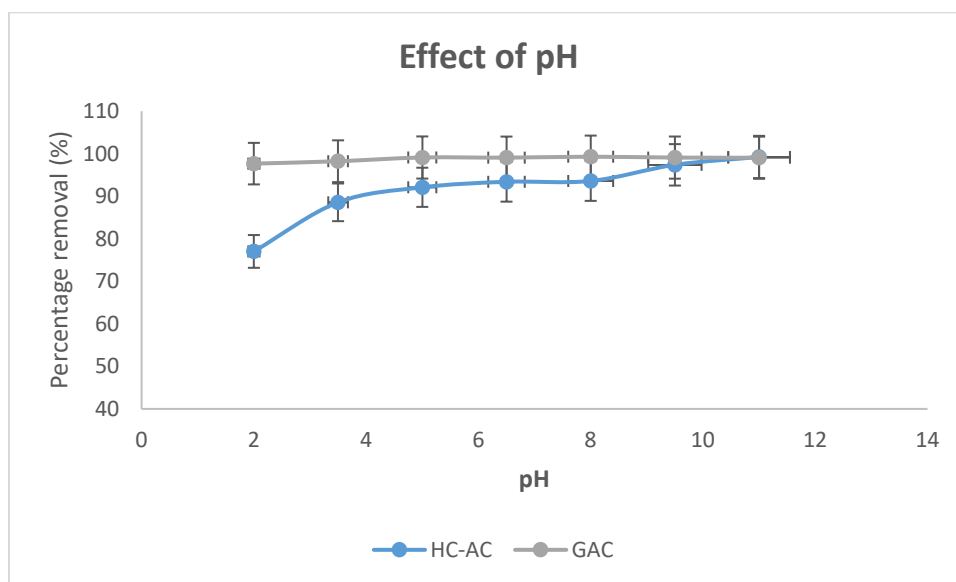


Figure 3.4: Effect of pH on Adsorption of MB (initial concentration: 7.5 mg/L; solution volume: 100 mL, contact time: 130 min for C-GAC, and 280 min for HC-AC; adsorbent dose: 0.2 g/100 mL); pH: 2-11).

The results indicate that the adsorption of MB is more favourable under alkaline conditions. This could be because of the net negative charge that the adsorbent surface develops due to its deprotonation at high pH resulting in the presence of negatively charged functional groups such as the carboxyls and hydroxyls which then enhance the electrostatic attraction between the MB dye and the adsorbent. The reason for the lower removal of the cationic dye in the lower pH range has been attributed to the abundant presence of hydrogen ions which then compete with the dye molecules for vacant active sites (Pirbazari et al. 2014; Singh et al. 2019). Another reason for this observation in the lower pH range has been ascribed to the release of positively charged ions by the cationic dye when it is dissolved in water, leading to electrostatic repulsion between the ions and the positively charged adsorbent, thus lowering removal (Singhet al. 2019; Pathania et al. 2017; Patawat *et al.*, 2020).

The presence of numerous functional groups on the surface of the activated carbons as confirmed by FTIR characterization suggest that the functional groups on the surface of the adsorbent play a large role in the adsorption of MB as they undergo protonation /deprotonation depending on the solution pH. These results also confirm that pH is an important parameter for MB dye adsorption as the removal of MB dye by both HC-AC and GAC changes as the pH of the solution changes.

Effect of Contact Time

The effect of contact time on the adsorption of MB was investigated at time intervals ranging from 5 to 370 min after contact with the adsorbent. The pH was maintained at 6.5. The time required to reach equilibrium was also determined in this phase of the experiments. The effect of contact time on the removal of MB is shown in Figure 3.5.

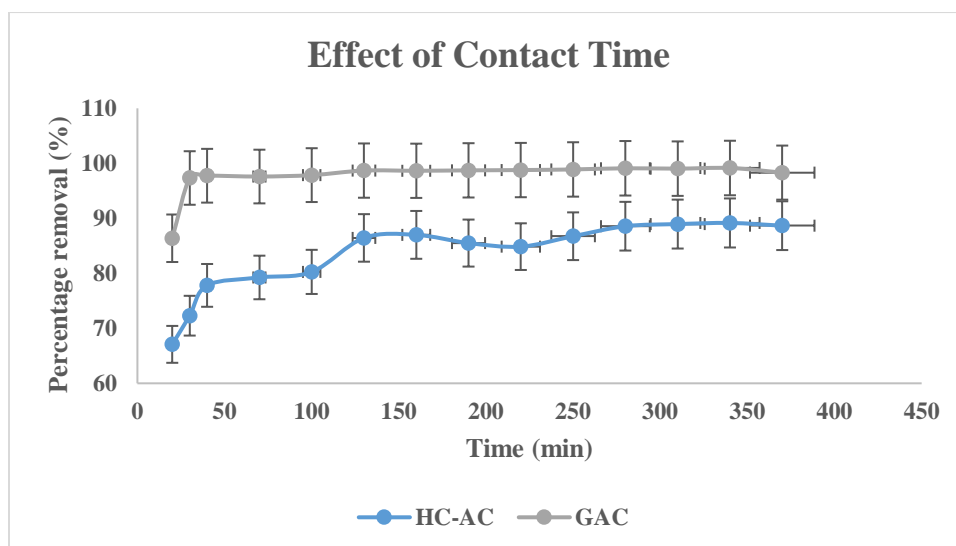


Figure 3.5: Effect of Contact Time on Adsorption of MB (initial MB concentration: 7.5 mg/L; solution volume: 100 mL, contact time: 370 min; adsorbent dose: 0.2 g/100 mL; pH 6.5).

The trends indicate an increase in dye removal with time for both HC-AC and C-GAC, until a certain point when the removal becomes constant. This point is referred to as the equilibrium time and it is described in literature as a state at which the amount of dye being adsorbed onto the activated carbon is equal to the amount being desorbed from the adsorbent. The adsorbent's maximum capacity for adsorption is taken as the quantity of dye adsorbed at the equilibrium time. The rapid rate of MB adsorption during the initial stages might be due to the high solute concentration gradient and the availability of vacant active sites on the adsorbent. Gradually, the number of vacant sites on the adsorbent surface decreases leading to a reduction in the rate of adsorption and constant removal values indicating that the system has reached equilibrium (Singh et al., 2019). The maximum percentage removal was observed around 130 and 280 minutes for C-GAC and HC-AC respectively. These times were taken as the equilibrium times and subsequent optimization experiments were conducted at these times for each adsorbent.

Effect of Adsorbent Dosage

The optimum dosage of the adsorbents was determined by fixing the contact time, initial adsorbate concentration, pH and the volume of solution and varying the amount of adsorbent in each flask. The dose for each adsorbent was varied between 0.1 to 1 g/100 ml (Figure 3.6).

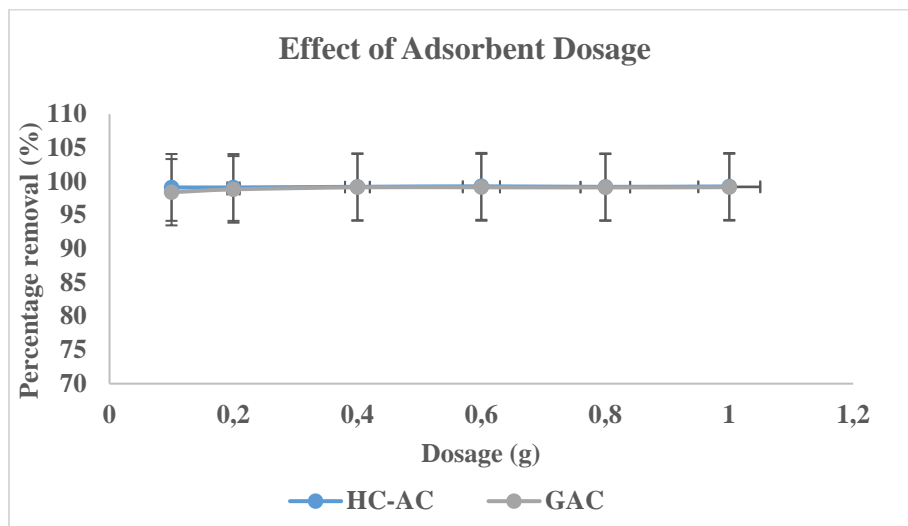


Figure 3.6: Effect of Adsorbent Dosage on Adsorption of MB (initial MB concentration: 7.5 mg/L; solution volume: 100 mL, contact time: 130 min for C-GAC, and 280 min for HC-AC; adsorbent dose: 0.1-1(g/100 ml); pH 8 for C-GAC and pH 11 for HC-AC).

The optimal dosage is useful to estimate the cost of adsorbent to be used for each unit of the solution to be treated. The removal of MB by HC-AC appeared to be almost constant and approached 100% removal over the dosage range, with the highest removal observed at 0.6 g at 99.3%. It can be concluded that removal of MB by HC-AC was more pH dependent than it was on the on the adsorbent dosage. HC-AC

showed slightly higher removal than C-GAC. The removal by C-GAC showed a slight increase from 98.4% at 0.1 g to 99.0% at 0.4 g, with the latter taken as the optimal dose for C-GAC as no significant change in removal was observed beyond 0.4 g. The increase in removal as the dosage increased could be attributed to the availability of sufficient adsorption sites as well as that of specific surface area. However, the lack of significant change in percentage removal past a certain dosage increment has been reported as being the result of adsorbent particle aggregation or the saturation of adsorbent sites by the dye (Pathania et al. 2017, Fan *et al.*, 2017).

Adsorption Kinetics and Capacities

The kinetics for the adsorption of MB by the two adsorbents were investigated for a contact time of 370 minutes using the pseudo-first order and pseudo-second order model equations as described by Tejada-Tovar et al. (2022). The pseudo-second order kinetic model best fitted the kinetic data for C-GAC and HC-AC with R^2 values of 0.999 and 0.9994, respectively. The adsorptive capacity of an adsorbent is a critical parameter that can be used to characterize and compare adsorbents. This value should be obtained by a single-point isotherm study (Raposo et al., 2009). The adsorption capacities and kinetic parameters for C-GAC and HAC are given in Table 3-5. The adsorption capacities (q_e) values for HC-AC and C-GAC for both the pseudo first and second order kinetic models were closely similar and the data also shows that the q_e values for C-GAC and HC-AC (3.9 and 3.4 mg/g, respectively) were close to the calculated q_e values of, 3.9 and 3.5 mg/g respectively. With an R^2 value greater than 0.996 the results also indicate that the rate limiting step of the sorption system is chemisorption (Ho and McKay, 1999a).

Table 3-3: Adsorption Capacities and Kinetic parameters for MB Adsorption onto GAC and HC-AC

Kinetic Model	Parameter	Units	C-GAC	HC-AC
Pseudo-first order	q_e	(mg/g)	0.9917	0.9893
	K_1	min ⁻¹	0.007692	0.003571
	R^2		0.3628	0.3793
Pseudo-second order	q_e	(mg/g)	3.8890	3.5202
	q_e^2	(mg/g)	15.125	12.392
	K_2	min ⁻¹	0.2244	0.0317
	R^2		0.9999	0.9994

Isotherms Studies

Adsorption isotherms represent the relationship between the adsorbate in the surrounding phase and adsorbate adsorbed on the surface of the adsorbent at equilibrium and constant temperature. Adsorption isotherms are crucial to comprehending the mechanism of adsorption by illustrating the interaction between the adsorbate and the surface of the adsorbent and providing information regarding the adsorption capacity at given operating conditions (Yagub et al., 2014; Musah et al., 2022; Tejada-Tovar et

al., 2022). A number of isotherms including Elovich, Freundlich, Langmuir, Redlich-Peterson, and Temkin have been published in literature. The Langmuir (1918) and Freundlich (1906) are the two most widely employed isotherms.

The experimental data of the two adsorbents were analysed using the Langmuir and Freundlich isotherm model equations. The parameters obtained from the analysis showed that the data for C-GAC best fitted to the Langmuir 2 equation with R^2 values of 0.9993. The data for HC-AC showed good high correlation with the Langmuir 1 isotherm equation with an R^2 value of 0.9877. The maximum adsorption capacity (q_{max}) of the GAC and HC-AC were similar at 7.500 and 7,467 mg/g respectively.

The results suggest that sorption onto the two adsorbents was a monolayer operation, and that the isotherm was favourable as the R_L values were within the range of $0 < R_L < 1$ (Hameed, Din and Ahmad, 2007).

Table 3-4: Isotherm Parameters for MB Adsorption onto GAC and HC-AC

Adsorption isotherm	Parameters	Unit	C-GAC	HC-AC
Langmuir 1	q_{max}	(mg/g)	8.4965	7.4667
	K_L	min^{-1}	72.1903	55.7512
	R_L		0.0018	0.0024
	R^2		0.9982	0.9877
Langmuir 2	q_{max}	(mg/g)	7.5001	-1.3225
	K_L	min^{-1}	56.2520	1.7490
	R_L		0.0024	0.0708
	R^2		0.9993	0.8094
	R^2		0.9942	0.9503

3.5.2 Lead (II) Adsorption

Lead (Pb) is a chemical element with an atomic number of 82. Its presence in the aqueous environment is due to its release from natural sources (mineral deposits) as well as untreated effluent from industrial activities (e.g. manufacture of lead-acid batteries, solders and alloys). It is widely used due to its important physio-chemical properties such as resistance to corrosion, poor conductivity and malleability. Consequently, it is a persistent poison that is not biodegradable and accumulates in the environment as well as the human body where it affects multiple body functions such as neurodevelopment in children, fertility, and cardiovascular function leading to death. Its main channels of entry into the human body are via the ingestion of food or water that are contaminated with lead. Due to its toxicity at low concentrations the World Health Organization and the South African National Standard (SANS) have set the guideline value for lead in drinking water at 10 $\mu g/l$ (Herschy, 2012; SANS 241, 2015).

For the adsorption studies, working concentrations were prepared for the adsorption tests by diluting the prepared stock solution containing the Pb (II) ions with deionized water. The concentrations of the solutions were determined using Inductively Coupled Optical Emission Spectroscopy (ICP-OES). The effect of pH, adsorbent dosage, initial concentration and contact time were investigated using the same procedures as for the MB adsorption studies. The fixed and varied parameters for the experiments are summarised in Appendix A. Adsorption kinetics and adsorption isotherms studies were conducted.

Effect of pH

The solution pH is a crucial parameter in adsorption as it not only facilitates the removal of lead by adsorption by influencing the properties of the metal ion, but also plays a significant role by influencing the surface charge of the adsorbent (Kavand et al. 2020; Mandal *et al.*, 2021). The effect of pH on the removal of Pb (II) by the two activated carbons is shown in Figure 3.7.

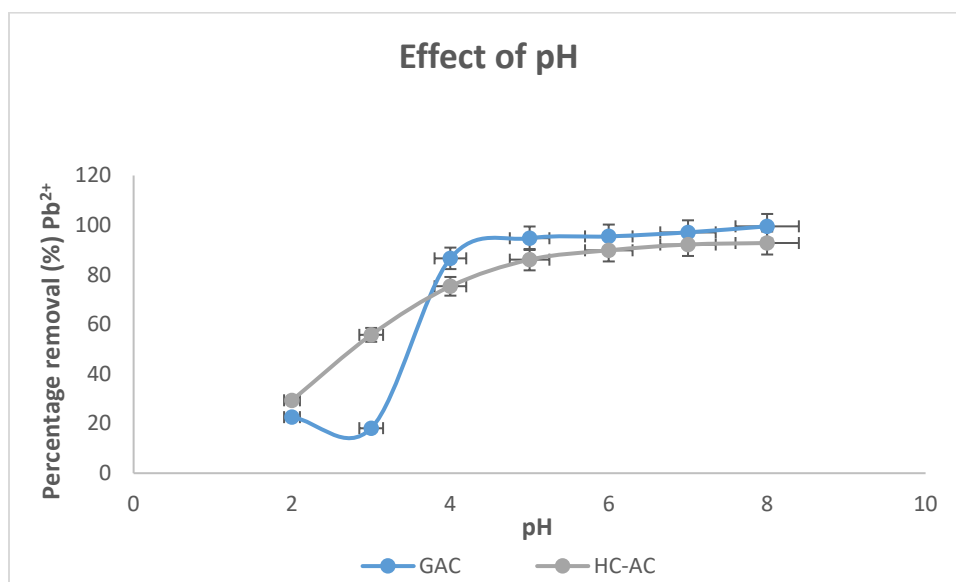


Figure 3.7: Effect of pH on the adsorption of Pb (II) ions (initial Pb (II) concentration: 5.3 mg/L; solution volume: 100 mL, contact time: 120 min; adsorbent dose: 0.2 g/100 mL); solution pH: 2-8).

Removal of Pb (II) was lowest in the low pH range (pH 2-4). This has been widely discussed in literature and is attributed to the competition for active sites by the Pb^{2+} ions and the H^+ ions which are highly concentrated in acidic environments. The gradual increase in pH saw an increase in adsorption of Pb (II), owing to the negative charge of functional groups present on the surface of the adsorbents which made them readily available for lead adsorption (Guyo and Moyo, 2017 Kavand et al. 2020). A pH of 7 was taken as the optimal value to attain maximum Pb (II) adsorption for both adsorbents, as it is believed that pH values greater than 7 facilitate the precipitation of Pb ions into hydroxide species (Alghamdi *et al.*, 2019; Kavand et al. 2020; Mohan *et al.*, 2020; Mandal *et al.*, 2021). It is also reported in the literature that high Pb removal (above 90%) are achieved. Treatment of wastewater at a neutral pH is also preferred because

it is more economical compared to treatment at higher pH with only marginal gains in Pb removal and an increased risk of hydroxide precipitation.

Effect of Adsorbent Dosage

The use of the optimum dosage of the adsorbent during the adsorption process is crucial for the effective uptake of the Pb (II) ions as it ensures the availability of active sites that the ions have access to (Tejada-Tovar *et al.*, 2022). Figure 3.8 shows how the removal efficiency of Pb (II) ions varied with adsorbents dosage for C-GAC and HC-AC.

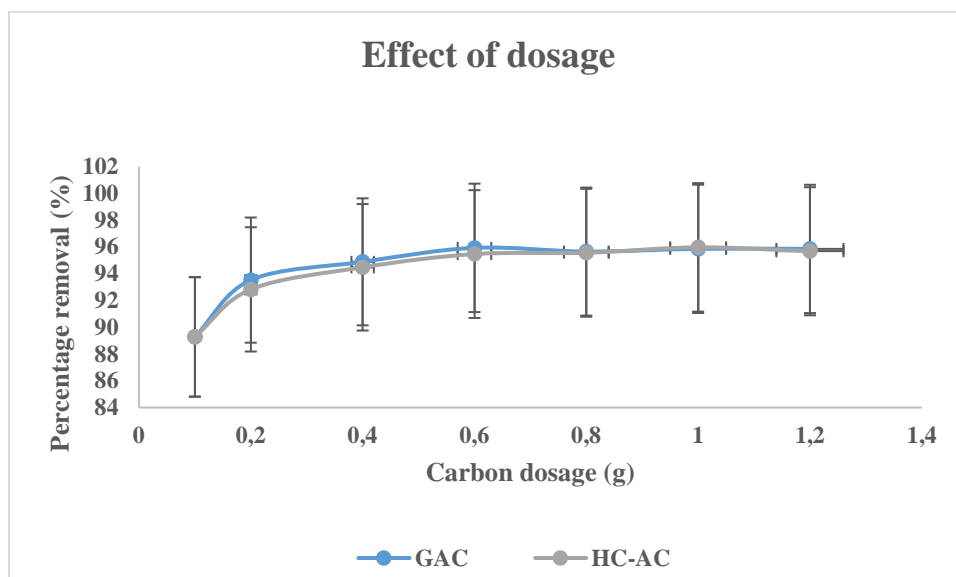


Figure 3.8: Effect of Adsorbent Dosage on the Adsorption of Pb (II) ions (initial concentration: 5.3 mg/l; solution volume: 100 ml, contact time: 120 min; adsorbent dose: 0.1-1 g/100 ml; solution pH: 7).

As the adsorbent dosage increased from 0.1 to 0.6 g, the percentage removal of the Pb (II) ions increased from 89.3 to 95.9% for C-GAC and 89.3 to 95.5% for HC-AC. This shows that the removal rate increased as the dosage of adsorbent increased. This phenomenon can be attributed to the increased availability of active sites or surface area, for the same quantity of adsorbate molecules, which facilitates better access for the Pb (II) ions onto the activated carbons adsorption sites. Subsequent increases in adsorbent dosage after 0.6 g for C-GAC and HC-AC did not result in significant increases in the percentage removal of the Pb (II) ions. This could be attributed to the overcrowding of adsorbent particles present in the solution, causing the adsorption sites to overlap (Onwordi *et al.*, 2019, Mandal *et al.*, 2021).

Effect of Contact Time

Adsorption tests were conducted at a contact time ranging from 10-150 minutes under optimal conditions (pH 7, adsorbent dosage of 0.6 g for C-GAC and HC-AC and initial concentration of 9.1 mg/l). The effect of the contact time on the percentage removal of lead is displayed in Figure 3.9.

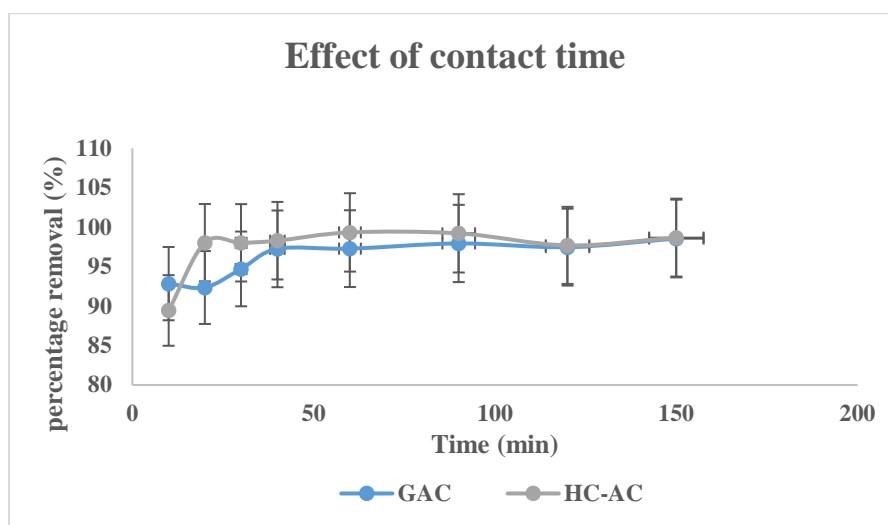


Figure 3.9: Effect of contact time on the adsorption of Pb (II) ions (initial Pb(II) concentration: 9.1 mg/L; solution volume: 100 mL, contact time: 150 min; adsorbent dose: 0.6 g for C-GAC and HC-AC, 0.8 g for AW-AC; solution pH: 7).

The adsorption was rapid in the initial stages. In the first 30 minutes C-GAC achieved a removal of 94.7%, while HC-AC achieved 98.0%. This observed trend showing rapid removal in the initial rate of adsorption may have been accelerated by the presence of a sufficient number of active functional groups and vacant active sites on the activated carbons exterior surface. It could also be explained as being a result of the concentration gradient between the adsorbate in solution and the quantity of vacant sites on the surface of the adsorbent. C-GAC reached equilibrium faster than HC-AC. From 40 minutes to 150 minutes the change in removal percentage was almost constant with a slight inflection at 150 minutes, indicating that equilibrium had been achieved. HC-AC showed a slight decrease in uptake after 90 minutes which could be as a result of the saturation of the active sites after equilibrium has been reached. The increment of contact time after this point has been linked to a decrease in percentage removal due to reduction in available Pb (II) ions to bind to the remaining active sites (Moyo *et al.*, 2013; Guyo and Moyo, 2017 ; Onundi *et al.*, 2010; Mandal *et al.*, 2021).

Adsorption Kinetic and Capacities

The kinetics for the two adsorbents were investigated using the pseudo-first order and pseudo-second order model equations. The parameters obtained from the plots of the equations are listed in Table 3-5. The parameters of the two models were compared and it was found that the kinetic data was best suited to the Pseudo-second order (PSO) model for C-GAC and HC-AC. The R^2 values were 0.9999 for both adsorbents and the calculated q_e values for C-GAC and HC-AC were the same at 1.5 mg/g respectively. The calculated values were close to the experimental values which were both, 1.50 mg/g. This indicates that the correspondence between the PSO and the adsorption of the Pb (II) ions onto the adsorbents is

high. With, an R^2 value greater than 0.996 is suggestive of chemisorption being the rate limiting step of the adsorption process (Ho and McKay, 1999a).

Table 3-5: Kinetic Parameters for Pb(II) ions onto C-GAC and HC-AC

Kinetic model	Parameter	Units	C-GAC	HC-AC
Pseudo-first order	qe	(mg/g)	0.3413	0.9949
	K ₁	min ⁻¹	0.0111	0.0167
	R ²		0.683	0.2443
Pseudo-second order	qe	(mg/g)	1.501	1.499
	qe ²	(mg/g)	2.254	2.247
	K ₂	min ⁻¹	0.635	2.262
	R ²		0.9999	0.9999

Isotherm studies for the Adsorption of Lead (II) ions

Similar to MB, the experimental data of the two adsorbents were analysed using the Langmuir and Freundlich isotherm model equations. The modelled parameters are listed in Table 3-6.

Table 3-6: Isotherm Parameters for the Adsorption of Pb (II) Ions onto GAC and HC-AC

Adsorption isotherm	Parameters	Unit	C-GAC	HC-AC
Langmuir 1	q _{max}	(mg/g)	1.5360	24.0693
	K _L	min ⁻¹	2.3592	579.3293
	R _L		0.0407	0.0002
	R ²		0.7835	0.0023
Freundlich	n	(mg/g)	0.5725	2.3823
	K _f	(mg/g)	12.0749	1.4372
	R ²		0.7824	0.1643

The analysis of the experimental results using the Langmuir and Freundlich isotherms showed that the data for C-GAC had a similar fit for both the Langmuir 1 and Freundlich isotherms ($R^2 = 0.7835$ and 0.7824 respectively), with the best fit being with the Langmuir 1 isotherm. The R^2 value for HC-AC was generally low for both isotherms with the R^2 value for the Freundlich being the higher value at 0.164. These results suggest that there was monolayer coverage of the adsorbate on C-GAC while the coverage on HC-AC may be multilayer in nature.

3.5.3 Multi-Metal Adsorption Studies using Wastewater from BNR Plant

Once the optimum adsorbent dosage was determined, further batch adsorption experiments were carried out to evaluate the adsorption of Pb (II) and other heavy metals from a solution containing various metals and other organic contaminants. Effluent from the secondary clarifiers at the case study BNR activated sludge plant was used in the laboratory scale adsorption studies. The effluent was collected prior to chlorination. The same adsorption test procedure used for MB and Pb (II) was applied.

The effect of contact time and the adsorbent dosage on percentage pollutant and the adsorption capacity was investigated. The adsorption capacity for C-GAC and HC-AC and percentage removals for the identified heavy metals are given in Table 3-7. The performance of HC-AC and C-GAC was closely similar for all elements except for Fe where C-GAC exhibited a significantly higher adsorption capacity. The order of adsorption was Fe > Ni > Mn > Zn for C-GAC and Fe > Ni > Zn > Mn for HC-AC.

Table 3-7: Summary of Adsorption Capacities and % Removals-Laboratory Scale Studies

Laboratory Scale Studies				
Heavy Metal	Adsorption Capacity (mg/g)		% Removal (%)	
	HC-AC	C-GAC	HC-AC	C-GAC
Iron	47.2	63.1	78	78
Manganese	25.7	26.6	57	67
Nickel	16.8	15.8	73	69
Zinc	6.6	8.2	67	64

3.6 Summary and Discussion

The results from the study suggest that hydrochar derived from wastewater sludge could be converted successfully to activated carbon (HC-AC) which is effective in removing both MB and Pb (II) ions as model micropollutants from aqueous solution. Under optimum conditions, (pH, adsorbent dosage, initial solute concentration and equilibrium time). HC-AC performed better than C-GAC, thereby suggesting its potential application as a cost-effective alternative adsorbent for removal of heavy metals from wastewater effluent in support of wastewater reclamation and reuse. The following conclusions were drawn from the laboratory tests:

- Activated carbon was successfully produced by pyrolysis of hydrochar derived from a combination of primary sludge and waste activated sludge at 425°C under a nitrogen atmosphere with no further activation.
- HC-AC exhibited the lowest microporosity as determined by its low iodine number. However, it showed an abundance of oxygen and sufficient oxygen functional groups which were attributed to its high removal of MB dye and Pb (II) ions

- Removal of the MB dye and Pb (II) ions is largely dependent on the pH of the solution. The highest percentage removal for both pollutants was achieved under alkaline conditions. The optimum pH for MB adsorption was 8 for C-GAC and 11 for HC-AC. The optimum pH for the adsorption of Pb (II) ions was 7 for the two activated carbons.
- Removal of MB by HC-AC and C-GAC was similar (at 99.2% and 99.1% respectively). For the Pb (II) adsorption tests HC-AC performed slightly better than C-GAC, achieving a removal of 99.3% and 97.2% respectively.
- The analysis of the experimental results using the Langmuir and Freundlich isotherms show that the data for C-GAC had a similar fit for both the Langmuir 1 and Freundlich isotherms ($R^2 = 0.7835$ and 0.7824 respectively). The R^2 value for HC-AC was generally low for both isotherms with the R^2 value for the Freundlich being the higher value at 0.164 . These results suggest that there was monolayer coverage of the adsorbate on the adsorbent C-GAC, while the coverage on HC-AC was multilayer in nature.
- In the mono-metal adsorption of Pb (II) ions, removal efficiency was almost 100% for both C-GAC and HC-AC. The maximum removal capacity of Pb (II) was 1.5 mg/g for both C-GAC and HC-AC which was equivalent to 99% removal.
- In the multi-metal adsorption studies using secondary clarifier effluent collected at a full-scale BNR activated sludge plant, although Pb (II) was present in low concentrations, removal was however still detected. The evaluation and comparison of the adsorptive capacity of the adsorbents for various metal pollutants was limited to Fe, Mn, Ni and Zn, regulated metals from SANS 241 which were present in detectable amounts in the effluent.
- The adsorption experiments using secondary clarifier effluent showed an order of adsorption of $\text{Fe} > \text{Mn} > \text{Ni} > \text{Zn}$ for both C-GAC and HC-AC.

In conclusion, the batch adsorption studies discussed in detail in this Chapter comprised of different experiments focused on determining the adsorption kinetics and isotherms using methylene blue, Pb (II) ions and wastewater effluent collected from a full-scale BNR activated sludge plant. The MB adsorption studies provided baseline information on the adsorption properties of the two adsorbates C-GAC and HC-AC. The Pb (II) adsorption studies were carried out to determine the adsorption kinetics and isotherms for both C-GAC and HC-AC using Pb (II) ions as an indicator metal. Pb was selected as an indicator metal in this study because it is one of the most toxic heavy metal pollutants that is most likely to be encountered in wastewater receiving industrial effluent.

The first stage of the laboratory scale experiments provided information on the optimum conditions for the adsorption of Pb (II) ions on both adsorbents. Once the optimum adsorbent dosage was determined, further batch adsorption experiments were carried out to evaluate the adsorption of Pb (II) and other heavy metals from a multi-metal solution using secondary clarifier effluent from a full-scale WWTP.

In the multi-metal adsorption studies using wastewater effluent, Pb (II) was present in low concentrations. However, removal of Pb (II) was still detected. The evaluation and comparison of the adsorptive capacity of the adsorbents for various metal pollutants were limited to heavy metals that were present in higher concentrations and regulated in SANS 241, i.e. Fe, Mn, Ni and Zn.

The findings from the laboratory studies provided the baseline information, that was used in setting up the small pilot scale adsorption studies. A small pilot scale column rig was setup at the same full-scale BNR activated sludge plant where effluent for the laboratory scale adsorption tests was collected. The test assessed the performance of the activated carbons in removing heavy metals regulated in SANS 241 and selected endocrine disrupting compounds (carbamazepine, Bisphenol A and Triclosan) from secondary clarifier effluent. Details of the pilot scale study are given in Chapter 4.

CHAPTER 4 PILOT SCALE ADSORPTION STUDIES

4.1 Introduction

Before installing full-scale continuous packed bed column adsorption plants, it is recommended that the systems be evaluated at small scale. This is particularly important when using new adsorbents and/or treating solutions with multiple contaminants such as wastewater effluent. Currently there is a gap in the application of fixed bed columns for adsorption in continuous systems despite several research studies investigating the application of biosorption at higher scale in continuous systems, being conducted over the years. (Ramrakhiani et al. 2016; Martín-Lara et al. 2017). Therefore, pilot scale adsorption studies are required to demonstrate acceptable removal efficiencies before plant scale up can be carried out. Rapid small scale column tests (RSSCTs) and pilot scale adsorption columns are generally used to evaluate and predict adsorption media performance before scaling up. Using information collected from laboratory adsorption studies, a small pilot scale column rig was setup at a full-scale BNR activated sludge plant to assess the performance of the activated carbons in removing heavy metals regulated in SANS 241-1:2015.

4.2 Design of Pilot-Scale Adsorption Columns

The design of the pilot scale adsorption columns was based on recommended design and operation parameters for granular activated carbon filters from Cecen, (2012). A summary of these parameters is given in Table 4-1. Four identical adsorption columns running in parallel and operating in continuous mode were setup. The four columns enable testing of four activated carbon materials at a time. The design and operating parameters are summarised in Table 4.2 while Figure 4-1 shows the adsorption column rig assembly.



Figure 4-1: Pilot Scale Adsorption Column Rig before Installation at BNR Activated Sludge Case Study Plant

Table 4-1: Typical Values for Design and Operation in GAC filters (Cecen, 2012)

Parameter	Unit	Range
Empty bed Contact time (EBCT)		
General	min	10-50
Typical	min	30
Water treatment	min	5-30
Tertiary treatment of municipal wastewaters	min	17-50
Physicochemical treatment of municipal wastewater	min	20-66
Industrial wastewater treatment	min	30-540
Hydraulic loading rate, HLR		
General	m/h	5-25
Typical	m/h	12
Water treatment	m/h	5-15
Tertiary treatment of municipal wastewaters	m/h	7-16
Physicochemical treatment of municipal wastewater	m/h	-6-15
Carbon Usage Rate (CUR)		
Tertiary treatment of municipal wastewaters	kg/ m ³	0.12-0.23
Physicochemical treatment of municipal wastewater	kg/ m ³	0.29-1.04
Typical values of GAC bed		
Bed Volume, VB	m ³	10-50
Cross-sectional area, A	m ²	5-30
Length, L _B		
General	m	3-9
Water treatment	m	1.8-4
Tertiary treatment of municipal wastewaters	m	3-10
Physicochemical treatment of municipal wastewater	m	2.7-11
Void fraction in GAC bed, ε _B	m ³ / m ³	0.3-0.6
Apparent filter density, ρ _B	kg solids/ m ³ bed	430-480
GAC particle density, ρ _P	kg solids/ m ³ bed	0.92-1.5

Table 4-2: Design and operating parameters of adsorption columns

Parameter	Unit	Range
No. of Columns		4
Diameter	m	0.16
Height of column	m	1,75
Height of bed	m	1.23
Area (X-section)	m ²	0.0201
Empty bed Contact time (EBCT)	min	18
Hydraulic loading rate, HLR	m/h	5-12
Flowrate, Q	l/min	1.7-4

4.3 Small-scale Pilot Column Adsorption Tests

The column tests were carried out in two phases. The first phase was conducted while the production of hydrochar was in progress. The first column was filled with commercial coal-based GAC (C-GAC) that was used in the laboratory studies. To assist Municipality A with options for adsorbents to use in WR&R schemes the other 3 columns were filled with ACs derived from renewable sources as follows

- Commercial GAC from macadamia nuts (MN-GAC)
- Activated carbon produced from pyrolysis of waste alien wood (AW-AC) and pinecone (PC-AC)

In the second phase, two columns were operated, one filled with sludge derived hydrochar AC (HC-AC) that was used in the laboratory studies and the second filled with commercial coal based powdered activated carbon (PAC). PAC was selected because of its fine particles size similar to HC-AC. The pilot scale studies therefore enabled the performance of HC-AC to be compared with both conventional coal-based GAC and PAC.

The columns were fed with secondary settling tank (SST) effluent from the three SSTs, collected from the combined effluent channel. The flowrate to each column was constant at 1.7 l/min. The columns were run continuously for a period of 3 days. Three days was found to be the maximum period the columns could be operated before clogging from residual solids in the SST effluent. Samples were collected from the inlet and outlet of the columns over the duration of the test. Influent samples (SST effluent) were collected from the common influent feed tanks and effluent samples were collected from the exit tubing from each column. All collected samples were preserved and transported to the laboratory for analysis. The samples were analysed for mostly heavy metals. However, in the first phase of the tests some selected endocrine disrupting compounds were also analysed.

A wide range of heavy metals were analysed for in the samples collected during the column tests. However, the discussion of results in this report is focused on heavy metals that form part of the determinands monitored in the SANS 241-1:2015 potable water standards, which were present in relatively high concentrations. Iron (Fe), manganese (Mn), nickel (Ni) and zinc (Zn) were present in the SST effluent fed to the columns in relatively higher concentrations than lead (Pb). Zn, Ni and Fe average concentrations in the effluent exceeded the SANS 241 limits. Pb was present in very low concentrations and at times the concentrations were below the limit of detection of the analysis method applied by the laboratory.

Similarly, a wide range of EDCs were tested for in the SST effluent feed during the first phase of the experiments. A few selected compounds (carbamazepine, diclofenac, bisphenol A, caffeine and triclosan) were the only compounds found to be above the detection limits.

Table 4-3 shows the SANS 241-2015 standard limits for heavy metals and the SST effluent average concentration.

Table 4-3: Comparison between SST Effluent Average Concentrations and SANS 241-2015 Standard Limits

Parameter	Unit	Risk	SANS 241-2015 Standard Limit	SST Effluent Average Concentration	Comments
Sodium	µg Na/ℓ	Aesthetic	≤200		Not measured in SST effluent
Antimony	µg Sb/ℓ	Chronic Health	≤20		
Cyanide	µg CNI/ℓ	Acute Health	≤200		
Aluminium	µg Al/ℓ	Operational	≤300	33	SST effluent average concentration was below SANS 241-2015 limit
Arsenic	µg As/ℓ	Chronic Health	≤10	1	
Boron	µg B/ℓ	Chronic Health	≤2,400	77	
Barium	µg Ba/ℓ	Chronic Health	≤700	26	
Cadmium	µg Cd/ℓ	Chronic Health	≤3	1	
Total Chromium)	µg Cr/ℓ	Chronic Health	≤50	3	
Copper	µg Cu/ℓ	Chronic Health	≤2,000	3	
Iron	µg Fe/ℓ	Chronic Health	≤2,000	313	
		Aesthetic	≤300	1	SST effluent average concentration for Fe was above the aesthetic SANS 241-2015 limit
Mercury	µg Hg/ℓ	Chronic Health	≤6	1	SST effluent average concentration was below SANS 241-2015 limit
Manganese	µg Mn/ℓ	Chronic Health	≤400	92	
		Aesthetic	≤100	86	
Nickel	µg Ni/ℓ	Chronic Health	≤70	86	SST effluent average concentration was above SANS 241-2015 limit
Lead	µg Pb/ℓ	Chronic Health	≤10	1	SST effluent average concentration was below SANS 241-2015 limit
Selenium	µg Se/ℓ	Chronic Health	≤40	1	
Uranium	µg U/ℓ	Chronic Health	≤30 effluent	1	SST effluent average concentration was above SANS 241-2015 limit
Zinc	µg Zn/ℓ	Aesthetic	≤5	19	

4.3.1 Phase 1 Adsorption Column Tests Results

Adsorption of Heavy Metals

Figure 4-2 to Figure 4-5 show the measured concentrations in the effluent from the adsorption columns over the course of the experiment. Graphical representations of the results for the other heavy metals are given in Appendix B. The graphs show the rate of heavy metal adsorption during the first 180 minutes of the experiment. During this period, the adsorption rate follows an upward trend. However, with time, due to the decrease in the number of active sites on the adsorbent, the rate gradually decreases until it reaches a fixed value. This occurred after running the experiment for approximately 24 hrs (1,440 mins). Beyond this point, the heavy metal concentrations in the column effluent samples start to increase due to the exhausted adsorptive capacity of the ACs.

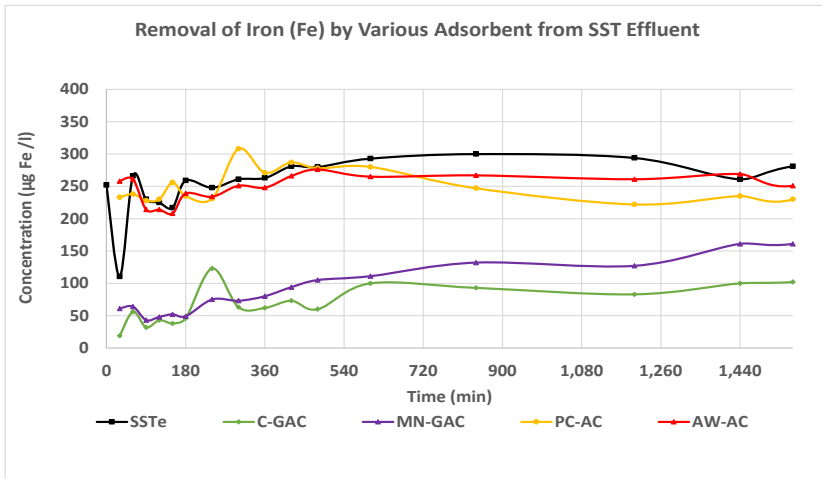


Figure 4-2: Removal of Iron from SST effluent by various adsorbents

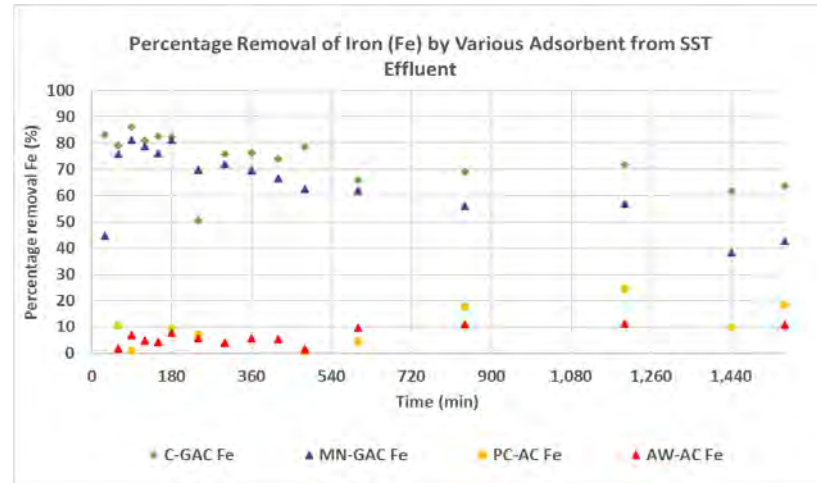


Figure 4-3: Percentage removal of Iron from SST effluent by various

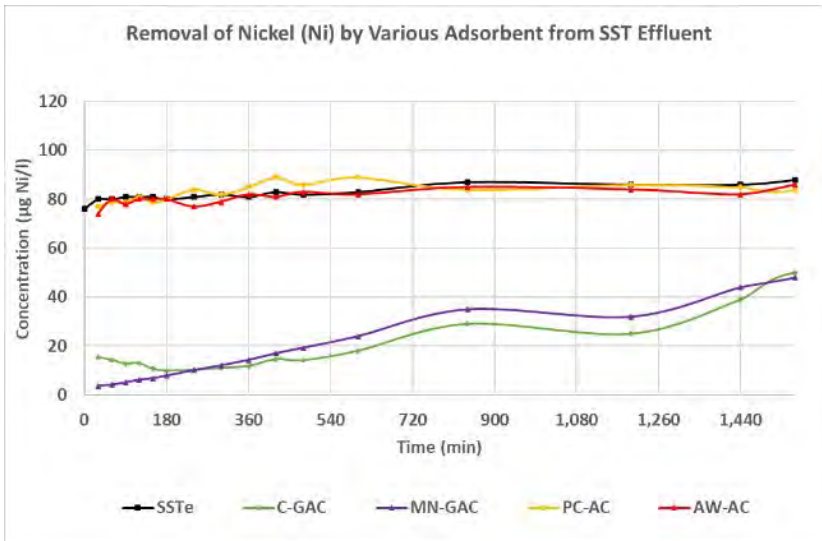


Figure 4-4: Removal of Nickel from SST effluent by various adsorbents

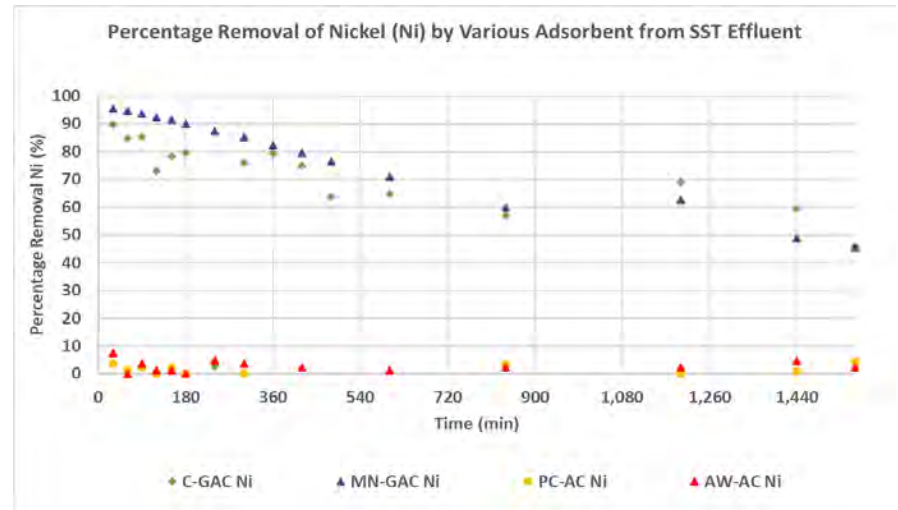


Figure 4-5: Percentage removal of Nickel from SST effluent by various

Data from the laboratory analysis was used to calculate the maximum adsorption capacities and percentage removal of the four selected heavy metals by each AC. A summary of these results is given in Table 4-4.

Table 4-4 Summary of Adsorption Capacities and Percentage Removals for Selected Heavy Metals in SST Effluent

Heavy Metal	C-GAC		MN-GAC		PC-AC		AW-AC	
	Adsorption Capacity (mg/g)	% Removal (%)						
Iron	43.6	84	38.7	81	3.6	24	51.4	90
Manganese	13.7	87	14.8	93	13.7	78	1.8	24
Nickel	12.2	81	14.6	95	*	*	14.7	77
Zinc	2.9	81	2.4	75	1.0	53	4.1	97

*no removal of heavy metal by adsorbent

The following was noted, from the results of the 3-day experimental run:

- C-GAC achieved removal for all the selected heavy metals (Fe, Mn, Ni and Zn). Percentage removals for Zn were $\geq 90\%$, while percentage removals for the rest of the heavy metals were between 55% and 88%.
- MN-GAC also achieved removal for all the selected heavy metals. Percentage removals for Mn and Ni were $\geq 90\%$, while percentage removals for the Fe and Zn were between 55% and 80%.
- PC-AC exhibited lower percentage removals (11-21%) for Fe and Ni. Improved percentage removals of 82% and 53% were recorded for Mn and Zn respectively.
- AW-AC exhibited very low percentage removals (7-47%) for most of the heavy metals. The highest percentage removal was for Mn at of 65%.

The results indicate that the waste wood derived ACs exhibited very low removal efficiencies for the selected heavy metals. Commercial macadamia nuts GAC (MN-GAC) performed as well as coal-based GAC (C-GAC).

The low removal efficiencies by the waste wood derived ACs is most likely due to poor activation during pyrolysis and grading as discussed in Appendix C.

Break through Curve Analysis-Heavy Metals

Breakthrough curve analysis is required for the successful design of adsorption columns (Han et al., 2006). The prediction of column breakthrough determines the operating lifespan of the bed. The breakthrough curves were obtained by plotting the dimensionless ratio, C_t/C_i defined as the ratio of effluent adsorbate

concentration, C_t (mg/l), to inlet adsorbate concentration, C_i (mg/l), as a function of time for a given bed height, giving a breakthrough curve. The breakthrough point is usually defined as the point when the ratio C_t/C_i becomes 0.05 to 0.90 (Chowdhury et al., 2015).

In industrial scale applications the adsorbent from the column is usually replaced when the C_t/C_i ratio is equal to 0.5, i.e. 50% breakthrough point. After the 50% breakthrough point, the column can still operate until the ratio C_t/C_i becomes 0.9 which is defined as the operating limit of the column. The column becomes completely exhausted when the pre-determined inlet concentration is almost equal to the outlet concentration.

Since there was no consistent heavy metal removal by waste wood activated carbons PC-AC and AW-AC, the breakthrough curves for these adsorbents did not display the expected characteristic graphs and the results were therefore not further analysed. Figure 4-2 to Figure 4-13 show the breakthrough curves for C-GAC and MN-GAC respectively. The 50% breakthrough point and the operating limit of each column are indicated on the plots.

The characteristic S-like shaped sigmoidal graphs were obtained (though not well defined) in the study for C-GAC and MN-GAC. The deviation of the breakthrough curves for C-GAC and MN-GAC from the characteristic S-shape was attributed to the following:

- Since wastewater contains various heavy metals, the adsorption process is more complex than that for single metal adsorption. When several heavy metals are present in solution, interference and competition phenomena for sorption sites may occur for the limited number of available binding sites. Furthermore, when the column capacity is approached, a species with a lower affinity is pushed off by other species with higher affinity and displacement of the species may occur (Trujillo et al., 1991).

The breakthrough curve for competing sorbates may also display C_t/C_i values greater than 1. This is referred to as overshooting and it occurs in different sorbents such as activated carbons (Mohan and Chan-der, 2001; Barros et al., 2013). Overshooting depends on the selectivity of the sorbent, the sorption mechanism and on the operational conditions of the adsorption system. MN displayed C_t/C_i values greater than 1 for both C-GAC and MN-GAC. This observation suggests that other heavy metals were preferentially adsorbed better than Mn.

Table 4-5 shows the adsorption capacities and 50% break through times for the various heavy metals for each AC.

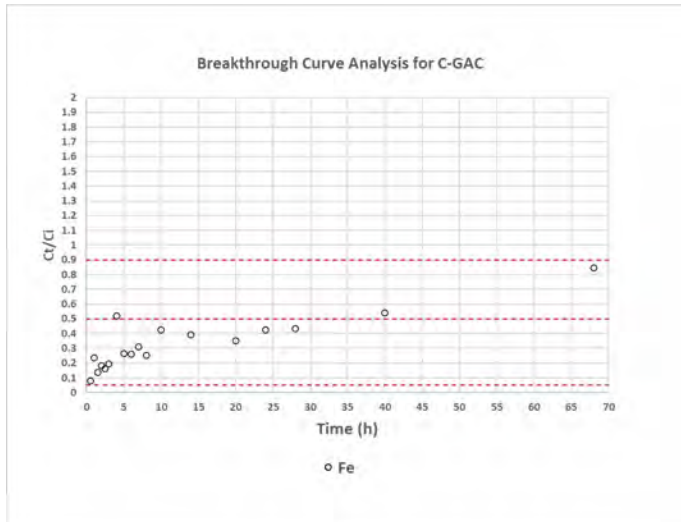


Figure 4-6: Breakthrough curve for Fe adsorption on C-GAC

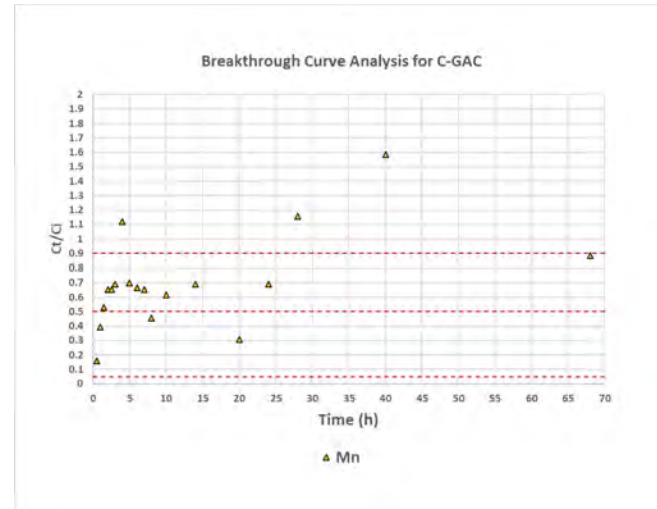


Figure 4-7: Breakthrough curve Mn adsorption on C-GAC

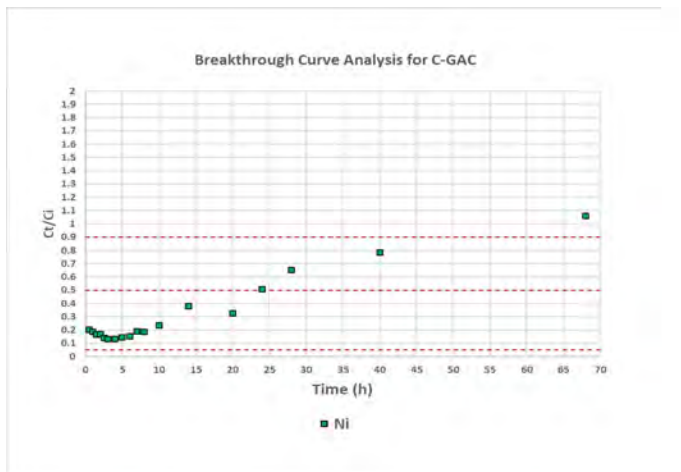


Figure 4-8: Breakthrough curve Ni adsorption on C-GAC

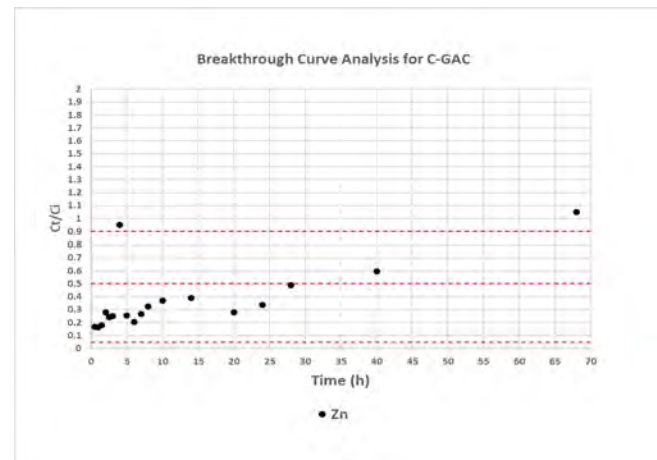


Figure 4-9: Breakthrough curve Zn adsorption on C-GAC

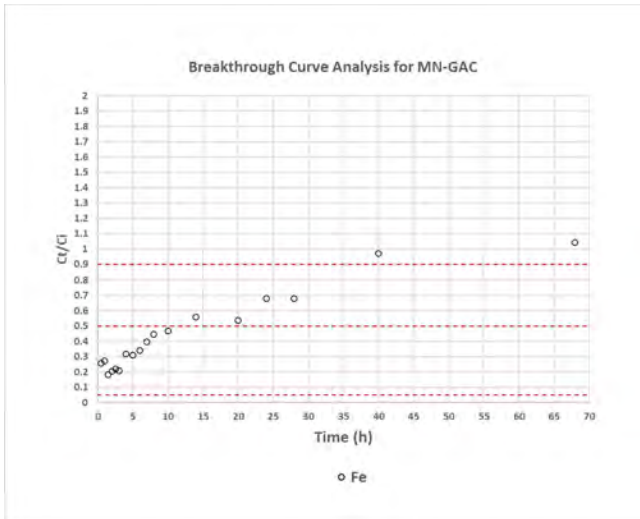


Figure 4-10: Breakthrough curve for Fe adsorption on MN-GAC

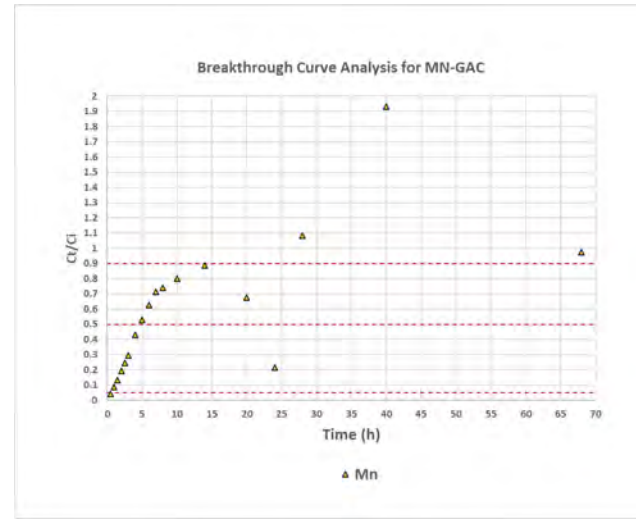


Figure 4-11: Breakthrough curve for Mn adsorption on MN-GAC

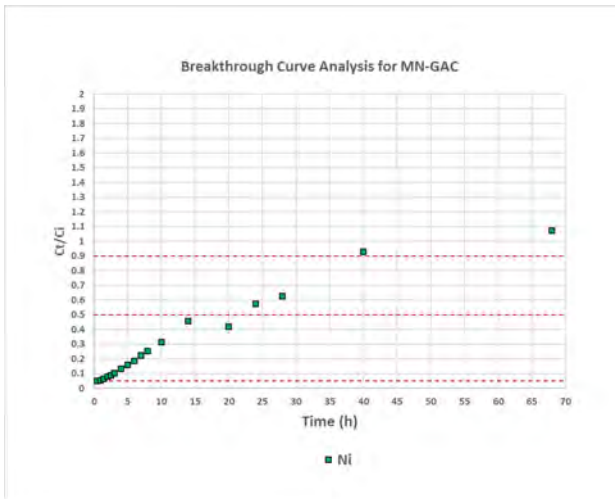


Figure 4-12: Breakthrough curve for Ni adsorption on MN-GAC

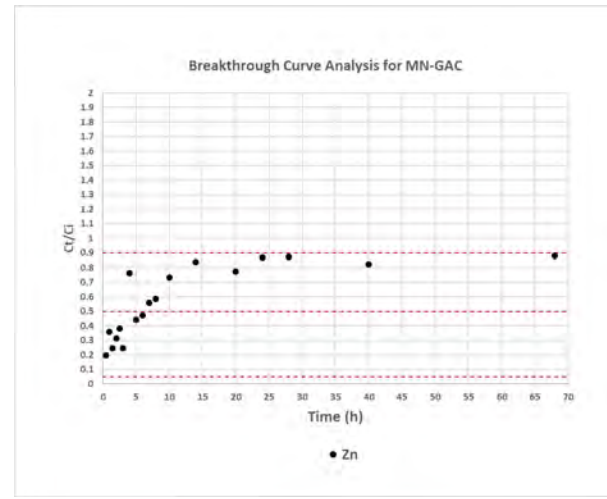


Figure 4-13: Breakthrough curve for Zn adsorption on MN-GAC

Table 4-5: Adsorption Capacity Break through Points for C-GAC and MN-GAC

Heavy Metal	C-GAC			MN-GAC		
	Adsorption Capacity (mg/g)	50% Breakthrough Point (hr)	Removal (%)	50% Breakthrough Point (min)	Adsorption Capacity (mg/g)	Removal (%)
Iron	43.6	10	84	10	38.7	81
Manganese	13.7	1.5	87	5	14.8	93
Nickel	12.2	17.5	81	15	14.6	95
Zinc	2.9	28	81	6	2.4	75

The breakthrough points for the various metals did not occur at the same time. The different breakthrough times implies that the four heavy metals were adsorbed at different rates. The adsorption sites were not readily available and easily accessed by all the four metal ions at similar times.

The adsorption capacity values indicate adsorption followed the order Fe > Mn > Ni > Zi for both C-GAC and MN-GAC. Percentage removals by C-GAC for all metals was 81-87% and 81-95% by MN-GAC.

Selected EDCs Removal

Five EDCs (bisphenol A, caffeine, carbamazepine, diclofenac and triclosan) were present in concentrations above the detection limits in the column effluent samples. Figure 4-8 and Figure 4-9 show the variation of concentration and the corresponding percentage removal of caffeine during the experiment. Similar plots for bisphenol A, carbamazepine, diclofenac and triclosan are presented in Appendix B. Table 4-6 presents a summary of the percentage maximum removals and corresponding removal capacities of EDCs observed from the study.

Table 4-6: Summary of adsorption capacities and % removals for selected EDC compounds in SST effluent

EDC	C-GAC		MN-GAC		PC-AC		AW-AC	
	Adsorption Capacity (mg/g)	Removal (%)						
Bisphenol A	0.79	82.0	0.87	90.8	0.50	70.6	*	*
Caffeine	2.41	99.6	2.42	99.9	*	*	*	*
Carbamazepine	0.027	74.6	0.036	81.4	0.036	77.8	0.038	91.9
Diclofenac	0.0047	82.6	0.0053	88.1	*	*	*	*
Triclosan	0.0098	77.2	*	*	*	*	*	*

*no removal

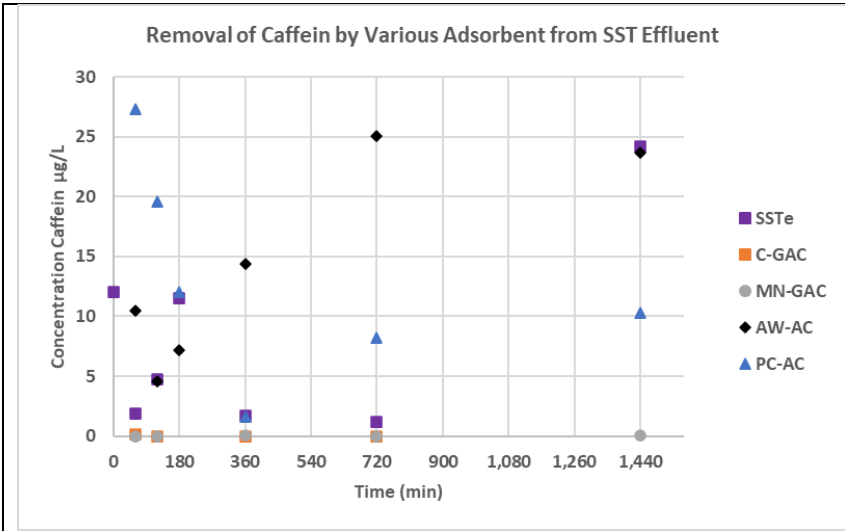


Figure 4-14: Removal of selected EDCs from SST effluent by various adsorbents

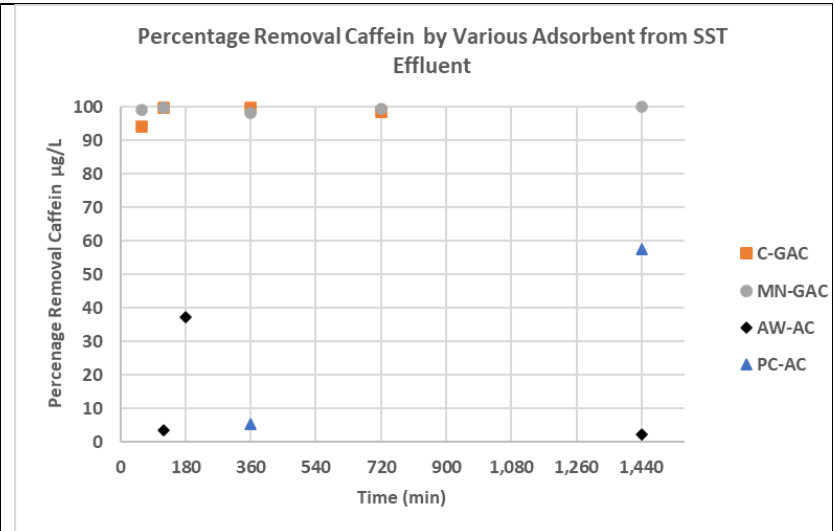


Figure 4-15: Removal of selected EDCs from SST effluent by various adsorbents

The results indicate the following:

- MN-GAC had the highest adsorption capacity and percentage removal at 0.87 mg/g and 90.8% respectively, followed by C-GAC with 0.79 mg/g and 82% respectively. Relatively lower adsorption of bisphenol A was recorded for PC-AC at 0.50 mg/g (70.6% removal), while no removal was observed for AW-AC.
- C-GAC and MN-GAC showed similar high removals for caffeine 2.42 mg/g (99.9% removal) for MN-GAC and 2.41 mg/g (99.6%) for MN-GAC. No removal of caffeine was observed for PC-AC and AW-AC.
- All the four adsorbents showed capacity to remove carbamazepine. The removal of carbamazepine was in the following order: AW-AC (0.038 mg/g, 91.9%)>MN-GAC (0.036 mg/g, 81.4%)>PC-AC (0.036 mg/g, 77.8%)>C-GAC (0.027 mg/g, 74.6%).
- C-GAC and MN-GAC showed similar removals for diclofenac; 0.0053 mg/g (88.1%) for MN-GAC and 0.0047 mg/g (82.6%) for MN-GAC. No removal of diclofenac was observed for PC-AC and AW-AC.
- Triclosan removal was observed on C-GAC (0.0098 mg/g, 77.2% removal). No removal of triclosan was observed for MN-GAC, PC-AC and AW-AC.

The findings from the study indicate that granular activated carbon CB-(GAC) and MN-GAC were the most effective adsorbents for the removal of the selected group of EDCs. Waste wood derived ACs indicated very poor removals of the EDCs except for carbamazepine.

4.3.2 Phase 2 Adsorption Column Test

The second phase of the small-scale pilot adsorption studies were conducted using HC-AC and coal based powdered AC (C-PAC). Coal based PAC was used in the adsorption column tests since its physical characteristic are similar to HC-AC. Using coal-based PAC enabled comparison of the performance of all coal based adsorbents that sludge derived HC-AC could be a substitute.

Two of the columns in the pilot test rig columns were each filled with HC-AC and C-PAC. To avoid entrapping of air bubbles inside the HC-AC and C-PAC particles, the ACs were soaked for 24 hours before packing into the column. The adsorbents were packed between two supporting layers of glass wool and wire gauze to prevent the floating of adsorbent particles. SST effluent was fed from the bottom of each column and the treated effluent was collected from the top of the column. Similar to the first phase, both columns received the same SST effluent flowrate of 1.7 l/min and were run continuously for a period of 3 days. Adsorption of the same four heavy metals (Fe, Mn, Ni and Zn) was evaluated.

Adsorption of Heavy Metals

The maximum adsorption capacity and percentage removals for Fe, Mn, Ni and Zn before breakthrough are given in Table 4-7. For ease of comparison, the performance of the ACs from Phase 1 are also included in Table 4-7.

Table 4-7: Summary of Adsorption Capacities and % Removals-Pilot Scale Studies

Heavy Metal	HC-AC		C-PAC		C-GAC		MN-GAC		AW-AC	
	Adsorption Capacity (mg/g)	Removal (%)								
Iron	35.4	94	30.7	93	43.6	84	38.7	81	51.4	90
Manganese	9.9	86	11.3	86	13.7	87	14.8	93	1.8	24
Nickel	13.6	90	10.3	89	12.2	81	14.6	95	14.7	77
Zinc	1.7	82	2.8	85	2.9	81	2.4	75	4.1	97

*no removal of heavy metal by adsorbent

It should be noted that during Phase 1, the SST effluent pumped to the columns had a lower heavy metal load (for each of the selected heavy metals) than during Phase 2.

Figure 4-16 and Figure 4-19 show the measured concentrations in the effluent from the adsorption columns over the course of the experiment and the calculated percentage removals, for Fe and Mn. Graphical representations of the results for the other heavy metals are given in Appendix B

The following is noted from the results:

1. The performances of HC-AC and C-PAC were closely similar for the selected heavy metals.
 - a) The order of removal was Fe > Ni > Mn > Zn for both HC-AC and C-PAC with removals ranging from 82-94% for HC-AC and 85-93% for C-PAC.
 - b) The adsorption capacity for Fe was 35.4 mg/g (94% removal) for HC-AC which was higher than 30.7 mg/g (93% removal) for C-PAC.
 - c) Although the percentage removal for Mn was the same at 86%, HC-AC had a lower adsorption capacity (9.9 mg/g) compared to C-PAC (11.3 mg/g).
 - d) For Ni, HC-AC recorded a higher adsorption capacity of 13.6 mg/g (90% removal) while C-PAC recorded 10.3 mg/g (89% removal).
 - e) The adsorption capacities for Zn and corresponding percentage removals for HC-AC and C-PAC were 1.7 mg/g (82%) and 2.8 mg/g (85%) respectively.

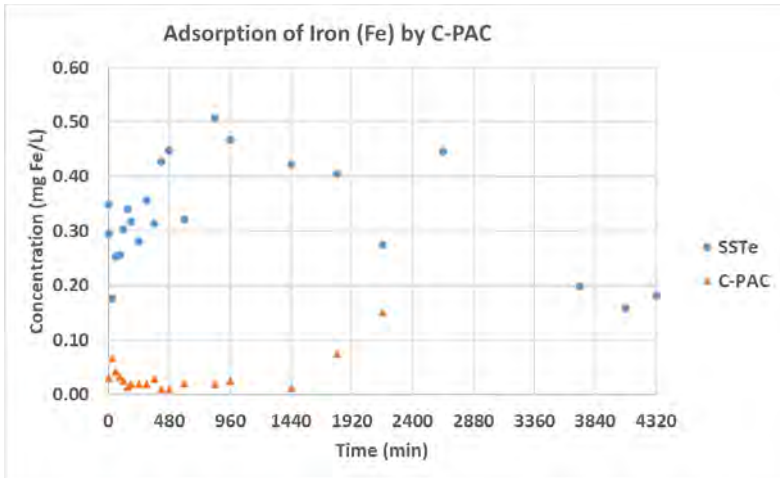


Figure 4-16: Removal of Iron from SST effluent by C-PAC

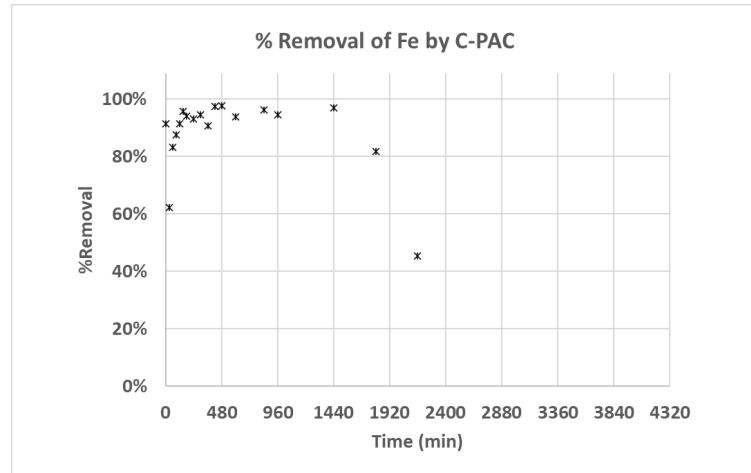


Figure 4-17: % Removal of Iron from SST effluent by C-PAC

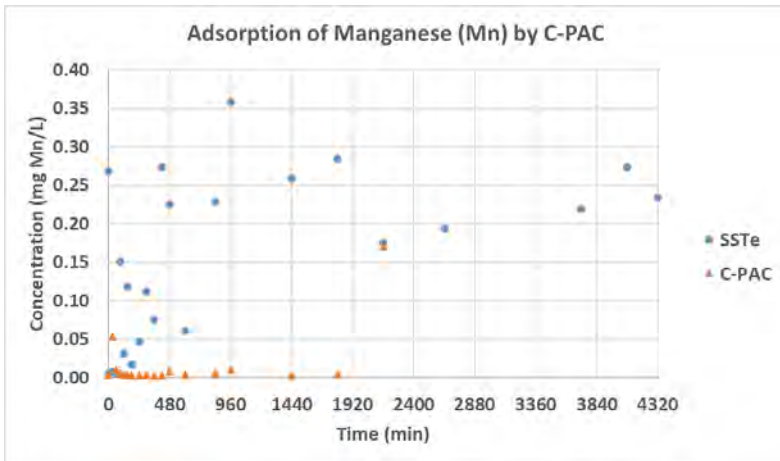


Figure 4-18: Removal of Manganese from SST effluent by C-PAC

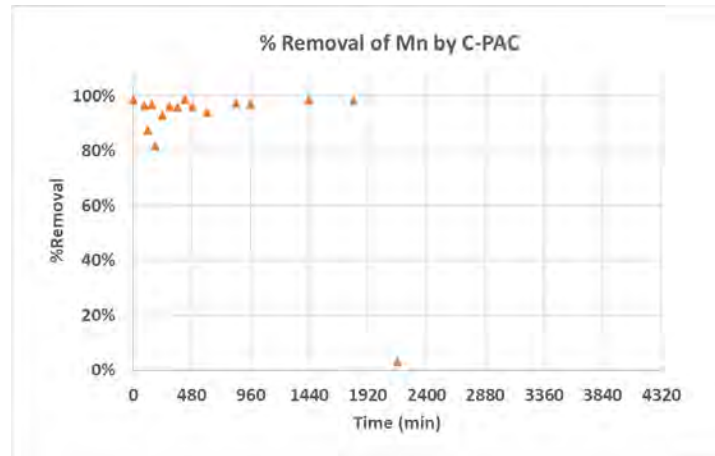


Figure 4-19: % Removal of Manganese from SST effluent by C-PAC

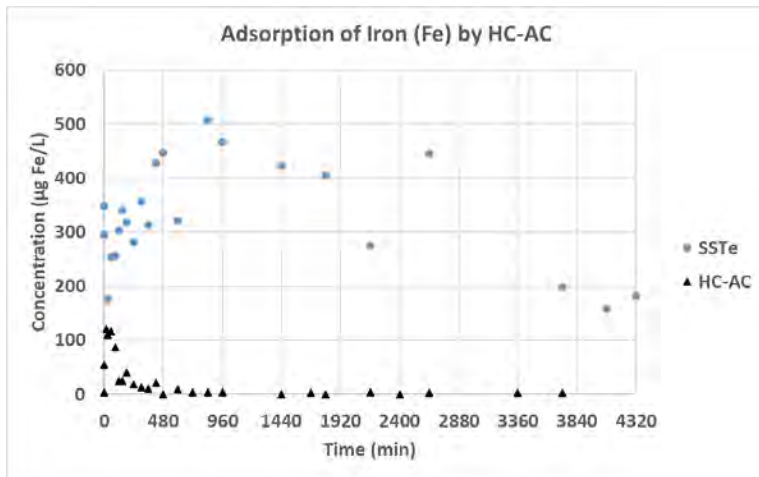


Figure 4-20: Removal of Iron from SST effluent by HC-AC

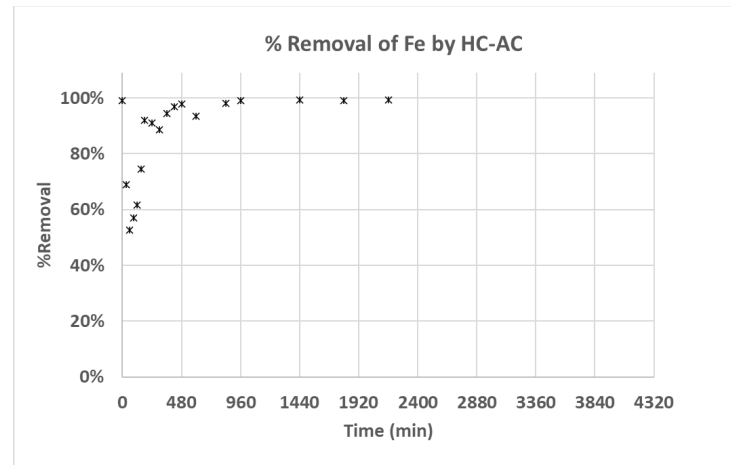


Figure 4-21: % Removal of Iron from SST effluent by HC-AC

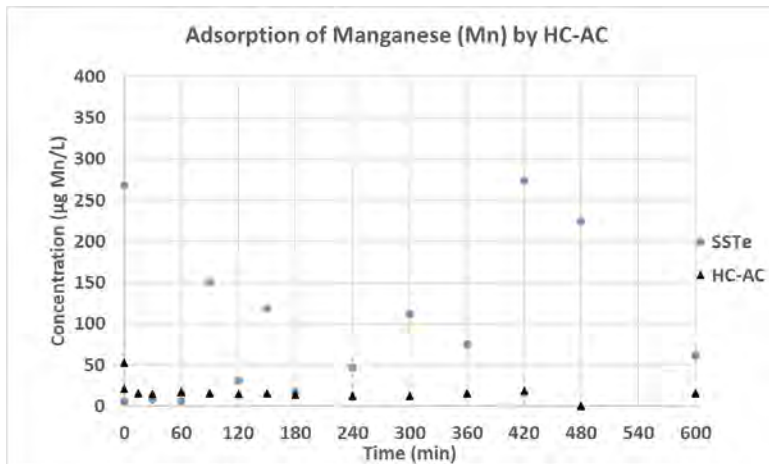


Figure 4-22: Removal of Manganese from SST effluent by HC-AC

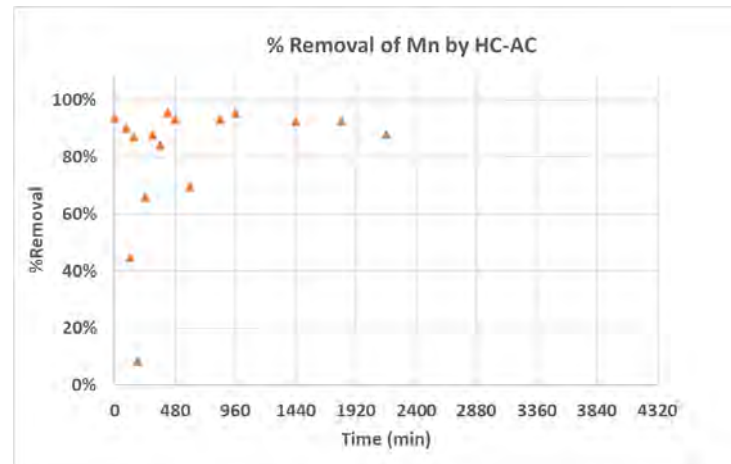


Figure 4-23: % Removal of Manganese from SST effluent by HC-AC

2. When compared to C-GAC and MN-GAC the performance of HC-AC was also closely similar.
 - a) The order of removal was Fe> Ni> Mn> Zn for both HC-AC and while for MN-GAC was Ni> Mn> Fe> Zn
 - b) The adsorption capacities were higher for C-GAC compared to HC-AC except for Ni where the later had a higher value. MN-GAC had higher adsorption capacities than HC-AC for all heavy.
3. HC-AC had higher percentage removals than AW-AC for all metals except for Ni where the later had a higher value. The HC-AC performance was also much higher than PC-AC which had the worst performance out of all the adsorbents.

The results indicate that sludge derived HC-AC performed as well as the commercial coal based ACs and commercial AC produced from waste macadamia nuts in removing heavy metals from SST effluent discharged at a full-scale WWTP. While the observed adsorption capacities for the heavy metals varied between adsorbents, the values did not differ significantly between HC-AC and the commercial ACs. Adsorption capacity depends on the characteristics of the individual adsorbent, the concentrations of the heavy metals in the secondary effluent as well as other factors.

Break through Curve Analysis-Heavy Metals for C-PAC and HC-AC

Figure 4-24 to Figure 4-29 show the breakthrough curves for C-PAC and HC-AC. The characteristic S-like shaped sigmoidal breakthrough curves were not obtained in the Phase 2 study for C-PAC and HC-AC. The results indicate that the adsorption capacity of each bed was not exhausted during the duration of the experiment. Hence, an attempt to plot the breakthrough does not give the expected S-like profile. The longer bed-life for C-PAC and HC-AC compared to C-GAC and MN-GAC is attributed to the fact that C-PAC and HC-AC have very small particles sizes (less than 100 μm in diameter) that allow a larger external surface area for adsorption compared to GAC particles that are relatively larger in size. The shape of the breakthrough curve also suggests that the selected column height contributed to the higher number of adsorbent sites and larger surface area available for adsorption, which extended the bed life inside the adsorption columns.

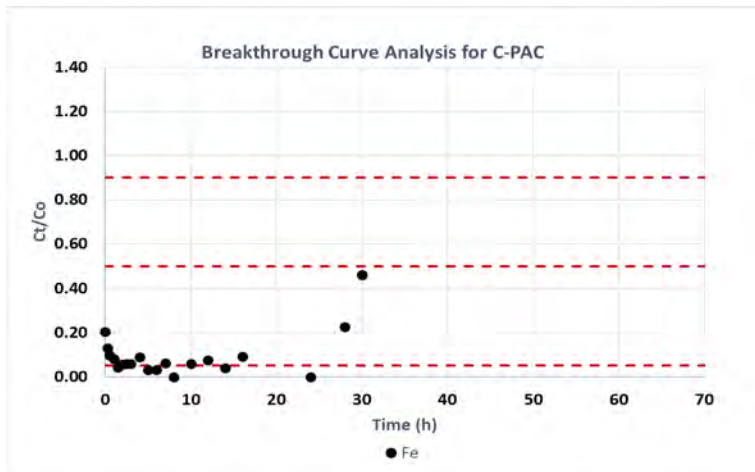


Figure 4-24: Breakthrough curve for Fe adsorption on C-PAC

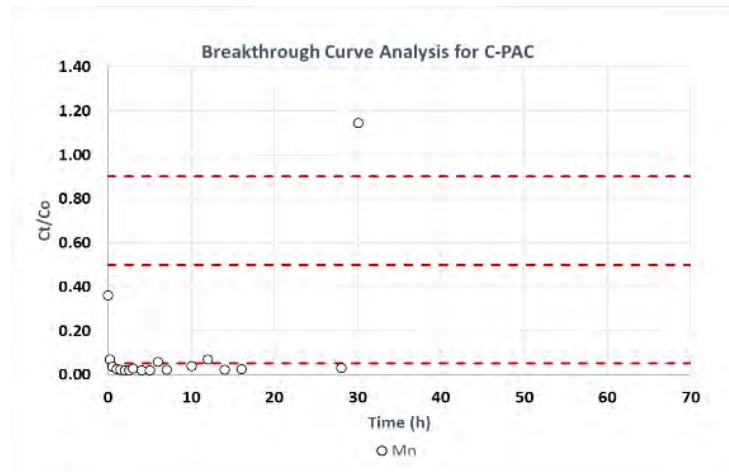


Figure 4-25: Breakthrough curve for Mn adsorption on C-PAC

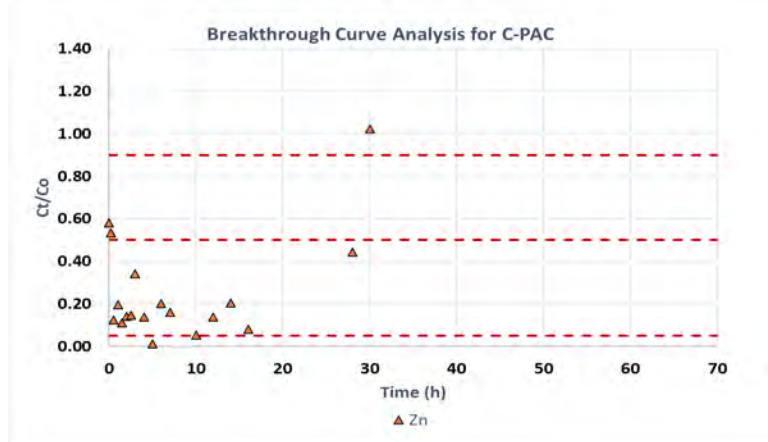


Figure 4-26: Breakthrough curve for Zn adsorption on C-PAC

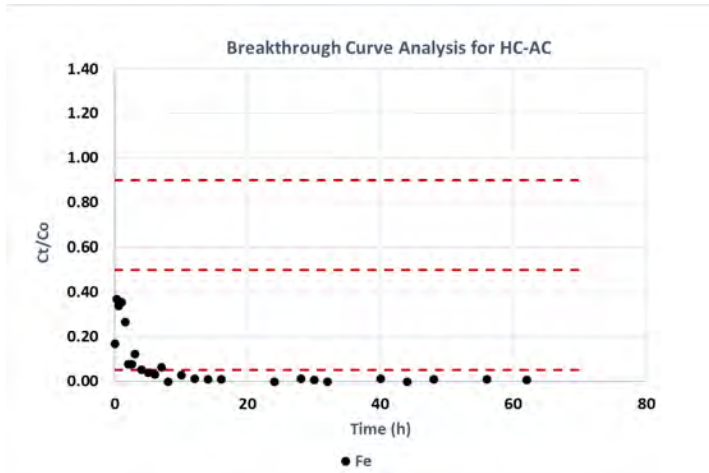


Figure 4-27: Breakthrough curve for Fe adsorption on HC-AC

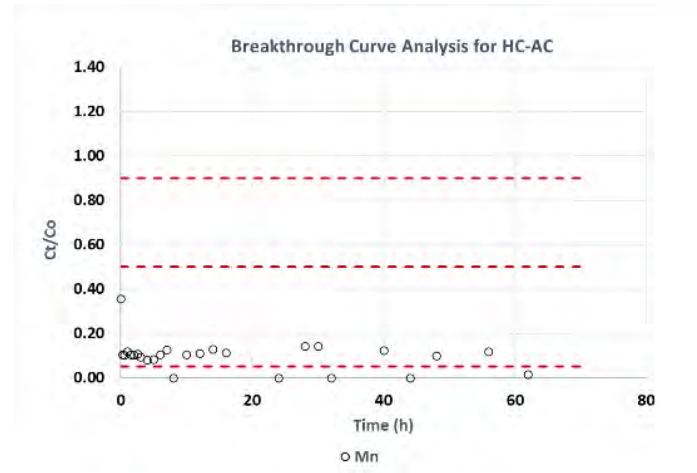


Figure 4-28: Breakthrough curve for Mn adsorption on HC-AC

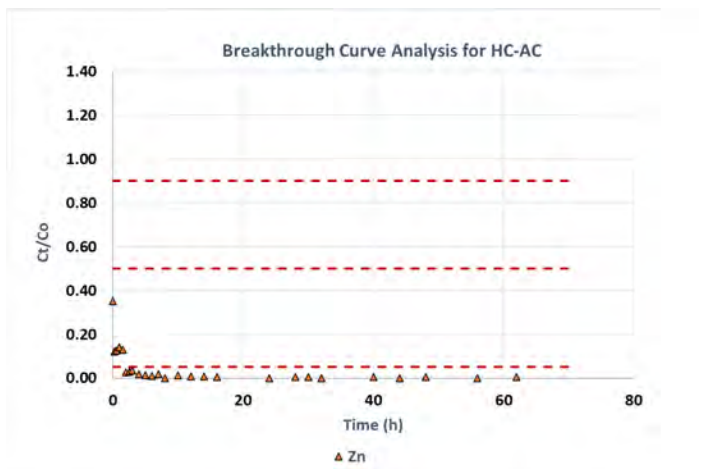


Figure 4-29: Breakthrough curve for Zn adsorption on HC-AC

CHAPTER 5 CONCLUSIONS AND RECOMMENDATIONS

This project investigated the feasibility of using activated carbon produced from pyrolysis of wastewater sludge hydrochar for micropollutant removal from wastewater. The hydrochar was derived from processing combined primary and waste activated sludge using the emerging enhanced hydrothermal polymerization (EHTP) technology (a catalysed hydrothermal carbonisation process). The performance of the sludge hydrochar-derived activated carbon was compared with commercial coal based activated carbons (both granular and powdered) and macadamia nuts derived AC as well as activated carbons derived from waste wood through laboratory-scale and small-scale column adsorption tests. The objective of the study was to assess the performance and viability of HC-AC as a low-cost alternative adsorbent, promoting the valorization of sludge within a circular economy framework.

Laboratory scale experiments were carried out in two phases. In the first phase standard laboratory scale jar adsorption tests were conducted to determine the adsorption kinetics and isotherms for coal granular activated carbon (C-GAC) and HC-AC using solutions containing (i) methylene blue dye and (ii) lead (II) ions. The second phase conducted similar jar adsorption tests to investigate the performance of HC-AC in removing selected heavy metals from secondary clarifier effluent collected from a full-scale biological nutrient removal (BNR) activated sludge plant.

The following conclusions were drawn from the laboratory tests:

- Activated carbon was successfully produced by pyrolysis of hydrochar derived from a combination of primary sludge and waste activated sludge at 425°C under a nitrogen atmosphere with no further activation.
- HC-AC exhibited the lowest microporosity as determined by its low iodine number. However, it showed an abundance of oxygen and sufficient oxygen functional groups which were attributed to its high removal of MB dye and Pb (II) ions
- The analysis of the experimental results using the Langmuir and Freundlich isotherms show that the data for C-GAC had a similar fit for both the Langmuir 1 and Freundlich isotherms ($R^2 = 0.7835$ and 0.7824 respectively). The R^2 value for HC-AC was generally low for both isotherms with the R^2 value for the Freundlich being the higher value at 0.164 . These results suggest that there was monolayer coverage of the adsorbate on the adsorbent C-GAC, while the coverage on HC-AC was multilayer in nature
- In the mono-metal adsorption of Pb (II) ions, removal efficiency was almost 100% for both C-GAC and HC-AC. The maximum removal capacity of Pb (II) was 1.5 mg/g for both C-GAC and HC-AC which was equivalent to 99% removal.

- In the multi-metal adsorption studies using secondary clarifier effluent collected at a full-scale BNR activated sludge plant, the evaluation and comparison of the adsorptive capacity of the adsorbents for various metal pollutants was limited to Fe, Mn, Ni and Zn, regulated metals from SANS 241 which were present in detectable amounts in the effluent.
- The adsorption experiments using secondary clarifier effluent showed an order of adsorption of Fe > Mn > Ni > Zn for both C-GAC and HC-AC.

During the pilot scale studies, the performance of HC-AC was compared with the performance of coal granular activated carbon (C-GAC) and powdered activated carbon (C-PAC), macadamia nuts granular activated carbon (MN-GAC) and activated carbons derived from waste alien wood (AW-AC) and pine cone (PC-AC). Evaluation of the adsorption of various metal pollutants was limited to Fe, Mn, Ni and Zn, regulated metals from SANS 241 which were present in detectable amounts in the effluent. The following conclusions were drawn from the results of the pilot scale studies:

- The performance of HC-AC was closely similar to commercial adsorbents C-GAC, C-PAC and MN-GAC. Both percentage removal and adsorption capacity values for HC-AC did not differ significantly from those of the other three adsorbents. The order of removal was Fe (94%) > Ni (90%) > Mn (86%) > Zn (82%) for HC-AC while the adsorption capacities were 35.4 mg/g, 9.9 mg/g, 13.6 mg/g and 1.7 mg/g for Fe, Ni, Mn and Zn respectively.
- Overall HC-AC performed better than the waste wood derived activated carbons with higher percentage removals than AW-AC for all metals except for Ni and much higher removals than PC-AC which had the worst performance out of all the adsorbents.

The findings from the laboratory studies and small scale pilot column tests demonstrated that hydrochar produced from processing sludge in a novel thermochemical conversion process can be successfully converted to activated carbon through pyrolysis under a nitrogen atmosphere. The HC-AC performed as efficiently as C-GAC in the removal of Pb (II) ions in a single-metal solution at laboratory scale. HC-AC performance was also demonstrated to be closely similar to that of C-GAC, C-PAC and MN-GAC in removing heavy metals from a multi-metal solution through laboratory and pilot column tests using final effluent from a BNR activated sludge plant as the adsorbate. Based on the study results, it is therefore feasible to process sludge in a catalysed hydrothermal carbonisation type technology such as the EHTP technology and convert the produced hydrochar to activated carbon that can be used for tertiary treatment of final effluent from WWTPs. It is recommended that further studies be conducted to investigate viability of using sludge derived hydrochar activated carbon for use in full-scale tertiary treatment adsorption plants.

To continue building the body of knowledge on application of sludge and other waste derived activated carbons for removal of contaminants from wastewater effluent in South Africa, the following is recommended:

- Further laboratory scale investigations into (i) other physical and chemical activation methods (ii) removal of ash and heavy metals and (iii) granulation and pelletisation to improve the characteristics of hydrochar derived activated carbon and (iv) regeneration and reuse of the activated carbon.
- Pilot scale investigations into feasible configurations for tertiary treatment processes that incorporate adsorption using sludge hydrochar derived activated carbon with other tertiary treatment technologies, leading to innovative low-cost treatment processes for WR&R schemes within a circular economy.
- Co-processing of sludge with waste wood in thermochemical conversion processes like EHTP that co-processes a wide range of biomass. The resultant hydrochar can be converted to activated carbon and evaluated for feasibility to remove heavy metals and micropollutants from wastewater effluent.

REFERENCES

- (Al-Sayed A, El-Senousy WM, Al-Herrawy AZ, Abo Aly MM and El-Gahary FA (2018). Membrane Bioreactor Technology for Wastewater Reclamation. *Egyptian journal of chemistry*, 61 (5), pp 883-896
- Alyüz B and Veli S (2009). Kinetics and Equilibrium Studies for The removal of Nickel and Zinc from Aqueous Solutions by Ion Exchange Resins. *J Hazard Mater* 167, pp 482-488.
- Asano T and Bahri A (2011). Global challenges to Wastewater Reclamation and Reuse. *On the Waterfront*, Vol 2, pp 64-72.
- Asano T, Burton F, Leverenz H, Tsuchihashi R, Tchobanoglous G (2007). *Water Reuse: Issues, Technologies, and Applications*. Publisher: McGraw-Hill Professional.
- Assaad, E.; Azzouz, A.; Nistor, D.; Ursu, A.V.; Sajin, T.; Miron, D.N.; Monette, F.; Niquette, P.; Hausler, R. Metal removal through synergic coagulation-flocculation using an optimized chitosan-montmorillonite system. *Appl. Clay Sci.* 2007, 37, 258-274.
- ASTM D2854-96 (2000). Standard Test Method for Apparent Density of Activated Carbon 96, pp. 1-3.
- ASTM D4607-94 (2006). Standard Test Method for Determination of Iodine Number of Activated Carbon 94, pp. 1-5.
- Bandosz T and Petit C (2009). On the Reactive Adsorption of Ammonia on Activated Carbons Modified by Impregnation with Inorganic Compounds. *Journal of Colloid and Interface Science* 338, pp. 329-345
- Barros, M. & Arroyo, Pedro & da Silva, Edson. (2013). General Aspects of Aqueous Sorption Process in Fixed Beds. 10.5772/51954.
- Blázquez G, Hernáinz F, Calero M, Martín-Lara MA & Tenorio G. (2009). The Effect of pH on the Biosorption of Cr (III) and Cr (VI) With Olive Stone. *Chemical Engineering Journal* 148, pp 473-479.
- Boehler M, Zwicklenpflug B, Hollender J, Ternes T, Joss A and Siegrist H (2012). Removal of Micropollutants in Municipal Wastewater Treatment Plants by Powder-Activated Carbon. *Water Science Technology*, 66(10), 2115-2121
- CEFIC E. (1986). Test Methods for Activated Carbon. European Council Of Chemical Manufacturers Federation/European Chemical Industry Council, pp. 9-43.
- Chowdhury, Z. Z., Hamid, S. B. A., and Zain, S. M. (2015). Evaluating design parameters for breakthrough curve analysis and kinetics of fixed bed columns for Cu(II) cations using lignocellulosic wastes. *BioRes.* 10(1), 732-749.
- Chung HY, Kim WH, Park J, Cho J, Jeong TY and Park P K (2015). Application of Langmuir and Freundlich Isotherms to Predict Adsorbate Removal Efficiency or Required Amount of Adsorbent. *Journal of Industrial and Engineering*, 28, 241-246
- Clement RE, Eiceman GA, Koester CJ (1995). Environmental Analysis. *Analytical Chemistry* 67 (12), 221R-255R.
- Daneshvar E, Daneshvar A, Niazi A, Sillanpää M & Bhatnagar A (2019). CSIR Green Book: Adapting South African Settlements to Climate Change. Available at: www.greenbook.co.za
- A Comparative Study of Methylene Blue Biosorption Using Different Modified Brown, Red and Green Macroalgae – effect of Pre-treatment (2017). *Chemical Engineering Journal* 307, 435-446.

- De Farias Silva CE, Da Silva Gonçalves AH & De Souza Abud AK (2016). Treatment of Textile Industry Effluents Using Orange Waste: A Proposal to Reduce Colour and Chemical Oxygen Demand. *Water Science and Technology* 74 (4), 994-1004.
- Diamanti-Kandarakis E, Bourguignon JP, Giudice LC, Hauser R and Prins GS (2009). Endocrine Disrupting Chemicals: An Endocrine Society Scientific Statement. *Endocrine Reviews* 30: 293-342.
- Dogan M, Alkan M and Yavuz Onganery (2000). Adsorption of Methylene Blue from Aqueous Solution onto Perlite. *Water, Air, and Soil Pollution*, 120, 229-248
- DWS (Department of Water and Sanitation) 2018. National Water and Sanitation Master Plan (NW & SMP). Volume 1: Call to Action. Ready for the Future and Ahead of the Curve. V10.1, 31 October 2018. Available at: <https://static.pmg.org.za/200818national-water-and-sanitation-master-plan.pdf>
- El-Bery HM, Saleh M, El-Gendy R A (2022). High Adsorption Capacity of Phenol and Methylene Blue Using Activated Carbon Derived from Lignocellulosic Agriculture Wastes. *Sci Rep* 12, 5499 (2022). Available at: <https://doi.org/10.1038/s41598-022-09475-4>
- El-Wakil AM, El-Maaty WM and Awad FS (2014). Removal of Lead from Aqueous Solution on Activated Carbon and Modified Activated Carbon Prepared from Dried Water Hyacinth Plant. *Journal of Analytical & Bioanalytical Technology*, 5(2), 1-14
- Erdem A, Ngwabebhoh FA, Çetintaş S, Bingöl D and Yildiz U (2017). Fabrication and Characterization of Novel Microporous Jeffamine/Diamino Hexane Cryogens for Enhanced Cu (II) Metal Uptake: Optimization, isotherms, kinetics and thermodynamic studies. *Chem Eng Res Des.* 117, 122-138. doi: 10.1016/j.cherd.2016.10.010
- F Raposo, MA De La Rubia, R Borja, J Hazard Mater (2009). Methylene Blue Number as Useful Indicator to Evaluate the Adsorptive Capacity of Granular Activated Carbon in Batch Mode: Influence of Adsorbate/Adsorbent Mass Ratio and Particle Size 165, pp. 291-299, 10.1016/j.jhazmat.2008.09.106
- FJ Real, FJ Benitez, JL Acero, F Casas (2017). Adsorption of Selected Emerging Contaminants onto PAC and GAC: Equilibrium Isotherms, Kinetics, and Effect of the Water Matrix. *Journal of Environmental Science Health A*, 52 (8), pp. 727-734, 10.1080/10934529.2017.1301751.
- Fenglian Fu a, Qi Wang b (2011). Removal of Heavy Metal Ions from Wastewaters: A review *Journal of Environmental Management*, Volume 92, Issue 3, March 2011, Pages 407-418
- Ferhan Cecen, Özgü Akatas (2012). *Activated Carbon for Water and Wastewater Treatment: Integration of Adsorption and Biological Treatment*. WILEY-VCH Verlag & Co.
- Flint S, Markle T, Thompson S and Wallace E (2012). Bisphenol A Exposure, Effects, and Policy: A Wildlife Perspective. *Journal of Environmental Management*, 104:19-34.
- Fu F and Wang Q (2011). Removal of Heavy Metal Ions from Wastewaters: A review. *Journal of Environmental Management*, 92(3), pp. 407-418. doi: 10.1016/j.jenvman.2010.11.011.
- Geçgel Ü, Özcan G and Gürpınar GÇ (2013). Removal of methylene blue from aqueous solution by activated carbon prepared from pea shells (*Pisum sativum*). *Journal of Chemistry*. doi: 10.1155/2013/614083.
- Graham N (2019). Barriers and Opportunities for Water Reuse PPPs in South Africa. Draft paper written for the European Union-South Africa Partners for Growth. Available at: <https://www.euchamber.co.za/wpcontent/uploads/2020/03/Barriers-to-water-reuse-Final-Report-20200113.pdf>

- Grégorio Crini, Eric Lichtfouse, Lee D. Wilson & Nadia Morin-Crini (2019). Conventional and Non-Conventional Adsorbents for Wastewater Treatment Review Published: 31 July 2018 Volume 17, pp 195-213.
- Grover D, Zhou J, Frickers P and Readman J (2011). Improved Removal of Estrogenic and Pharmaceutical Compounds in Sewage Effluent by Full Scale Granular Activated Carbon: Impact on Receiving River Water. *Journal of Hazardous Materials*, 185(2), 1005-1011
- Gupta VK , Suhas I, Tyagi S, Agarwal R, Singh M, Chaudhary A, Harit S, Kushwaha Glob (2016). *Journal of Environmental Science Management*, 2 (1), 1-10.
- Han R, Zou W, Li H, Li Y and Shi J (2006). Copper (II) and Lead (II) Removal from Aqueous Solution in Fixed-bed Columns by Manganese Oxide Coated Zeolite. *Journal of Hazardous Materials*, vol. B137, no. 1, pp. 934-942.
- Harrison P, Humfrey C, Litchfield M, Peakall D and Shuker L (1995). Environmental oestrogens: consequences to human health and wildlife: Institute for Environment and Health.
- Ho YS, Huang CT and Huang HW (2002). Equilibrium Sorption Isotherm for Metal Ions on Tree Fern. *Process Biochemistry*, 37, 1421-1430
- Honarpour M (2012). Bulk Density and Tapped Density of Powders. World health organization, XXXIII(2), pp.81-87.
- Hube S, Eska M, Hrafnkelsdóttir KF, Bjarnadóttir B, Bjarnadóttir MÁ, Axelsdóttir S (2020). Direct Membrane Filtration for Wastewater Treatment and Resource Recovery: a Review. *Sci Total Environ*. 710, 136375. doi: 10.1016/j.scitotenv.2019.13637
- Huisman JL, Schouten G, and Schultz C (2006). Biologically Produced Sulphide for Purification of Process Streams, Effluent Treatment and Recovery of Metals in the Metal and Mining Industry. *Hydrometallurgy* 83, 106-113. doi: 10.1016/j.hydromet.2006.03.017
- HO Pörtner, DC Roberts, ES Poloczanska, K Mintenbeck, M Tignor, A Alegría, M Craig, S Langsdorf, S Löschke, V Möller, A Okem (2022). IPCC (Intergovernmental Panel on Climate Change). Summary for Policymakers.
- Jamaliniya S (2018). Evaluating the Adsorption Performance of a Novel Green Adsorbent in Removing Inorganic Nitrogen from Surface Water and Comparing with Granular Activated Carbon. Master's degree Thesis, Carleton University, Ottawa, Ontario.
- Jimenez B and Asano T (2008). Water Reuse: An International Survey of Current Practice, Issues and Needs. Scientific and Technical Report No. 20. London, UK: International Water Association Publishing
- Joss A, Siegrist H, Ternes TA (2008). Are We About to Upgrade Wastewater Treatment for Removing Organic Micropollutants? *Water Science Technology* 57 (2): 251-255.
- Kalebaila N, E J Ncube, CD Swartz, S Marais and J Lubbe (2020). Strengthening the Implementation of Water Reuse in South Africa. Gezina: water Research Commission? (Water Research Commission Working Paper)
- Kanamarlapudi S, Chintalpudi VK, Muddada S (2018). Application of Biosorption for Removal of Heavy Metals from Wastewater Biosorption 18, 69-116.
- Kumar R, D Bhatia, R Singh, S Rami, NR Bishnoi (2011). *International Biodeterioration Biodegradable*, 65, 1133-1139.

- Lakshmipathy R, NC Sarada (2015). Environmental Science Water Research 1, 244.
- Kundu S and Gupta AK (2005). Analysis and Modelling of Fixed Bed Column Operations on As (V) Removal by Adsorption onto Iron Oxide-Coated Cement (IOCC). Journal of Colloid and Interface Science, vol. 290, no. 1, pp. 52-60.
- Lim AP, AZ Aris (2020). Engineered Biochar Production and Its Potential Benefits in a Closed-Loop Water-Reuse Agriculture System (3). Environmental Science and Biotechnology, 13, 163 (2014).
- M. Suzuki (1991). Application of Fibre Adsorbents in Water Treatment Water Science and Technology, 23 (7-9), pp. 1649-1658, 10.2166/wst.1991.0619.
- MacCarthy P, Klusman RW, Cowling SW, Rice JA (1993). Water analysis. Analytical Chemistry 65 (12), 244R-292R.
- Mahajan OP and Walker PL (1978). Porosity of Coals and Coal Products. United States Department of Energy, Technical Report 7
- Marques-Pinto A, Carvalho D (2013). Human Infertility: Are endocrine disruptors to blame? Endocrine Connections, 2(3),15-29.
- Martín-Lara MA, Calero M, Rond A, Pérez A & Trujillo MC (2016). Assessment of the Removal Mechanism of Hexavalent Chromium from Aqueous Solutions by Olive Stone. Water Science and Technology 73, 2680-2688.
- Mashile PP, Mpupa A, Nomngongo PN (2018). Adsorptive Removal of Microcystin-LR from Surface and Wastewater Using Tyre-based Powdered Activated Carbon: Kinetics and Isotherms. Toxicon 145, 25-31.
- Matthiessen P and Gibbs EP (1998). Critical Appraisal of the Evidence for Tributyltin-mediated Endocrine Disruption in Mollusks. *DOI, 10*, 1002
- Mills LJ and Chichester C (2005). Review of Evidence: Are Endocrine-Disrupting Chemicals in the Aquatic Environment Impacting Fish Populations? Science of The Total Environment, 343(1-3), 1-34.
- Minerals BC (2014). Comparison of European Biochar Certificate Version 4. European Biochar Certificate first publication March 2012. Available at: <http://www.european-biochar.org/en/home> IBI Biochar Standards first publication May 2012, (October), pp. 1-5.
- Montazer-Rahmati MM, Rabbani P, Abdolali A & Keshtkar AR (2011). Kinetics and Equilibrium Studies on Biosorption of Cadmium, Lead, and Nickel Ions from Aqueous Solutions by Intact and Chemically Modified Brown Algae. Journal of Hazardous Materials 185, 401-407.
- Mohan, D. and Chander, S., Single Component and Multi-component Adsorption of Metal Ions by Activated Carbons, Colloids and Surfaces A: Physicochemical and Engineering Aspects, 177, 2-3, 183-196, 2001.
- Morris JC, Georgiou I, Guenther E (2021). Barriers in Implementation of Wastewater Reuse: Identifying the Way Forward in Closing the Loop. 1, 413-433 (2021).
- Musvoto E, Mgwenya N, Mangashena H and Mackintosh A (2018). Energy Recovery from Wastewater Sludge – A Review of Appropriate Emerging and Established Technologies for the South African Industry. Water Research Commission, Report No. TT 752/18, Pretoria, South Africa.
- Namasivavam and Kavitha (2002). Removal of Congo Red from Water by Adsorption onto Activated Carbon Prepared from Coir Pith, an Agricultural Solid Waste. Dyes and Pigments, 54, 47-58.

- Ncibi MC, Mahjoub B, Mahjoub O, Sillanp M (2017). Remediation of Emerging Pollutants in Contaminated Wastewater and Aquatic Environments: Biomass-based technologies. *Clean Soil Air Water* 45 (5), 1700101.
- Nepu SahaDanhui, XinDanhui Xin Pei C, Chiu M, Toufiq Reza M (1974). Standard for Granular Activated Carbon. *Journal of American Water Works Association*, 66(11), pp. 672-681. doi: 10.1002/j.1551-8833.1974.tb02114.x.
- Nowicki P, Kazmierczak-Razna J, Skibiszewska P, Wiśniewska M, Nosal-Wiercińska A and Pietrzak (2015). Production of Activated Carbons from Biodegradable Waste Materials as an Alternative Way of their Utilisation. *Adsorption* 22, 489-502
- Nunell G, Fernandez M, Bonelli P and Cukierman A (2015). Nitrate Uptake Improvement by Modified Activated Carbons Developed from two Species of Pinecones. *Journal of Colloid and Interface Science*, 440, 102-108.
- Omo-Okoro PN, Daso AP, Okonkwo JO (2018). A Review of the Application of Agricultural Wastes as Precursor Materials for the Adsorption of Per-and Polyfluoroalkyl Substances: A Focus on Current Approaches and Methodologies.
- Ozcimen D and Mericboyu A (2008). A Study on the Carbonization of Grapeseed and Chestnut Shell. *Fuel Processing Technology* 89(11), 1041-1046.
- Özverdi A and Erdem M (2006). Cu²⁺, Cd²⁺ and Pb²⁺ Adsorption from Aqueous Solutions by Pyrite and Synthetic Iron Sulphide. *J Hazard Mater.* 137, 626-632. doi: 10.1016/j.jhazmat.2006.02.051
- Pillai S.B 2024. Adsorption in water and used water purification. In *Handbook of water and used for water purification* (pp. 99-120). Cham: Springer International Publishing.
- Ramrakhiani L., Ghosh S and Majumdar S (2016). Surface modification of naturally available biomass for enhancement of heavy metal removal efficiency, upscaling prospects, and management aspects of spent biosorbents: a review. *Applied Biochemistry and Biotechnology* 180 (1), 41-78.
- Rangabhashiyam, S, Nandagopal M.G, Nakkeeran E and Selvaraju N. 2016. Adsorption of hexavalent chromium from synthetic and electroplating effluent on chemically modified Swietenia mahagoni shell in a packed bed column. *Environmental monitoring and assessment*, 188, 411.
- Raposo F, Rubia MDL and Borja R (2009). Methylene Blue Number as useful Indicator to Evaluate the Adsorptive capacity of Granular Activated Carbon in Batch Mode: Influence of Adsorbate/Adsorbent Mass Ratio and Particle Size. *Journal of Hazardous Materials*, 165(1-3):291-299.
- Renge V. C, Khedkar S. V, Pandey Shraddha V (2012). Removal of heavy metals from wastewater using low-cost adsorbents: a review. *Scientific Reviews and Chemical Communications* 2 (4), 580-584.
- Rosenfeld P.E, Lydia G.H and Feng, L (2011). Risks of hazardous wastes. William Andrew. pp 215-222.
- Saif M.J, Zia K.M, Ur-Rehman F, Usman M, Hussain A.I. and Chatha S.A.S (2015). 'Removal of Heavy Metals by Adsorption onto Activated Carbon Derived from Pinecones of Water Environment Research, 87(4), pp. 291-297. doi: 10.2175/106143015x14212658613433.
- Saleh T.A (2022). *Surface Science of Adsorbents and Nano adsorbents: Properties and Applications in Environmental Remediation*. Academic Press.
- Sawyer CN and McCarty PL (1978). *Chemistry for Environmental Engineering* (3rd ed.). New York: McGraw-Hill Book Co.

- Schug T.T, Janesick A, Blumberg B and Heindel J.J (2011). Endocrine disrupting chemicals and disease susceptibility. *The Journal of Steroid Biochemistry and Molecular Biology*, 127, 204-215.
- Sepúlveda MEL and Salsa JJ (2011). Wastewater Reclamation by Unconventional Technologies. 3rd International Congress: at Seville.
- Singh B. Dolk M.M., Shen Q and Camps-Arbestain, M (2017). Biochar pH, electrical conductivity and liming potential', *Biochar: A Guide to Analytical Methods*, (June 2018), pp. 23-38.
- Soares A, Guieysse B, Jefferson B, Cartmell E and Lester J.N (2008). Nonylphenol in the environment: a critical review on occurrence, fate, toxicity and treatment in wastewaters. *Environment International*, 34(7), 1033-49.
- Tetreault GR, Bennett CJ, Shires K, Knight B, Servos MR and McMaster ME (2011). Inter-sex and Reproductive Impairment of Wildfish Exposed to Multiple Municipal Wastewater Discharges. *Aquatic Toxicology*, 104, 278-290
- Sonthheimer H., Crittenden J.C and Summers S (1988). Activated carbon for water treatment, *DVGW-Forschungsstelle am Engler-Bunte Institut der Universität Karlsruhe (TH), Germany*
- Tetreault GR, Bennett CJ, Shires K, Knight B, Servos MR and McMaster ME (2011). Inter-sex and Reproductive Impairment of Wildfish Exposed to Multiple Municipal Wastewater Discharges. *Aquatic Toxicology*, 104, 278-290
- Tetreault GR, Brown CJM, Bennett CJ, Oakes KD, McMaster ME and Servos M (2011). Fish community responses to multiple municipal wastewater inputs in a watershed. *Integrated Environmental Assessment and Management* 9(3)
- Toles C. A, Marshall W.E, Johns M.M, Wartelle L.H and McAloon A (2000). Acid-activated carbons from almond shells: Physical, chemical and adsorptive properties and estimated cost of production', *Bioresource Technology*, 71(1), pp. 87-92. doi: 10.1016/S0960-8524(99)00029-2.
- Tortajada C (2021). Water reuse to address water security. *International Journal of Water Resources Development* 2021, Vol. 37, No. 4, 581-583, <https://doi.org/10.1080/07900627.2021.1928911>
- Toze S (2006). Reuse of effluent water—benefits and risks, *Agricultural water management*, 80(1-3), pp.147-159.
- Trujillo, E. M., T. H. Jeffers, C. Freguson, and H. Q. Stevenson (1991) Mathematically modelling the removal of heavy metals from a waste water using immobilized biomass. *Environ. Sci. Technol.* 25: 1559-1565.
- Vassileva P, Tzvetkova P, Lakov L and Peshev O (2008). Thiouracil modified activated carbon as a sorbent for some precious and heavy metal ions. *Journal of Porous Mater.*, 15, pp. 593-599.
- Vinodhini V and Das N (2010). Packed bed column studies on Cr (VI) removal from tannery wastewater by neem sawdust. *Desalination*, 264(1-2), pp.9-14.
- Vitidsant T, Suravattanasakul T and Damronglerd, S (1999). Production of activated carbon from palm-oil shell by pyrolysis and steam activation in a fixed bed reactor. *Science Asia*, 25(4), pp.211-222.
- World Bank (2018). Wastewater: From waste to resource. Water Global Practice. The Case of Durban, South Africa.
- World Health Organization (WHO) (2013). State of the Science of Endocrine Disrupting Chemicals.

APPENDICES

APPENDIX A LABORATORY SCALE STUDIES

A.1 Analytical tests for Activated Carbon Characterisation

Analytical techniques such as scanning electron microscopy (SEM), Fourier-transform infrared (FTIR) spectroscopy, energy dispersive X-ray spectroscopy (EDS), Raman spectroscopy, thermogravimetric analysis (TGA), and Brunauer-Emmett-Teller (BET) are employed to determine the surface properties and thermal stability (TGA) of activated carbons. An overview of the techniques is given below.

Scanning Electron Microscopy (SEM)

Scanning electron microscopy is a surface imaging technique used to examine and analyse microstructure morphology and characterize chemical composition as well as providing information about surface topography, crystalline structure and electrical behaviour. As a result, it is not only one of the most versatile instruments available but also one of the leading instruments for insitu analysis of micro areas (K D Vernon-Parry, 2000; Zhou et al., 2007; Zhao and Li, 2018). SEM provides the ability to visually detect pores, crevices and surface deposits (Novak et al., 2019). The advantages of SEM include having a large depth field which ensures that most of the specimen surface is in focus, high magnification and resolution, strong stereoscopic vision, the ability to switch between different techniques allowing for a cross-correlation of information, no destruction of specimen during evaluation, and ease of preparation of specimen for evaluation (K D Vernon-Parry, 2000). A scanning electron microscope (SEM) creates an image by projecting a focused beam of electrons to systematically scan across the surface of a specimen, causing the specimen and electrons to interact, leading to the production numerous signals which are used to gather information regarding surface composition and topography (Zhou et al., 2007).

Fourier-Transform Infrared (FTIR) Spectroscopy.

Fourier transform infrared spectroscopy is a non-invasive analytical technique that uses infrared light to scan and obtain chemical properties of samples in situ. As a form of vibrational spectroscopy, the FT-IR spectrum displays the molecular structure as well as the molecular environment. This technique works by exposing the sample to infrared radiation, which is absorbed by the sample stimulating vibrational motion by the transfer of energy, thereby producing spectral bands which are characterized by amplitude and frequency. Infrared radiation with a wave number range of between 4000 and 400 cm^{-1} is emitted by a blackbody source, then interferometer inside the spectrophotometer, measures the energy transmitted to the sample and then encodes the spectral signals and transmits them through the surface of the sample, where specific energy signals are absorbed. In time, the infrared beam passes through the detector, onto the processing computer for Fourier transformation of energy signals. (Sacksteder and Barry, 2001; Undavalli, Khandelwal and Fuels, 2021). The unique spectral absorption bands can be associated with fundamental vibrations which correspond to certain functional groups (Berthomieu and

Hienerwadel, 2009). Of the infrared based dispersive spectroscopy instruments, FT-IR is one of the most preferred because of its heightened sensitivity, precision, accuracy, speed, non-invasiveness and ease of operation. (Undavalli, Khandelwal and Fuels, 2021) The use of FT-IR spectroscopy covers a variety of applications such as the identification of unknown compounds and characterization of components in mixtures (e.g. liquids, solids, or films).

Energy Dispersive X-ray spectroscopy (EDS)

The energy dispersive X-ray spectroscopy EDS, which at times is referred to as EDX, is a technique that is used in conjunction with scanning electron microscopy and is widely applied for elemental analysis and chemical composition determination, associated with electron microscopy (Torres-Rivero et al., 2021). This technique is dependent on the characteristic X-rays emitted by a specimen. The investigated sample is irradiated by stream of high energy charged particles (electrons or protons). An electron from a higher binding energy electron level falls into the core hole and an X-ray with the energy of the difference of the electron level binding energies is emitted, and a spectrum that depicts the peaks correlated to the elemental composition of the investigated sample is displayed (Colpan et al., 2018).

The elements in an investigated sample are determined by the energies of the X-rays emitted from the area being excited by the high energy electron beam. The rate at which the characteristic X-rays are determined can be used to take the measurement of the elements present in sample. Though the EDS system is able to provide information regarding present chemical elements in the specimen it cannot identify the molecular structure. Applications of EDS are typically in quality control, material research, forensic science and failure analysis (Bergström, 2015).

RAMAN Spectroscopy

Raman spectroscopy is a non-destructive spectroscopic technique analyse vibrational, rotational, and other low-frequency modes in a material system. It relies on a laser in the visible, near infrared, or near ultraviolet range to disperse Raman scattering of monochromatic light. The energy laser photons are shifted up and down as a result system excitations being absorbed or emitted by laser light. This shift in energy provides information about photon modes in the system (Bergström, 2015). Raman spectroscopy has become one of the most sensitive analytical techniques due to recent developments. Not only does it achieve very low detection limits, it also allows easy identification of specimen by giving vibrational information which can be treated as its fingerprint. It allows for the study of complex samples as its signals are often characteristic for analysed compounds (Kudelski, 2008). Its non-destructive character, ability to deliver specific chemical identification and wide range of instrumental and sampling methodologies allows for it's a wide range of application including; chromatographic detection, environmental monitoring, and materials chemistry (Lyon *et al.*, 1998). The Raman Effect is the process by which most photons are elastically scattered when light is scattered from a molecule. The energy difference between the incident photon and the Raman scattered photon is equal to the energy of a vibration of the scattering molecule.

The Raman spectrum is made up of a plot of intensity of scattered light versus energy difference. Raman spectroscopy works by irradiating a spot on the sample being tested with a laser beam. The Raman effect then produces scattered radiation which includes information about the molecular vibrations and rotations, which depend on the particular atoms or ions that comprise the molecule (Bergström, 2015).

Thermogravimetric analysis (TGA)

Thermogravimetric analysis is a quantitative chemical engineering experimental technique, applied to derive mass changes and thermal stabilities of samples as a function of increasing temperature. (Bottom, 2008). The temperature in the furnace can be ramped up as high as 1600 C depending on the information required about the sample, in addition the atmosphere in which the experiment is carried out can be reactive, inert or oxidizing (Saadatkah *et al.*, 2020). The technique provides information to do with some physical and chemical phenomena such as:

- Decomposition or carbonization which is carried out in an inert environment and results in the formation of gaseous products.
- Oxidative degradation which occurs in air or oxygen environment
- adsorption and desorption of gases and other volatile components
- vaporization of water

Solid-gas reactions where a products evolve or where hydrogen gas is purged causing a reduction reaction to occur (Bottom, 2008). However, the technique cannot provide information for reactions in which mass remains unchanged, phase transitions or polymorphic transformations. The thermogravimetric analyser is fitted with a precise microbalance coupled with a sample pan closed inside a temperature programmed and controlled furnace. The mass changes of the sample under investigation are represented graphically by a thermogram which depicts the mass change vs temperature or time. The thermogram is unique for each sample and it provides information such as the thermal and oxidative stability, moisture and volatile content, decomposition kinetics, component composition and sample lifetime. Thermograms generally consist of multiple stage or sections; at temperatures below 150 °C, volatile compounds, trapped gases and physisorbed water are usually lost. Between 150 °C and 250 °C, a loss of mass occurs due to the loss of chemisorbed water and volatile decomposition products. Compounds begin to decompose above 250 °C, and materials such as metals and non-volatile inorganic ashes remain above the end temperature. Metallic compounds gain mass and increase the oxidation state when an oxidizing environment is created (Saadatkah *et al.*, 2020) .

Brunauer-Emmett-Teller (BET)

The Brunauer–Emmett–Teller (BET) Method developed by Brunauer, Emmett and Teller in 1938, is an analytical technique used to measure the specific surface area of a material based on its multilayer adsorption of nonreactive gas molecules such as nitrogen at 77K or argon at 87K at a range of pressures (Brunauer, Emmett and Teller, 1938; Sinha *et al.*, 2019). During the procedure, known amounts of a

noncorrosive gas are released into a cell containing the material to be analysed in steps. A partial vacuum is then created to achieve saturation pressure after which no more adsorption takes place regardless of any increases in pressure. The pressure changes due to the adsorption process are monitored by pressure transducers. Adsorption layers are formed and then the sample is removed from the gaseous atmosphere and heated to release the adsorbed gaseous molecules so that they can be quantified. A BET isotherm is formed from the collected data and a linearized plot of the gas adsorbed as a function of relative pressure is displayed making it possible to determine the surface area of the material (Hwang and Barron, 2011).

A.2 Characterization of Activated Carbons

Characterization tests were conducted on both GAC and HC-AC. The activated carbons were tested for (i) moisture content, (ii) ash content, (iii) iodine number, (iv) particle size, (v) attrition, (vi) bulk density, (vii) pH and (viii) surface area. The moisture content and ash content were determined using the procedure adopted from (CEFIC, 1986). The iodine test was conducted as outlined in the American Society for Testing and Materials (ASTM D4607-94, 2006). The particle size distribution was determined as outlined in the American Water Works Association (AWWA B604-74) (Comm Rep, 1974). The attrition test was determined as reported by (Toles et al., 2000). The bulk density was determined as outlined in (ASTM D2854-96, 2000). The pH was determined as outlined in (Singh et al., 2017b). Analytical techniques such as scanning electron microscopy (SEM), Fourier-transform infrared spectroscopy (FTIR), energy dispersive X-ray spectroscopy (EDS), Raman spectroscopy, thermogravimetric analysis (TGA), and Brunauer-Emmett-Teller (BET) were used to determine the surface properties and thermal stability of the activated carbons. Results attained from these tests are summarise in Table 3-2.

Table 5-1: Properties of adsorbents

Properties	GAC		HC-AC
Moisture content (%)	3.78		3.36
iodine number (mg/g)	1198.48		110.66
Surface area (BET N ₂) (m ² /g)	1050 ^a		97.20
Particle size (µm)	850-1180		75-150
Attrition (%)	32		-
Bulk density (g/cm ³)	0.48		0.31
Ash content (%)	2.4		62.8
pH	5.1		2.6

^a value from supplier

Moisture Content (%):

The moisture content of GAC and HC-AC were 3.8 and 3.4% respectively. The moisture content of the two activated carbons is less than 8%, which is ideal as stated in the GAC requirements by the American Water Works Association (AWWA) (Comm Rep, 1974).

Iodine Number

The iodine number is a parameter used to measure the microporosity of activated carbon and to indicate the surface area with good precision. It is also used as a measure of the activation level of an adsorbent (Saka, 2012). The American Society for Testing and Materials (ASTM D4607-94, 2006) procedure defines it as the amount of iodine adsorbed in milligrams per gram of carbon at a residual iodine concentration of 0.02 N. The iodine numbers obtained for GAC and HC-AC were, 1198 and 111 mg/g respectively. The iodine number of GAC is within the range of 500-1200 mg/g which is indicative of a high degree of activation (Saka, 2012). Applying the same measure, it can be said that HC-AC has a low level of activation. Though the relationship between the iodine number and the surface area cannot be generalized as per the American Society for Testing and Materials (ASTM D4607-94, 2006) procedure, the results obtained support the BET results which show that the surface area of the adsorbents is in the order of GAC > HC-AC.

Ash Content and Surface Area

When compared with HC-AC which has a high ash content (62.8%) and a low surface area (97 m²/g), GAC has a significantly lower ash content, (2.7%) and a high surface area (109 m²/g). The link between high ash content and low surface area has been vastly discussed in literature and has been mainly attributed to the blockage of pores by the ash (Bernardo *et al.*, 2020; Jawing *et al.*, 2021; Mkungunugwa *et al.*, 2021). The high ash content values for HC-AC in this study are fairly comparable to values reported in literature for sludge derived adsorbents (Smith *et al.*, 2009; Pedroza *et al.*, 2014; Almahbashi *et al.*, 2021). In this regard, Rengaraj *et al.*, (2002) and Mkungunugwa *et al.*, (2021) have also reported a correlation between high ash content and low carbon content.

pH

The measured pH for GAC and HC-AC were 5.1 and 2.6 respectively. Most activated carbons found in literature have alkaline pH values as a result of washing with deionized water after activation and carbonization to neutralize the pH (Hameed, Din and Ahmad, 2007; Ebrahimian Pirbazari *et al.*, 2014). The presence of the sharp peak at 1710 cm⁻¹ on the IR spectrum of HC-AC is indicative of an oxygen containing acidic surface functional group (carboxyl group) which could have contributed to the low pH value obtained (Chen, Jeyaseelan and Graham, 2002; Shen, Li and Liu, 2012).

Bulk Density

The bulk density is an important parameter of activated carbon which is used to determine the volume capacity of a carbon material. A high density is generally associated with a carbon's ability to hold more adsorbate per unit volume during adsorption (Asuquo *et al.*, 2017; Ravichandran *et al.*, 2018). The bulk density values of GAC and HAC were determined as 0.48 and 0.31 g/cm³ respectively. The American Water Works Association (AWWA, 1991) has set a lower limit of 0.25 gm/l for activated carbon to be of practical use (Qureshi *et al.*, 2008; Yakout *et al.*, 2015; Ravichandran *et al.*, 2018). In this regard, all two carbon materials have bulk density values above 0.25 gm/l, an acceptable value for use of the adsorbent in wastewater treatment. The bulk density of a carbon material is highly dependent on its precursor and treatment method used (Chowdhury, 2013). Adsorbents derived from woody biomass have been reported as having higher bulk densities when compared to urban and industrial solid wastes such as sludge (Tomczyk, 2020). However, having a bulk density below 1.2 g/cm³ has been reported as being indicative of an adsorbent with small particle sizes which improves its adsorption capacity (Moyo *et al.*, 2013; Guyo and Moyo, 2017).

Attrition

Resistance to attrition is among the parameters of importance considered when selecting granular adsorbents for wastewater treatment (Dąbrowski, 2001). This provides information on the mechanical strength and ability to resist disintegration of the carbon during transportation, normal handling and regeneration (Ravichandran *et al.*, 2018). Due to the nature of the particles of granular carbons and their applications, there is a high possibility of intraparticle abrasion (Toles *et al.*, 2000) which could lead to the formation of fine particles associated with low attrition resistance (high losses) which can result in the blockage of systems (Asuquo *et al.*, 2017). The attrition test was only performed on GAC. GAC exhibited attrition of 32%. The attrition test could not be conducted for HC-AC since HC-AC was in powdered form (fine in nature) and it would be difficult to determine loss on attrition accurately.

Particle Size

To determine the particle size of the adsorbents sieves with openings ranging from 425 to 2 360 µm were used to determine which sieves would have the largest retention of GAC when 100 g was. It was found that 91.6% of the carbon was retained on the 850 and 1180 µm sieves collectively therefore this portion was used for all tests. The particle size of HC-AC was determined using sieves ranging from 45 to 150µm, 99.8% of the carbon was retained on the 75 and 150 µm sieves collectively and this portion was used for testing.

Scanning Electron Microscopy (SEM)

The scanning electron micrographs of GAC and HC-AC were carried out at three different magnifications, 500,5kX, and 50kX at a scale of 1, 10, and 100 µm. The micrograph of GAC shows a rough surface with numerous crevices and pores present for possible the dye and metal adsorption. high surface roughness and macro porosity (>50nm) are important factors for adsorption and can be attributed for GACs' high

surface area, making it a good adsorbent (Mansour *et al.*, 2020). The derived carbon, HC-AC is characterized by a rough, uneven, fibrous surface with a wide variety of loose pores of different sizes that resemble canals. Similar micrographs were reported in studies dealing with sludge derived activated carbons (Li, Yue, Gao, Ma *et al.*, 2011; Pradhan, 2011; Oumabady *et al.*, 2021).

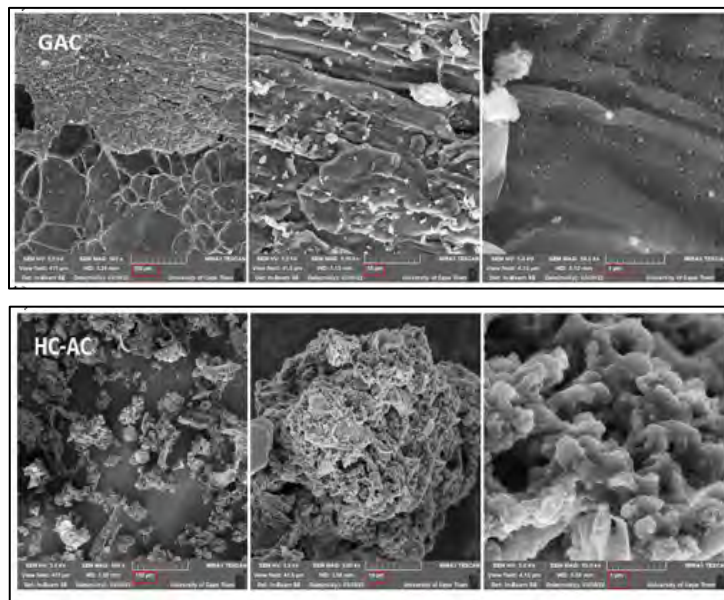


Figure 5.1: Scanning electron micrographs of C-GAC and HAC

Raman Spectroscopy

The Raman spectra was recorded over a range of 10-3000 cm^{-1} . Three distinct peaks were observed on all the carbon samples as can be seen in Figure 5.1. The Raman spectra of the two carbon samples GAC, and HAC have bands present at 1336 and 1368 cm^{-1} respectively. Bands in this range are referred to as the D band peaks which highlight defects and disorder in the crystalline structure of the carbon (Chia *et al.*, 2012; Liu *et al.*, 2017; Medhat *et al.*, 2021). Sharp peaks are observed around 1586 and 1597 cm^{-1} for the samples C-GAC and HAC respectively. Peaks in this range are distinctive of the graphitic arrangement known as the G-band which is the primary signature for sp^2 carbon in Raman spectra. The G-band indicates that pairings of sp^2 atoms in both rings and chains are stretched by a c-c link (Chia *et al.*, 2012; Medhat *et al.*, 2021). Ill-defined second order Raman peaks were observed around 2879 and 2948 cm^{-1} for C-GAC and HAC respectively. Peaks within this range are referred to as 2D bands and they identify these carbons as materials with low order in aromatic domains but rich in sp^3 (González-García, 2018; Giorcelli *et al.*, 2021). The combination of D and G bands found are proof that the carbons are polyaromatic and graphitic (Chia *et al.*, 2012). In GAC, the D band is more intense than the G band which is indicative of the disorder of a large number of carbon atoms. For HC-AC the D band is less intense than the G band inferring just a slight disorder of the carbon atoms. The measure of the extent of disorder in the carbon materials is expressed by the intensity ratio between the D and G band ($R = I_D/I_G$) (Medhat

et al., 2021). The intensity ratio of the activated carbons, GAC and HC-AC are 0.84 and 0.86 respectively. The similarity of the values suggests that the carbons have similar graphitic structures (Kristianto *et al.*, 2016)

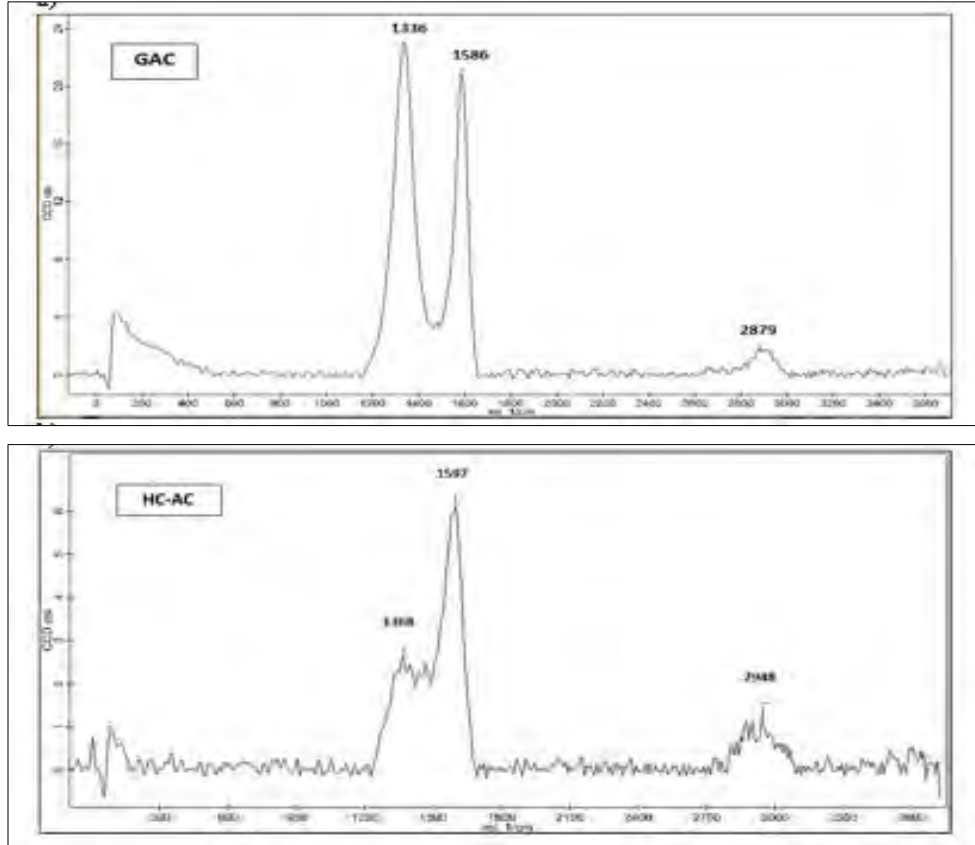


Figure 5.2: Raman spectra of GAC and HC-AC

Energy Dispersive Spectroscopy (EDS) mapping

Five spectra were marked on each activated carbon and the elemental results of one were displayed. The main elements observed in the activated carbons are carbon and oxygen as can be seen in Figure 5.2. There was a greater ratio of carbon compared to oxygen in the GAC samples while the ratio observed in HC-AC was almost 1:1. C-GAC and HAC contained 78.8% and 43.4% carbon and lasty HC-AC (43.4%). Though HC-AC contained the least carbon of the three it contained the most oxygen (40.5%) which was almost thrice the amount of oxygen in GAC (13.5%).

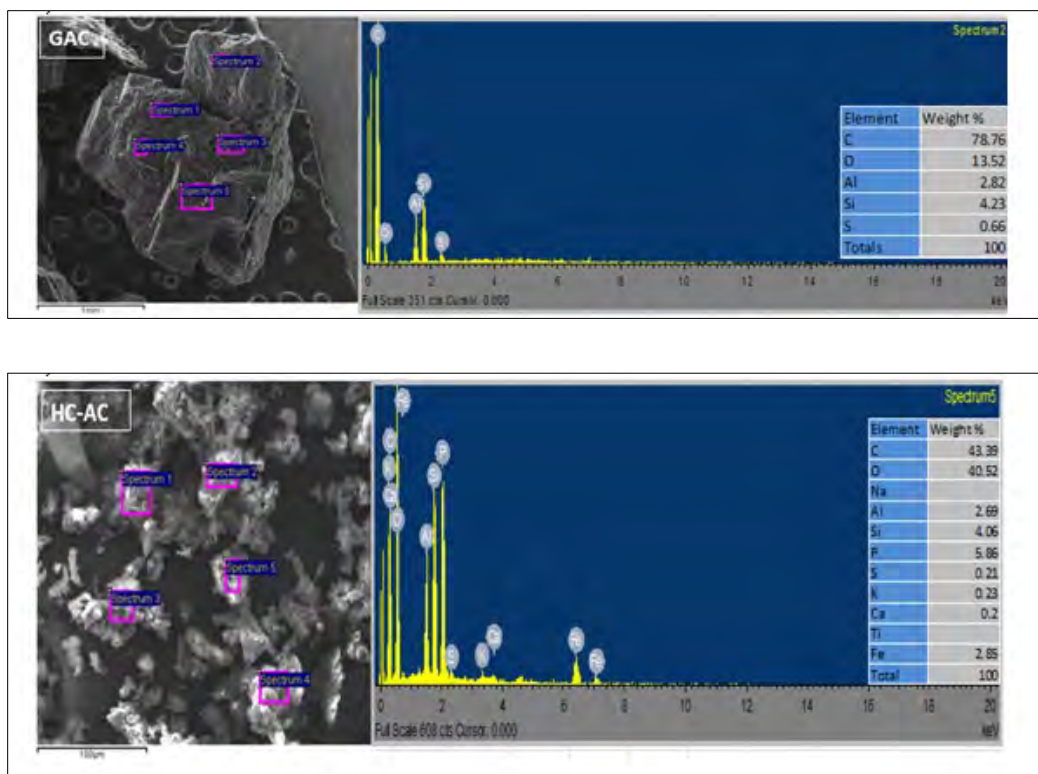


Figure 5.3: EDS spectrum of GAC, and HC-AC

Fourier Transform Infrared (FT-IR) Spectroscopy

The FT-IR spectra of the two carbons are displayed Figure 5.3 below. The presence of surface functional groups is an important characteristic of adsorbents since the functional groups influence the adsorptive capacity (Onundi *et al.*, 2010; Yagub, Sen and Ang, 2014; Tomczyk, 2020) by complexation, electrostatic attraction and ion exchange between the surface groups on the adsorbent and the adsorbate in solution (Ullah *et al.*, 2020; Dutta *et al.*, 2021). In some cases the presence of functional groups has been reported as being more important to the removal process than the surface area (Saleem *et al.*, 2019). The presence of oxygen containing functional groups on the surface of adsorbents such as the carboxyl and hydroxyl groups has been identified as having a strong influence on their adsorption performance (Gupta and Suhas, 2009; Badawi, Abd Elkodous and Ali, 2021). From Figure 5.3, it is clear that HC-AC contained both the hydroxyl and carboxyl peaks as indicated by the sharp peaks at 3406cm^{-1} and 1102cm^{-1} re. GAC, also displayed peaks within the ranges of $1000\text{-}1200\text{cm}^{-1}$ and $3200\text{-}3500\text{cm}^{-1}$ similar to HC-AC, but these peaks were shorter and not as pronounced as those of GAC.

A.3 ADSORPTION EXPERIMENTS

Effect of Initial Concentration

A series of batch adsorption experiments with initial concentrations of 2.5, 5 and 7.5 mg/L of methylene blue solution at optimal pH of 6.5 and using 0.2 g/L of adsorbent, were carried out to investigate the effect of the initial concentration on the adsorption capacity and the removal percentage of methylene blue. The adsorbate concentration which showed the highest removal capacity as calculated was chosen as the optimum concentration and was maintained in the subsequent batch studies. Parameters for this test are displayed in Table 5-2 below.

Table 5-2: Parameters for the methylene blue initial concentration test

		<u>Adsorbents</u>	
		GAC	HC-AC
Fixed parameters	Carbon dosage (g)	0.2	0.2
	pH	6.5	6.5
	Volume (ml)	100	100
Varied parameters	Concentration (mg/L)	2.5-5-7.5	2.5-5-7.5

Effect of contact time

The effect of contact time on the adsorption of methylene blue in the solution was investigated at time intervals falling in the range of 5-370 min after contact with the adsorbent. The pH was maintained at 6.5. The time required to reach equilibrium was also determined in this phase of the experiments. Parameters for this test are displayed in Table 5-3 below.

Table 5-3: Parameters for the methylene blue contact time test

		<u>Adsorbents</u>	
		GAC	HC-AC
Fixed parameters	Carbon dosage (g)	0.2	0.2
	pH	6.5	6.5
	Volume (ml)	100	100
Varied parameters	Time (min)	5-370	5-370

The effect of contact time on the removal of methylene blue dye (MB) is shown in Figure 5.4 below.

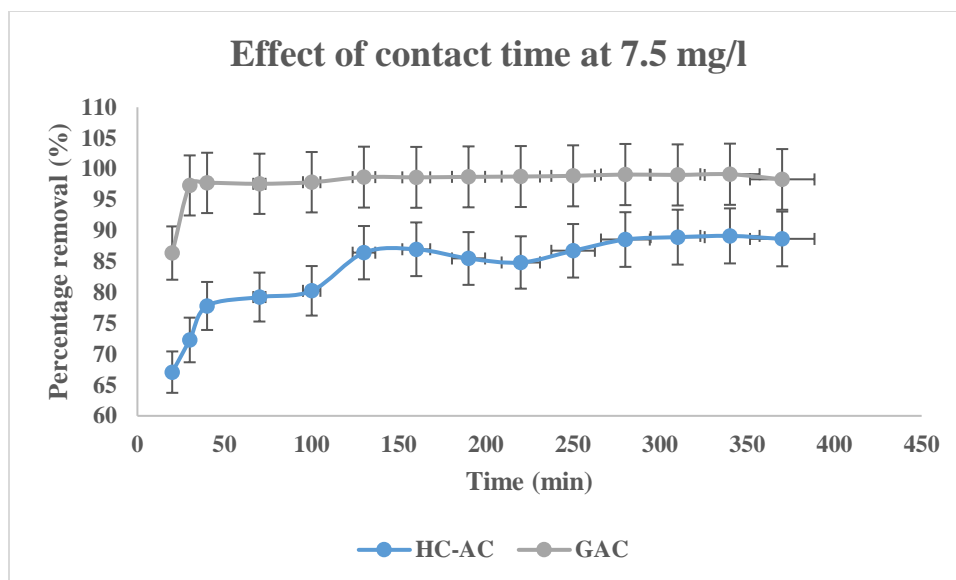


Figure 5.4: Effect of contact time on adsorption of MB (initial concentration: 7.5 mg/L; solution volume: 100 mL, contact time: 370 min; adsorbent dose: 0.2 g/100 mL; pH 6.5).

The trends indicate an increase in dye removal with time for both HC-AC and GAC, until a certain point in time after which the removal becomes constant. This point is referred to as the equilibrium time and it is described in literature as a state at which the amount of dye being absorbed onto the activated carbon is equal to the amount being desorbed from the adsorbent (Bello *et al.*, 2008). The adsorbents maximum capacity for adsorption under the employed operating conditions is taken as the quantity of dye absorbed at the equilibrium time (Hameed, Din and Ahmad, 2007). The rapid rate of methylene blue adsorption during the initial stages might be due to the high solute concentration gradient and the availability of vacant active sites on the adsorbent (Pathania, Sharma and Singh, 2017). Gradually, the number of vacant sites on the adsorbent surface decreases leading to a reduction in the rate of adsorption and constant removal values indicating that the system has reached equilibrium (Singh, Sidhu and Singh, 2019). The percentage removal was observed as stabilizing around 130 and 280 minutes for GAC and HC-AC respectively. These times were taken as the equilibrium times and subsequent optimization experiments were conducted at the above-mentioned times for each adsorbent.

Effect of pH

The determination of the optimum pH for the adsorption process was investigated as follows: 30 mL solutions of the optimized methylene blue concentration determined in step 1 were added to 100 mL conical flasks containing a fixed amount of adsorbent (0.06 g). The pH of the solutions was varied between

2 and 11 using the prepared 0.1 M HCL and NaOH solutions Parameters for this test are displayed in Table 5-4: parameters for the methylene blue pH test below.

Table 5-4: parameters for the methylene blue pH test

		Adsorbents	
		GAC	HC-AC
Fixed parameters	Carbon dosage (g)	0.06	0.06
	Concentration (mg/L)	optimum	optimum
	Volume (ml)	30	30
	Time (min)	equilibrium	equilibrium
Varied parameters	pH	2-3-4-...11	2-3-4-...11

Figure 5.4: clearly show that the adsorption of MB is favourable under alkaline conditions.

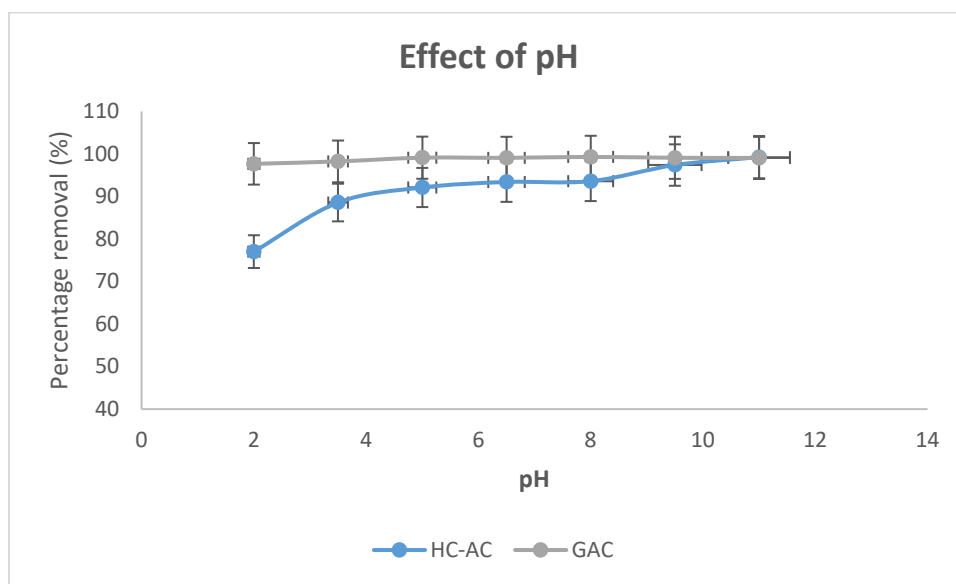


Figure 5.5: Effect of pH on adsorption of MB (initial concentration: 7.5 mg/L; solution volume: 100 mL, contact time: 130 min for GAC, 160 min AW-AC and 280 min for HC-AC; adsorbent dose: 0.2 g/100 mL); pH: 2-11).

The effect of pH on methylene blue adsorption was investigated for values between the pH ranges of 2-11. The percentage removal of MB by GAC increased from 97.7% at pH 2 to attain maximum removal of 99.1% at pH 8. This slight increment over the pH range indicates that the adsorbent performed reasonably effectively across the whole pH range studied. However, the derived carbon HC-AC, attained its maximum removal of 99.0% at pH of 11 which was similar to the optimum pH for MB removal reported by Fan *et al.*, (2017). This could be as a result of the net negative charge that the adsorbent surface develops due to its

deprotonation at high pH (Patawat *et al.*, 2020) resulting in the presence of negatively charged functional groups such as the carboxyls and hydroxyls (Pirbazari et al. 2014; Singhet al. 2019) which then enhance the electrostatic attraction between the MB dye and the adsorbent (Pathania et al. 2017). The reason for the low removal of the cationic dye in the lower pH range, has been attributed to the abundant presence of hydrogen ions which then compete with the dye molecules for vacant active sites (Yagub et al. 2012; Pirbazari et al. 2014; Singh et al. 2019). Another reason for this observation in the lower pH range has been ascribed to the release of positively charged ions by the cationic dye when it is dissolved in water, leading to electrostatic repulsion between the ions and the positively charged adsorbent, thus lowering removal (Pirbazari et al. 2014; Pathania et al. 2017; Patawat *et al.*, 2020). The increased percentage removal observed at higher pH ranges has been ascribed to the electrostatic attraction between the positively charged ions released by the cationic methylene blue dye when it dissolves in water and the surface of the adsorbents that become negatively charged due to deprotonation at increased pH levels (Pirbazari et al. 2014; Pathania et al. 2017; Patawat *et al.*, 2020). The presence of numerous functional groups on the surface of the activated carbons as confirmed by FTIR characterization suggest that the functional groups on the surface of the adsorbent play a large role in the adsorption of MB as they undergo protonation /deprotonation depending on the solution pH. (Pirbazari et al. 2014). These results also confirm that pH is an important parameter for MB dye adsorption as it can be seen that the removal of HC-AC was greater than that of GAC. and AW-AC when its optimum pH of 11 was reached.

Effect of adsorbent dosage

The optimum dosage of the adsorbents was determined by fixing the following parameters: contact time, initial adsorbate concentration, pH, and the volume of solution. and varying the amount of adsorbent in each flask. The adsorbent dosage was varied within a range of 0.03 g and 0.3 g. The optimum adsorbent dosage was chosen and maintained in the following experiments.

Table 5-5: parameters for the methylene blue dosage test

		Adsorbents	
		GAC	HC-AC
Fixed parameters	pH	optimum	optimum
	Concentration (mg/L)	optimum	optimum
	Volume (ml)	30	30
	Time	equilibrium	equilibrium
Varied parameters	Adsorption dosage (g)	0.03-0.3	0.03-0.3

The dose for each adsorbent was varied between 0.1 to 1 g /100 ml as can be seen in Figure 5.6.

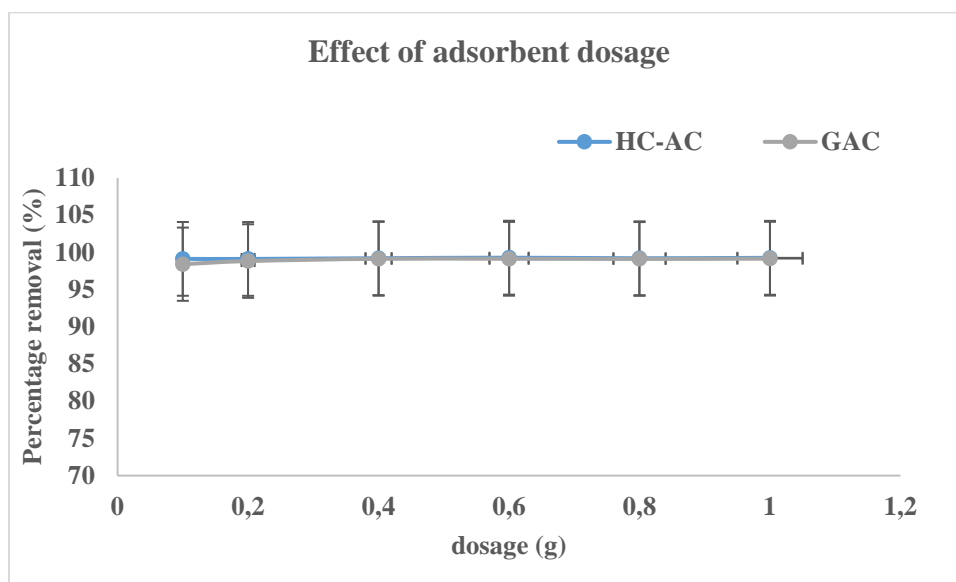


Figure 5.6: Effect of adsorbent dosage on adsorption of MB (initial concentration: 7.5 mg/L; solution volume: 100 mL, contact time: 130 min for GAC, 160 min for AW-AC and 280 min for HC-AC; adsorbent dose: 0.1-1(g/100 ml); pH 8 for GAC and AW-AC, pH 11 for HC-AC).

The optimal dosage is useful to estimate the cost of adsorbent to be used for each unit of the solution to be treated (Alam *et al.*, 2021). The removal of MB by HC-AC appeared to be almost constant and approach 100% removal over the dosage range. Its highest removal was observed at 0.6 g at 99.3%. It can be said that removal of MB by HC-AC was more pH dependent than it was dosage dependent as it achieved high removal even at low dosage. HC-AC showed higher removal than GAC. The removal of GAC showed a slight increase from 98.4% at 0.1 g to 99.0% at 0.4 g. 0.4 g was taken as the optimal dose for GAC as no significant change in removal was observed beyond 0.4 g. The increase in removal as the dosage increased could be attributed to the availability of sufficient adsorption sites as well as that of specific surface area

(Fan *et al.*, 2017; Pathania *et al.* 2017). However, the lack of significant change in percentage removal past a certain dosage increment has been reported as being the result of adsorbent particle aggregation (Pathania *et al.* 2017) or the saturation of adsorbent sites by the dye (Fan *et al.*, 2017). The percentage removal of the dye at the optimum conditions was in the following order: HC-AC (99.21%)> GAC (99.13%).

Single Metal Lead Adsorption Studies

Lead

Lead (Pb) is a chemical element with an atomic number of 82. Its presence in the aqueous environment is due to its release from natural sources (mineral deposits) as well as untreated effluent from industrial activity (such as the manufacture of lead-acid batteries, solders and alloys) (Papanikolaou, Hatzidaki and Belivanis, 2005; Herschy, 2012). It is widely used due to its important physio-chemical properties such as resistance to corrosion, poor conductivity, and malleability. Consequently, it is a persistent poison that is not biodegradable and accumulates in the environment as well as the human body where it affects multiple body functions such as the neurodevelopment in children, fertility, as well as cardiovascular function leading to death. Its main channels of entry into the human body are via the ingestion of food or water that are contaminated with lead (Herschy, 2012; Wani, Ara and Usmani, 2015). Due to its toxicity at low concentrations the World Health Organization and the South African National Standard (SANS) have set the guideline value for lead in drinking water at 10µg/L (Herschy, 2012; SANS 241, 2015).

Working concentrations were prepared for the adsorption tests by diluting the prepared stock solution containing the lead (II) ions with deionized water. The concentrations of the solutions were obtained by ICP-OES. The effect of pH, adsorbent dosage, initial concentration and contact time were investigated in a similar approach as for the methylene blue adsorption studies. Table 5-6 show the parameters for each test that was conducted.

Table 5-6: Parameters for the Lead pH test

		Adsorbents	
		GAC	HC-AC
Fixed parameters	Adsorbent dosage (g)	0.06	0.06
	Concentration (mg/L)	5.3	5.3
	Volume (ml)	30	30
	Time (min)	120	120
Varied parameters	pH	2-3-4-5-6-7-8	2-3-4-5-6-7-8

The solution pH is a crucial parameter in adsorption as it not only facilitates the removal of lead by adsorption by influencing the properties of the metal ion, but also plays a significant role by influencing the surface charge of the adsorbent (Alghamdi *et al.*, 2019; Onwordi *et al.*, 2019; Kavand *et al.* 2020; Mandal *et al.*, 2021). The effect of pH on the removal of lead by the three activated carbons is shown in Figure 5.7

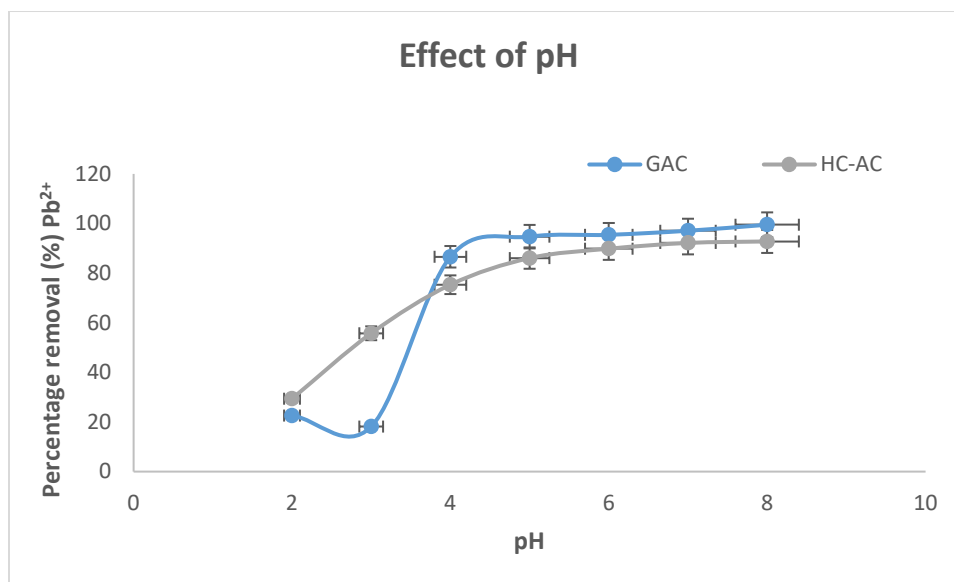


Figure 5.7: Effect of pH on the adsorption of Pb (II) ions (initial concentration: 5.3 mg/L; solution volume: 100 mL, contact time: 120 min; adsorbent dose: 0.2 g/100 mL; solution pH: 2-8).

The removal of lead was the lowest in the low pH range (pH 2-4). This has been widely discussed in literature and is attributed to the competition for active sites by the Pb^{2+} ions and the H^+ ions which are highly concentrated in acidic environments (Mohan *et al.*, 2007, 2020; Onundi *et al.*, 2010; Boontham, 2016; Kavand *et al.* 2020). The gradual increase in pH saw an increase in adsorption of lead, owing to the negative charge of functional groups present on the surface of the adsorbents which made them readily available for lead adsorption (Guyo and Moyo, 2017). A pH of 7 was taken as the optimal value to attain

maximum lead adsorption for all three adsorbents, as it is believed that pH values greater than 7 facilitate the precipitation of lead ions into hydroxide species (Alghamdi *et al.*, 2019; Kavand *et al.* 2020; Mohan *et al.*, 2020; Mandal *et al.*, 2021).

Table 5-7: Parameters for the Lead adsorbent dosage test

		Adsorbents	
		GAC	HC-AC
Fixed parameters	pH	optimum	optimum
	Concentration (mg/L)	5.3	5.
	Volume (ml)	30	30
	Time (min)	120	120
Varied parameters	Adsorbent dosage (g)	0.03-0.3	0.03-0.3

The use of the optimum dosage of the adsorbent during the adsorption process, is crucial for the effective uptake of the lead ions as it ensures the availability of active sites that the ions have access to (Wahi, Ngaini and Jok, 2009; Tejada-Tovar *et al.*, 2022). Figure 5.8 shows how the removal efficiency of Pb (II) ions varied with adsorbents dosage for GAC and HC-AC.

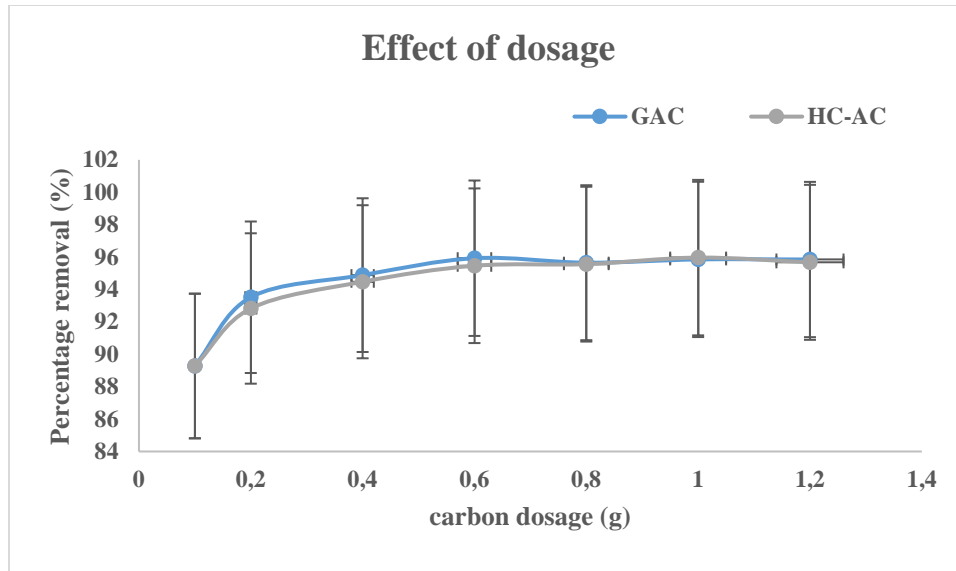


Figure 5.8: Effect of adsorbent dosage on the adsorption of Pb (II) ions (initial concentration: 5.3 mg/L; solution volume: 100 mL, contact time: 120 min; adsorbent dose: 0.1-1 g/100 mL; solution pH: 7).

GAC and HC-AC showed greater efficiency in the removal of lead ions when compared to AW-AC. As the adsorbent dosage increased from 0.1 to 0.6 g, the percentage removal of the lead ions increased from 89.3 to 95.9% for GAC, and 89.3 to 95.5% for HC-AC. This shows that the removal rate increased as the dosage of adsorbent increased. This phenomenon can be attributed to the increased availability of active sites or surface area, for the same quantity of adsorbate molecules, which facilitates better access for the Pb(II) ions onto the activated carbons adsorption sites (Moyo *et al.*, 2013; Onwordi *et al.*, 2019; Mandal *et al.*, 2021). Subsequent increases in adsorbent dosage after 0.6 g for GAC and HC-AC did not result in significant increases in the percentage removal of the Pb (II) ions. This could be attributed to the overcrowding of adsorbent particles present in the solution, causing the adsorption sites to overlap (Bernard, Jimoh and Odigure, 2013; Onwordi *et al.*, 2019).

Table 5-8: Parameters for the Lead initial concentration test

		Adsorbents	
		GAC	HC-AC
Fixed parameters	pH	optimum	optimum
	Adsorbent dosage (g)	optimum	optimum
	Volume (ml)	30	30
	Time	120	120
Varied parameters	Concentration (mg/L)	1.9-14.3	1.9-14.3

Effect of initial concentration on adsorption of lead (II) ions

The starting concentration of the adsorbate serves as a crucial driving factor to overcome all Pb(II) mass transfer resistances between the solid and aqueous phases (Guyo and Moyo, 2017). It also governs the rate of the adsorption process, therefore, making it an important component to take into account for efficient adsorption. The effect of concentration on the adsorption process was tested for a concentration range of 1.9 to 14.3 mg/l. Figure 5.9 presents the variation of removal efficiency with concentration for GAC and HAC-AC.

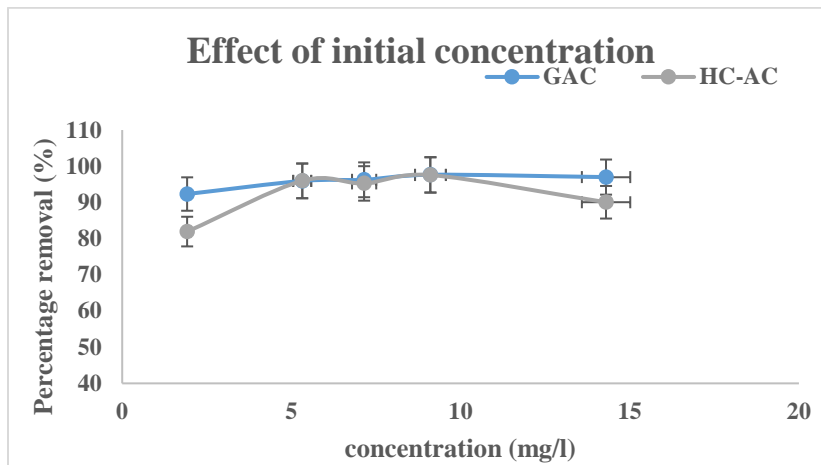


Figure 5.9: Effect of initial concentration on the adsorption of Pb (II) ions (initial concentration: 1.9-14.3 mg/L; solution volume: 100 mL, contact time: 120 min; adsorbent dose: 0.6 g for GAC and HC-AC, 0.8 g for AW-AC; solution pH: 7).

The percentage removal of the lead ions initially increased with an increase in concentration of lead ions for all adsorbents up until a concentration of 9.1 mg/l was reached. The percentage removal of the Pb (II) ions at 9.1 mg/l was 97.6% and 96.1% for GAC and HC-AC respectively. A further increment in concentration by 5 mg/l saw a decrease in metal ion uptake for both adsorbents. The observed phenomena can be linked to the strong interaction between the adsorbate and the numerous active sites of the adsorbent available for adsorption at lower adsorbate concentrations, hence higher removal (Guyo and Moyo, 2017). The decrease in removal at higher concentration can be attributed to the saturation of active sites as the amount of lead ions increases while the number of active sites on the activated carbon remains unchanged, resulting in a remnant of ions in solution after the adsorption process is complete (Moyo *et al.*, 2013; Musumba *et al.*, 2020). This decrease in removal at higher concentrations could also be explained by the involvement of active sites that are energetically less favourable to adsorption as the favourable sites will already be at capacity. Additionally, the increase in ion concentrations, results in high ion collision rates and high diffusion rates which lead to decreased removal (Musumba *et al.*, 2020).

Table 5-9: Parameters for the Lead contact time test

		<u>Adsorbents</u>	
		GAC	HC-AC
Fixed parameters	Carbon dosage (g)	0.2	0.2
	pH	6.5	6.5
	Volume (ml)	100	100
Varied parameters	Time (min)	5-370	5-370

Effect of contact time on adsorption of lead (II) ions

The effect of contact time experiment was conducted at a contact time ranging from 10-150 minutes using the optimum conditions (pH 7, adsorbent dosage of 0.6 g for GAC and HC-AC and initial concentration of 9.1 mg/l). The effect of the contact time on the percentage removal of lead is displayed in Figure 5.9

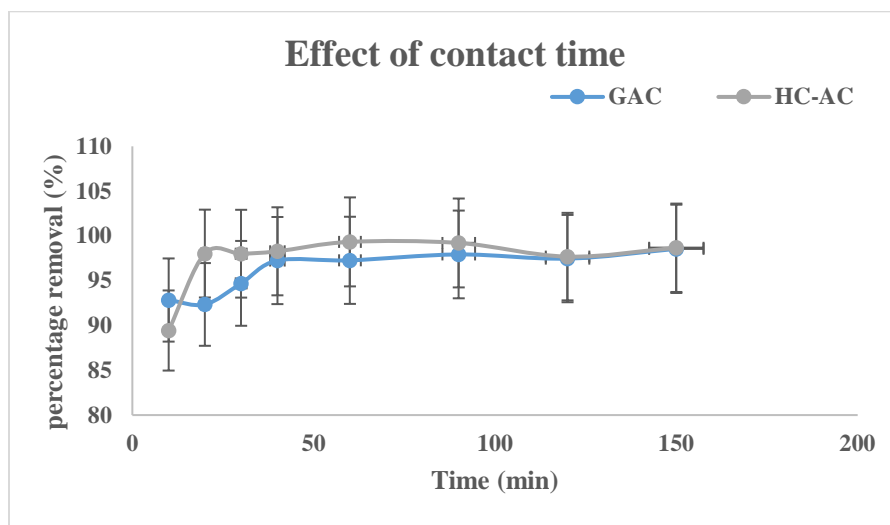


Figure 5.10: Effect of contact time on the adsorption of Pb (II) ions (initial concentration: 9.1 mg/L; solution volume: 100 mL, contact time: 150 min; adsorbent dose: 0.6 g for GAC and HC-AC, 0.8 g for AW-AC; solution pH: 7).

The adsorption was rapid in the initial stages. In the first 30 minutes GAC achieved a removal of 94.7%, while HC-AC achieved 98.0%. This observed trend showing rapid removal in the initial rate of adsorption may have been accelerated by the presence of a sufficient number of active functional groups and vacant active sites on the activated carbons exterior surface (Moyo *et al.*, 2013; Guyo and Moyo, 2017; Mandal *et al.*, 2021). It could also be explained as being a result of the concentration gradient between the adsorbate in solution and the quantity of vacant sites on the surface of the adsorbent (Acharya *et al.*, 2009; Onundi *et al.*, 2010). GAC reached equilibrium faster than HC-AC, from 40 minutes to 150 minutes the change in removal percentage was almost constant with a slight inflection at 150 minutes, indicating

that equilibrium had been achieved. HC-AC showed a slight decrease in uptake after 90 minutes which could be as a result of the saturation of the active sites after equilibrium has been reached (Guyo and Moyo, 2017). The increment of contact time after this point has been linked to a decrease in percentage removal due to reduction in available Pb (II) ions to bind to the remaining active sites (Mandal *et al.*, 2021).

Multi-ion Adsorption Studies using Wastewater from BNR Plant

Once the optimum adsorbent dosage was determined, further batch adsorption experiments were carried out to evaluate the adsorption of Pb (II) and other heavy metals from a multi-metal solution system. The effect of contact time and the adsorbent dosage on percentage pollutant and the adsorption capacity was investigated. Table 5-10 and Table 5-11 show the parameters for each test that was conducted.

Table 5-10: Parameters for adsorbent dosage test using wastewater.

		<u>Adsorbents</u>	
		GAC	HC-AC
Fixed parameters	pH	7.8	7.8
	Concentration (mg/L)	*	*
	Volume (ml)	100	100
	Time (min)	120	120
Varied parameters	Adsorbent dosage (g)	0.3-5.5 g	0.3-5.5 g

* Concentration of heavy metals in SSTe

Table 5-11: Parameters for contact time test using wastewater.

		<u>Adsorbents</u>	
		GAC	HC-AC
Fixed parameters	Carbon dosage (g)	0.6	0.6
	pH	7.8	7.8
	Volume (ml)	1 000	1 000
Varied parameters	Time (min)	0-420	0-420

The adsorption capacity for C-GAC and HAC and percentage removals for the identified heavy metals are given in Table 1. The performance of HAC and C-GAC was closely similar for all elements except for Fe where C-GAC exhibited a significantly higher adsorption capacity. The order of adsorption was Fe > Ni > Mn > Zn for C-GAC and Fe > Ni > Zn > Mn for HAC.

Table 5-12: Summary of Adsorption Capacities and % Removals-Laboratory Scale Studies

Laboratory Scale Studies				
Heavy Metal	Adsorption Capacity (mg/g)		% Removal (%)	
	HAC	C-GAC	HAC	C-GAC
Iron	47.2	63.1	78	78
Manganese	25.7	26.6	57	67
Nickel	16.8	15.8	73	69
Zinc	6.6	8.2	67	64

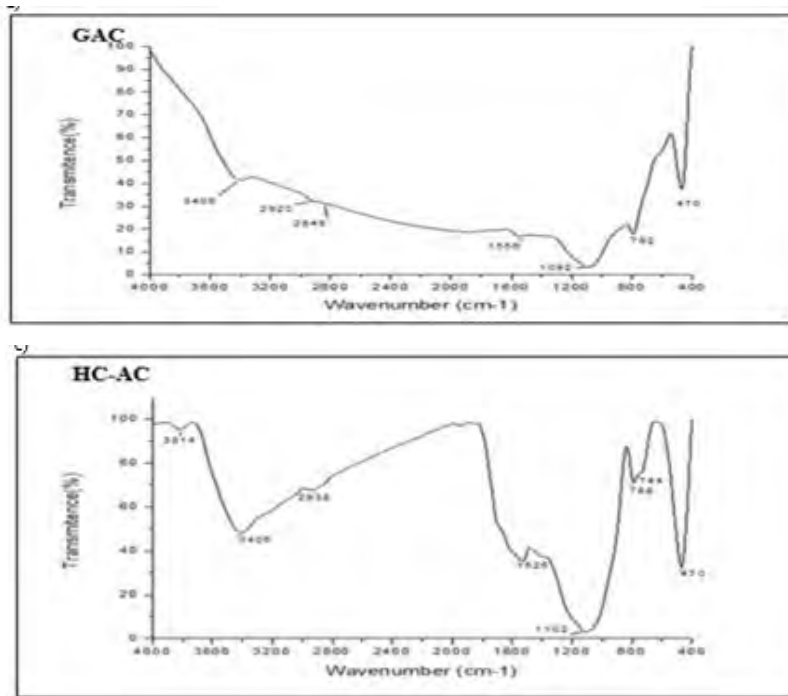


Figure 5.11: FT-IR spectra of GAC and HAC

Table 5-13: Summary of the presence and absence of functional groups on GAC and HC-AC.

	GAC	HC-AC
Group or functionality		
C-O in ethers (stretching)	✓	✓
Alcohols	✓	✓
-C-OH (stretching)	✓	✓
Quinones	✓	✗
C-H (stretching)	✓	✓
N-H, C=N	✗	✗
N-O-	✓	✓
✓ present ; ✗ absent		

APPENDIX B ADSORPTION COLUMN TESTS RESULTS – HEAVY METALS

B.1 Phase 1 – Heavy Metals

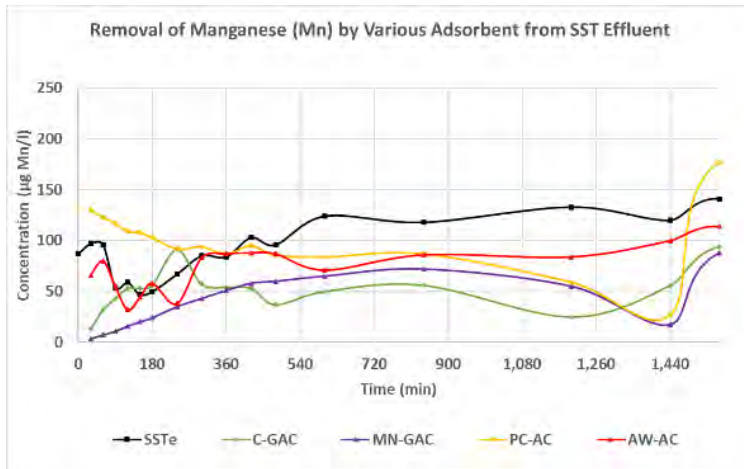


Figure 5-12: Removal of Manganese from SST effluent by various adsorbents

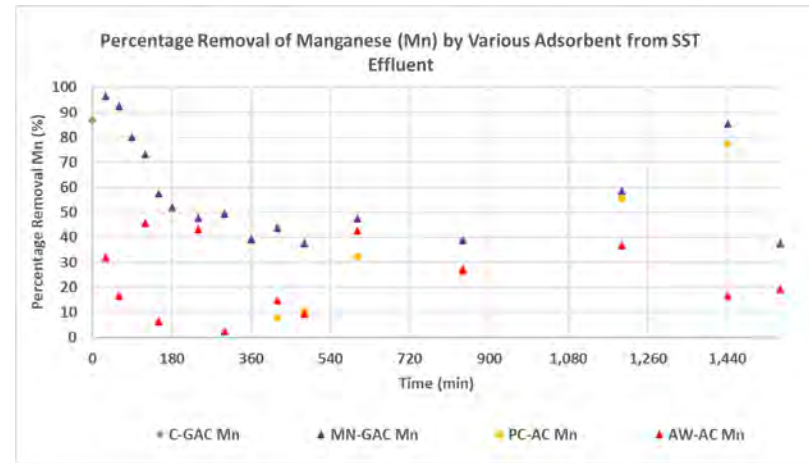


Figure 5-13: Percentage removal of Manganese from SST effluent by various adsorbents

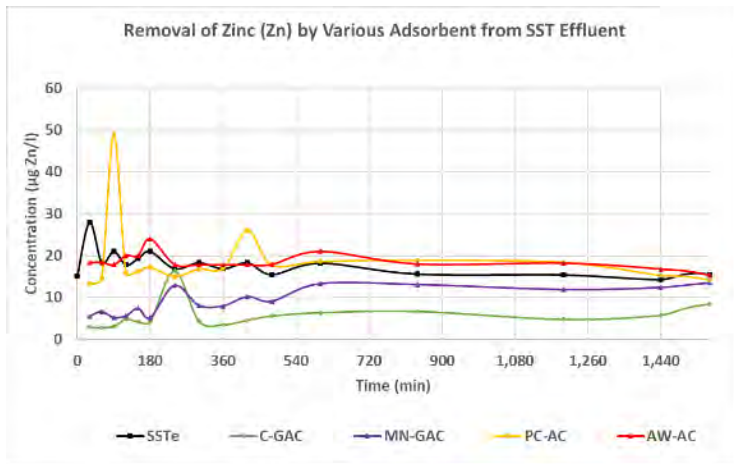


Figure 5-14: Removal of Zinc from SST effluent by various adsorbents

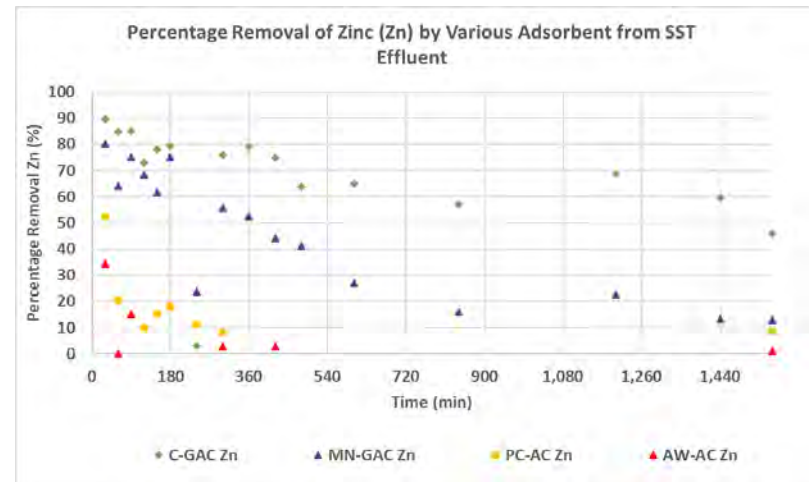


Figure 5-15: Percentage removal of Zinc from SST effluent by various adsorbents

B.2 Phase 1 Adsorption Column Tests Results – EDCs

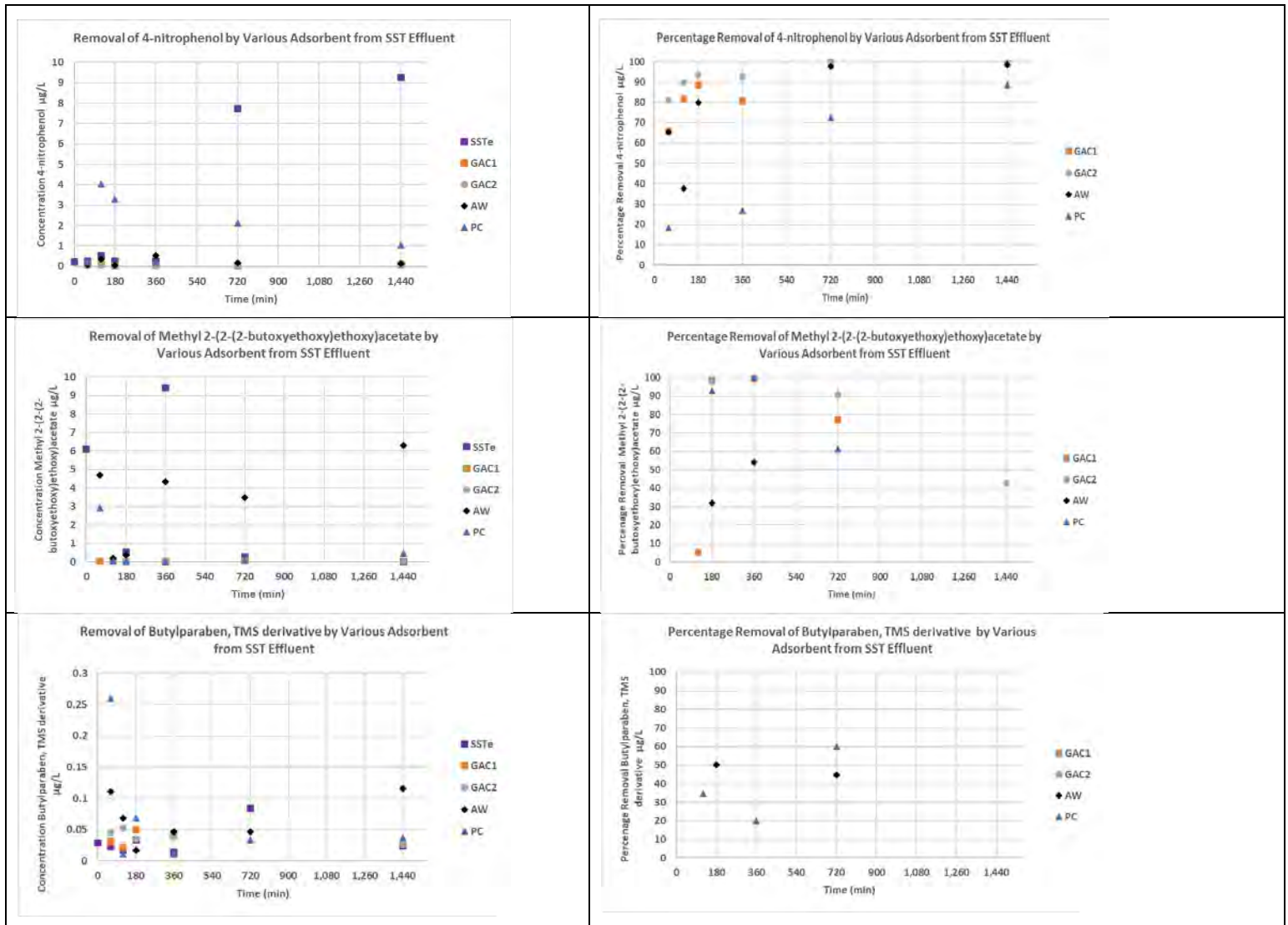


Figure 5-16: Removal of selected EDCs from SST effluent by various adsorbents

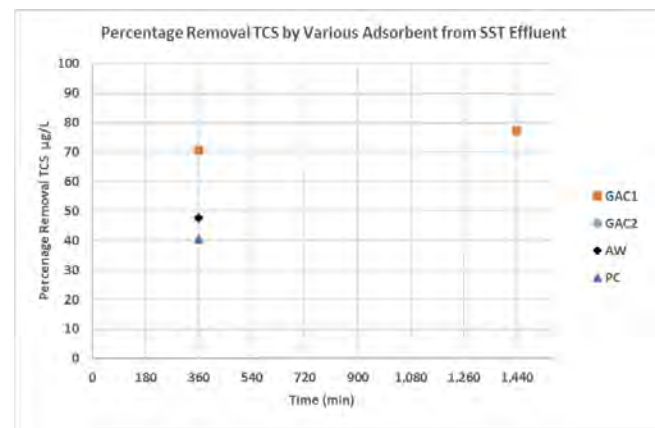
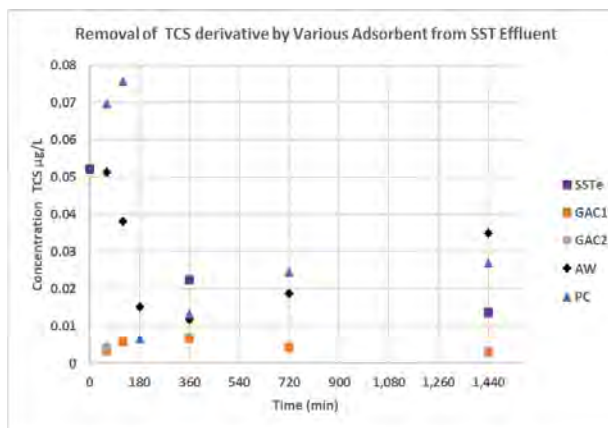
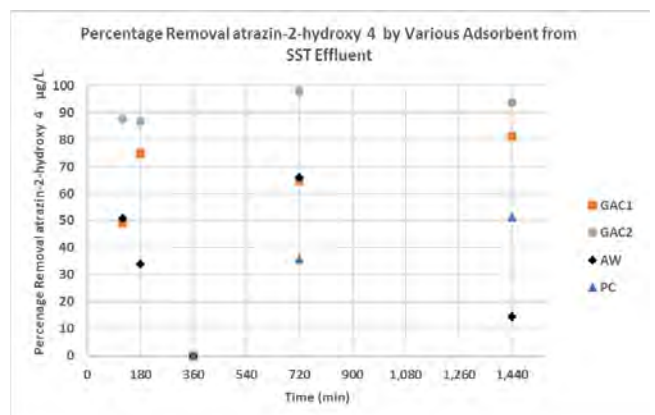
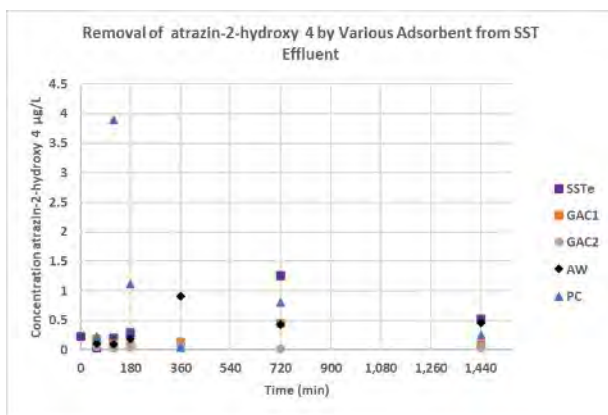
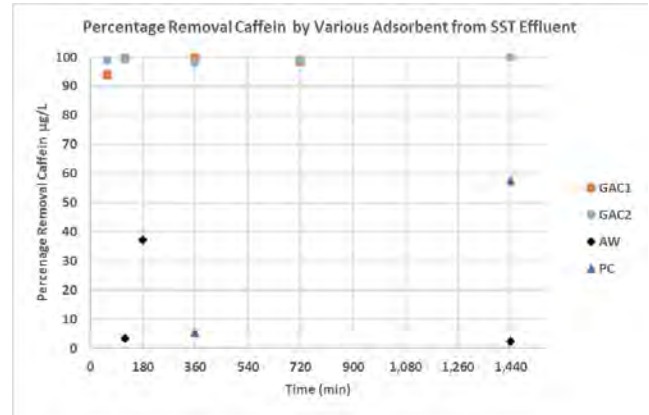
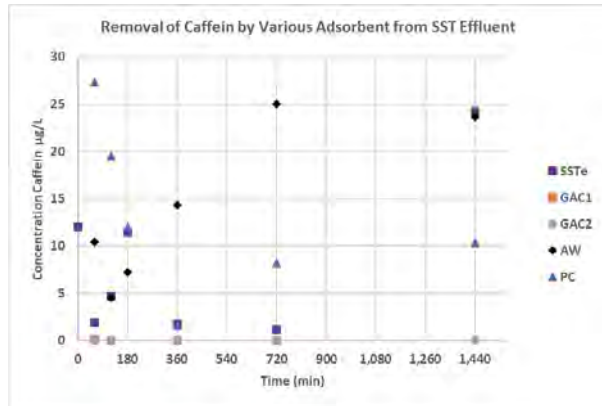


Figure 5-17: Removal of selected EDCs from SST effluent by various adsorbents

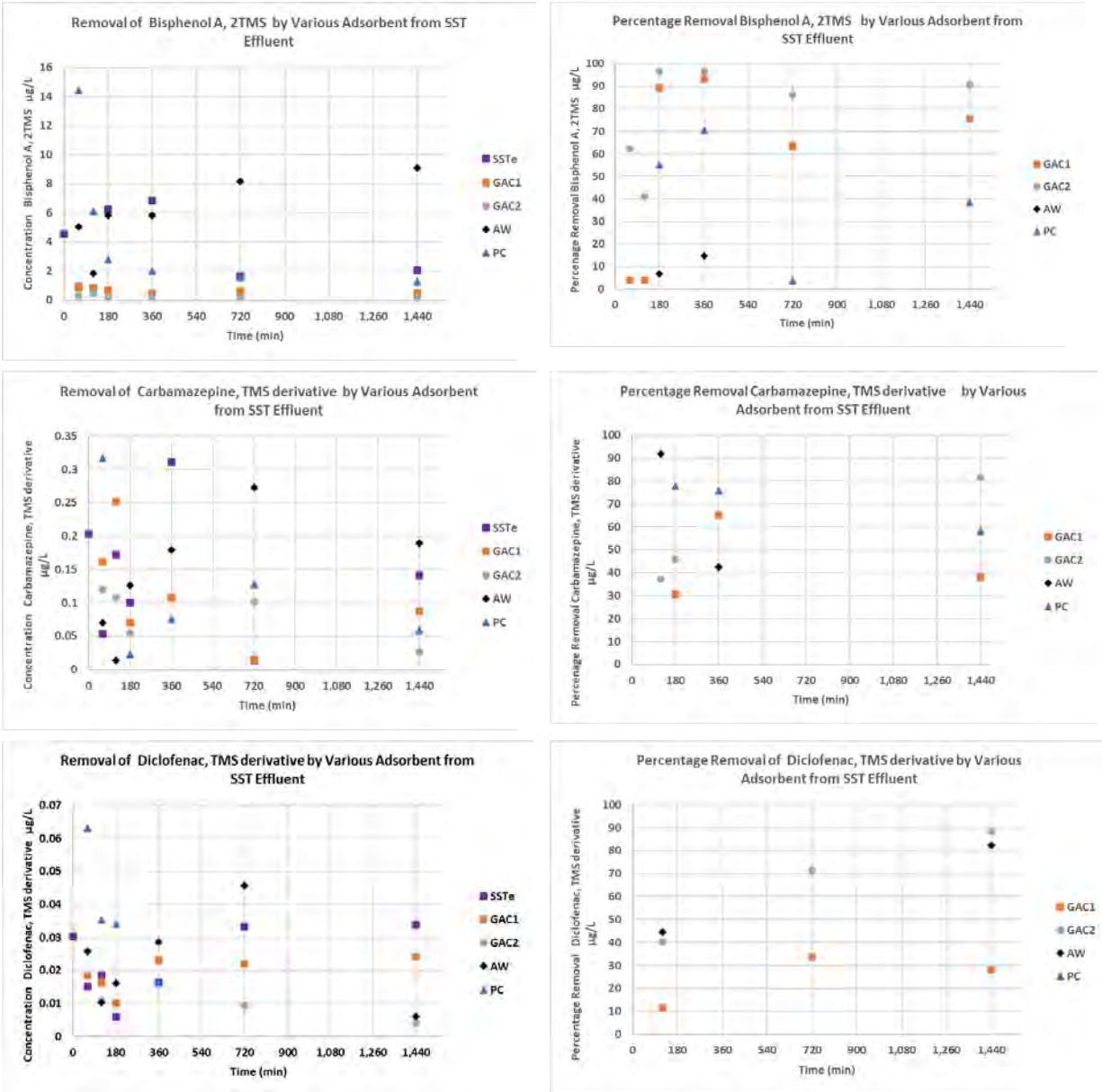


Figure 5-18: Removal of selected EDCs from SST effluent by various adsorbents

APPENDIX C TESTS ON WOOD DERIVED ADSORBENTS

C.1 Activated Carbons under Investigation

The following locally sourced activated carbons will be investigated in this project:

- Coal based granular activated carbon (C-GAC). This will be the baseline against which all the other green ACs will be compared
- Commercially generated GAC and PAC from macadamia nuts (M-GAC and M-PAC respectively)
- AC derived from hydrochar (HAC) from processing sludge and other waste biomass in the emerging EHTP process
- Green ACs derived from waste wood in Khula Village (KwaZulu-Natal) and supplied by eThekweni Municipality, i.e.
 - Alien wood AC (AW-AC) from pyrolysis of recently felled (December 2020) alien wood
 - Waste sawdust AC (SD-AC) from pyrolysis of fine (6 mm) dump sawdust
 - Pinecone AC (PC-AC) from pyrolysis of fallen pinecones from a plantation

Table5-14 shows some of the ACs that are part of the comparative study.

C.2 Conversion of Hydrochar to Activated Carbon

The hydrochar produced from the various feedstocks will be converted to activated carbon using the method outlined in the literature (Saha et al., 2019). The hydrochar will initially be thermally annealed at different temperature (400, 500 and 600°C) to determine the optimal temperature to produce activated carbon with characteristics that efficiently remove the selected micropollutants. Annealing will be conducted in two stages. In the first stage, the furnace will be heated from ambient temperature to 100°C at 10°C/min and kept constant for 1 min to stabilize the temperature and remove moisture from the hydrochar. In the final stage, the furnace will be heated from 100°C to the set annealing temperature at a rate of 20°C/min followed by an isothermal period of 60 min at the same temperature. The furnace will then be cooled to 200°C at a rate of 20°C/min using the built-in forced draft fan and then naturally cooled to room temperature. Nitrogen will be passed through the furnace at 1.0 ml/min during the annealing to prevent combustion or gasification of the hydrochar. Proximate analysis, BET analysis, ultimate analysis, ESC measurement, pH, pH at point of zero charge (pHPZC), Boehm titration and FTIR analysis will be conducted on the hydrochar and produced activated carbon.

Table 5-14: Photos of Some of the Locally Sourced Activated Carbons used in the Laboratory and Pilot Scale Adsorption Tests

			
<p>Coal Based GAC (C-GAC)</p>	<p>Coal Based PAC (C-PAC)</p>	<p>Hydrochar from Combined Primary and Waste Activated Sludge</p>	<p>HAC</p>
			
<p>Pinecone AC (PC-AC)</p>	<p>Waste Saw Dust AC (SD-AC-)</p>	<p>Alien Wood AC (AW-AC)</p>	

C.3 Laboratory and column scale AC Characterisation

Research Approach

The following will be undertaken during the laboratory scale study to achieve the objectives of this study:

1. Thermal annealing of hydrochar from the EHTP process to convert it to activated carbon
2. Characterization of ACs
3. Methylene blue adsorption tests
4. Heavy metal and micropollutant adsorption tests

Thermal annealing of hydrochar to convert to HAC has been completed and characterisation is in progress. Coal based GACs and other green ACs have been fully characterised. Methylene blue and micropollutant removal adsorption tests are still in progress. The available results are given below.

Physical Appearance and Preparation for Testing

The commercial GACs have uniform particles and did not need any pre-preparation prior to characterisation. The ACs derived from pyrolysis of waste wood from Khula Village however did not have uniform particles. Therefore, the activated carbons were ground to produce uniform particles prior to characterization as required by the standard characterisation tests that were applied. Table 5-15 summarises the physical appearance of the waste wood derived ACs from Khula Village and the pre-preparation required prior to characterisation and jar tests to determine adsorption efficiency.

Table 5-15: Physical Characteristics of Waste Wood Derived Green ACs from Khula Village

AC	Appearance	Behaviour when Mixed with Water	Additional Preparation for Characterisation
AW-AC	Very chunky particles with appearance similar to charcoal with fine dust particles	Well distributed when mixed with water	Required extensive grinding and milling
SD-AC	Relatively small wood chips and powder like sawdust	Dispersed on water surface	Did not require much grinding and milling
PC-AC	Distinct particles consisting of pine stalk and pine scales	Scale component floated while the stalk component settled as it was heavier	Required extensive grinding and milling

The above physical characterisation showed that the ACs from pyrolysis of waste wood from Khula village did not have uniform particles and required additional preparation in order to be characterised and used for adsorption tests. Furthermore, SD-AC and PC-AC did not mix well with water and had floating particles on the water surface. AW-AC was well distributed when mixed with water.

Standard Characteristics of ACs

A summary of the results of standard characterisation tests conducted on the ACs is given in Table 5-16. The results for the hydrochar derived activated carbon (HAC) are still pending.

Table 5-16: Characteristics of the Activated Carbons Analysed to Date

Parameter	C-GAC	M-GAC	M-PAC	AW-AC	SD-AC	PC-AC
pH	5.1	10.2	10.3	7.0	6.2	6.5
Attrition (%)	32			60	70	50
Ash content (%)	2.4	5.2	6.6	2.7	26.8	1.8
Moisture content (%)	3.9	2.8	2.9	7.9	1.9	5.4
Bulk density (kg/m ³)	476	358	349	377	284	237
Particle size(μm)	425-2,360	425-2360	45-250	45-250*	45-250	45-250*
Iodine number (mg/g)	1,198	585	899	266	70	36

The following is noted from the results:

Attrition

Attrition is an important physical property of AC which defines the intraparticle abrasion due to the adsorbent application's nature. Lower attrition has been found to indicate a longer operating life in the process. C-GAC has the lowest attrition. Of the waste wood derived ACs, PC-AC has the lowest attrition and SD-AC the highest.

Bulk Density

Bulk density is an important parameter for characterizing the mass/volume ratio of the adsorbents. A higher bulk density potentially indicates a higher adsorption capacity.

- C-GAC has the highest bulk density
- Of the waste wood derived ACs, AW-AC has the highest bulk density and SD-AC and PC-AC have closely similar values

Particle Size

The particle size cannot be accurately compared since the waste wood derived ACs particles varied widely from very small particles to large chunks. Therefore, extensive grinding to a uniform particle size was required before any characterisation could be carried out.

Iodine Number

The Iodine number is used as a compensatory parameter in addition of BET analysis to characterize the internal surface area of the adsorbents. The iodine molecule gives information about the surface area contributed by pores larger than 1 nm. Therefore, this characterization defines the microporosity of the adsorbents. The determination is based on the adsorption experiment with iodine as adsorbate with defined initial and residual concentrations. Iodine number is a measure of activity level and the micropore content of the activated carbon. A higher number indicates a higher degree of activation.

- Of the commercially produced ACs, C-GAC has the highest iodine number (1,198 mg/g) followed by M-PAC (899 mg/g) and M-GAC (585 mg/g) has the lowest. The iodine number for the commercially produced ACs is significantly higher than the waste wood derived ACs

- Of the waste wood derived ACs, AW-AC has the highest iodine number of 265 mg/g. The iodine numbers for SD-AC and PC-AC were significantly lower at 70 mg/g and 36 mg/g respectively

C.4 Pilot Scale Column Tests

A fixed bed column pilot scale rig with four columns was installed at Northern Works WWTW to test the performance of adsorbents and obtain results that can be applied at full-scale operation. Before the actual performance testing adsorption tests could be conducted, initial testing was conducted to test the suitability of the various ACs and optimize the operation of the rig. The results are given below.

Results with all ACs as Manufactured

After setting up the adsorption column test tubes, each AC was transferred to a column in the test rig. Each column was filled with AC to the height which was predetermined during the design of the pilot column tests. The height was the same for all the 4 columns. Once the columns were ready, the wastewater (effluent from the secondary settling tanks) feed-pumps were switched on and the columns received wastewater from the top of each column at the same flowrate.

Figure 5-19 shows the columns filled with C-GAC and the ACs derived from wood waste AW-AC, SD-AC and PC-AC. The initial runs of the experiment highlighted that some of ACs had poor characteristics that made them unsuitable for the adsorption tests as described below.

Alien Wood AC (AW-AC)

- As observed during the laboratory scale tests the density of the particles was not uniform. The non-uniformity caused the adsorption media bed to break with lighter particles floating at the top and heavier particles staying at the bottom.
- The AC also had fine dust particles that clogged the outlet at the bottom of the column

Sawdust AC (SD-AC)

- SD-AC consists of mainly very fine particles derived from saw dust and relatively slightly bigger particles derived from wood chips. The porosity of the SD-AC appeared to be too low to allow the wastewater to flow through from the top to the bottom. As a result, the wastewater filled up in the column and the inlet valve had to be shut off to prevent an overflow.
- Some of the lighter wood chips floated on the water

Pinecone AC (PC-AC)

- As observed during the laboratory tests, the density of the particles was not uniform. The non-uniformity caused the adsorption media bed to break with lighter particles (consisting mainly of the pinecone scales) floating at the top and heavier particles (consisting mainly of pinecone stalks) staying at the bottom.

Coal GAC (C-GAC)

- The C-GAC column behaved as expected. Wastewater was able to flow from the top to the bottom of the column and the bed did not break.



Figure 5-19: Pilot Scale Column Test Calibration for the Various ACs. AW-AC and PC-AC had broken beds with some particles floating to the surface while wastewater could not flow through SD-AC causing pooling in the column. C-GAC had a normal bed.

Results with Additional Preparation of Waste Wood ACs

To try and mitigate the observed challenges with waste wood derived ACs from Khula village, additional steps were taken to prepare the ACs before transferring to the columns and running the test rig. The following steps were undertaken:

Alien Wood AC (AW-AC)

- AW-AC was washed to remove fine particles that clogged the column bottom outlet. Furthermore, to grade the particles and increase uniformity the AC was also soaked in a bin full of clean water and the lighter particles that floated on top of the water were removed. Only heavier particles that settled at the bottom of the bin were kept for use in the column.

Pinecone AC (PC-AC)

- Similar to AW-AC, the uniformity of the particles was improved by soaking the AC in a bin full of clean water, removing the floating lighter particles and retaining the heavier bottom particles for the column tests.

Sawdust AC (SD-AC)

- No additional preparation was done on the SD-AC and it was accepted that no improvements could be made

Additional preparation resulted in the following improvements:

- Washing off fines from the AW-AC eliminated the clogging at the bottom outlet of the adsorption column
- The grading through soaking and removing of floating particles also solved the problem of breaking of the bed through the reduction of the amount of lighter floating particles for both AW-AC and PC-AC.



Figure 5-20: Pilot Scale Column Test Calibration for the Various ACs. After washing off fines, soaking and removing floating particles, the AW-AC and PC-AC column beds remained intact similar to GAC.

C.5 Discussion and Conclusions

The results of the characterisation of the waste wood derived ACs from Khula Village indicated the following:

1. Laboratory Scale Tests

- Both AW-AC and PC-AC had non uniform particle sizes. The ACs required extensive grinding in to enable characterisation using the generally accepted scientific standard methods
- Jar tests showed that SD-AC could not mix with water and most of the particles floated on the surface. For PC-AC, particles which consisted mostly of pinecone scales floated while those consisting of pinecone stalks settled at the bottom of the jar. AW-AC mixed well with water
- Standard characterisation of the waste wood ACs indicated the following:
 - PC-AC has the lowest attrition (50%), AW-AC the second lowest (60%) and SD-AC (70%) the highest. Therefore PC-AC has potentially the highest operating time when used in a treatment process.
 - AW-AC has the highest bulk density (377 kg/m³) and SD-AC (284 kg/m³) and PC-AC (237 kg/m³) values are 25% and 37% lower respectively. AW-AC bulk density is 21% lower than that of C-GAC. This indicates that AW-AC has potentially a higher adsorption capacity than SD-AC and PC-AC
 - AW-AC has the highest iodine number of 265 mg/g. The iodine numbers for SD-AC and PC-AC were significantly lower at 70 mg/g (74% lower) and 36 mg/g (86% lower) respectively. The results indicate that AW-AC has a significantly higher degree of activation than SD-AC and PC-AC and therefore potentially better adsorption performance

2. Pilot Scale Column Tests

- Use of the ACs in the pilot column tests which represent use of the ACs in full scale plants indicated the following:
 - SD-AC as supplied had particles that were too fine and clogged the column. Feed wastewater could not flow through the column resulting in ponding on top of the column bed. No improvements could be made to the SD-AC
 - AW-AC as supplied had fine pores that clogged the column bottom outlet. Furthermore, due to non-uniformity of the particles, light particles floated on top of the wastewater in the column resulting in a broken bed. Additional preparation of the AC through (i) washing off fine particles and (ii) prior soaking of the AC in clean water and removing the floating particles and using the heavier particles in the column improved the performance of the AW-AC. No blockage of the outlet was observed and an intact bed, similar to C-GAC was retained in the column
 - PC-AC as supplied also exhibited a broken column bed due to floating of light particles. After similar prior soaking and discarding the floating particles, the heavier particles retained an intact column bed

Based on both the laboratory characterisation tests and the results from the setting up of the pilot column tests it was concluded that:

- Sawdust derived activated carbon (SD-AC) and pinecone derived activated carbon (PC-AC) as supplied (and after extensive additional preparation of PC-AC) do not have the characteristics to be successfully investigated as adsorbents for the removal of the selected contaminants from wastewater effluent at laboratory and pilot scale. No further tests will be conducted on these ACs
- While AW-AC required extensive additional preparation prior to use in the laboratory jar tests and pilot column tests, the standard characteristics indicate that it is suitable for further evaluation as an adsorbent to remove the identified contaminants from wastewater effluent. AW-AC was therefore included in further laboratory and pilot scale adsorption tests in this project.

It is recommended that the Supplier of the waste wood derived ACs improve the characteristics of these ACs to improve their potential use as adsorbents.

